JOHANNES GUTENBERG UNIVERSITÄT MAINZ

"The *Rbfox1* gene: expression analysis and study of the transcriptional regulation"

Dissertation
zur Erlangung des Grades
"Doktor der Naturwissenschaften"

Am Fachbereich Biologie
der Johannes Gutenberg-Universität Mainz

Sònia Casanovas Palau
geb. am 13.01.1982 in Reus-SPAIN

Mainz 2018

Summary

The *RBFOX1* gene, which is located on chromosome 16p13.2, encodes an RNA-binding protein that regulates pre-mRNA splicing events in specific cell types including neurons. In the mouse, the gene contains a large noncoding part in its 5' end with at least four alternative promoters, promoters 1B, 1C, 1D and 1E. Promoters 1B, 1C and 1D are brain specific and promoter 1E is muscle specific. The promoters drive the expression of the alternative *Rbfox1* transcript isoforms, which differ in their 5'UTR but not in their coding exons. Copy number variants (CNVs) in the human *RBFOX1* gene that are located in the 5'-noncoding part of the gene and that typically only affect some but not all *RBFOX1* transcript isoforms, have been associated with a range of neurodevelopmental disorders such as autism spectrum disorder, intellectual disability, epilepsy, attention deficit hyperactivity disorder and schizophrenia.

In this thesis, I analyzed the expression of the three brain-specific Rbfox1 transcript isoforms controlled by the promoters 1B, 1C and 1D during embryonic development of the cerebral cortex as well as in various brain regions of the juvenile mouse. Furthermore, through *in silico* analysis and luciferase assays, I characterized the alternative *Rbfox1* promoters and demonstrated that the expression of *Rbfox1* in primary cortical neurons is driven by promoters 1B and 1C. I identified three transcription factors (C-MYC, NEUROD2 and TCF4) that regulate the expression of *Rbfox1* in cortical neurons. Using transcript-specific studies, I was able to show that TCF4 regulates the expression of transcripts 1B and 1C, whereas NEUROD2 only controls the expression of transcript 1B.

Zusammenfassung

Das RBFOX1-Gen, das auf Chromosom 16p13.2 lokalisiert ist, kodiert für ein RNA-bindendes Protein, das Prä-mRNA-Spleißereignisse in bestimmten Zelltypen einschließlich Neuronen reguliert. In der Maus enthält das Gen einen großen nichtcodierenden Teil in seinem 5'-Ende mit mindestens vier alternativen Promotoren, den Promotoren 1B, 1C, 1D und 1E. Die Promotoren 1B-1D sind hirnspezifisch und der Promotor 1E ist muskelspezifisch. Die Promotoren steuern die Expression der alternativen Rbfox1-Transkript-Isoformen, die sich lediglich in ihren 5'UTR-Exons unterscheiden. Kopienzahlvarianten (CNVs) im humanen RBFOX1-Gen, die sich im 5'-nichtcodierenden Teil des Gens befinden und typischerweise nur einige, jedoch nicht alle RBFOX1-Transkript-Isoformen betreffen, sind mit einer Reihe von neurologischen Entwicklungsstörungen wie Autismus Spektrum Störung, geistige Behinderung, Epilepsie, Aufmerksamkeitsdefizit-Hyperaktivitätsstörung und Schizophrenie assoziiert.

In dieser Arbeit analysierte ich die Expression der drei durch die Promotoren 1B, 1C und 1D gesteuerten Gehirn-spezifischen Rbfox1-Transkript-Isoformen während der Embryonalentwicklung des zerebralen Kortex der Maus sowie in verschiedenen Hirnregionen der juvenilen Maus. Darüber hinaus charakterisierte ich die alternativen Rbfox1-Promotoren und zeigte, dass die Expression von Rbfox1 in primären cortikalen Neuronen von den Promotoren 1B und 1C gesteuert wird.

Ich identifizierte drei Transkriptionsfaktoren (C-MYC, NEUROD2 und TCF4), die die Expression von Rbfox1 in kortikalen Neuronen regulieren. Mittels transkriptspezifischer Untersuchungen konnte ich zeigen, dass TCF4 die Expression der Transkripte 1B und 1C reguliert, wohingegen NEUROD2 lediglich die Expression von Transkript 1B steuert.

Abbreviations

aCGH	Array comparative genomic hybridization
Anti-DIG-AP	Anti-digoxigenin antibody
ASD	Autism Spectrum Disorder
ATP	Adenosine triphosphate
bHLH	Helix-Loop-Helix
bp	Base pairs
BS	Binding site
C-Box	
cDNA	Complementary DNA
c-MYC	Mouse myelocytomatosis oncogene
CNS	Central nervous system
CNV	Copy number variants
CP	Cortical plate
cRNA	Complementary RNA
dH2O	Distilled water
DIF	Downstream intronic flanking
DIG	Digoxigenin
DIV	Days in vitro
DMEM	Dulbecco's Modified Eagle Medium
dNTP	deoxynucleotide triphosphate
DPBS	Dulbecco's phosphate buffered saline
E	Embryonic day
E-box	Enhancer box
E. *coli*	*Escherichia coli*
EST	Expressed sequence tag
EtBr	Ethidium Bromide
EtOH	Ethanol
et al	et alii
FBS	Fetal bovine serum
FISH	Fluorescence in situ hybridization
Fox gene	Feminizing on X gene
Gapdh	Glyceraldehyde 3-phosphate dehydrogenas
GWAS	Genome-wide association studies
ISH	In situ hybridization
IPCs	Intermediate progenitor cells
KLF7	Krüppel Like Factor 7
Kd	Knockdown
KO	Knockout
LASR	Large assembly of splicing regulators
LB	lysogeny broth
MZ	Marginal zone
MAX	MYC Associated Factor X
µl	Microliters
ml	milliliters
miR302	MicroRNA 302
miR-980	Micro-RNA 980
mRNA	Messenger Ribonucleic Acid
mut	Mutated
MYCN	v-myc myelocytomatosis viral related oncogene, neuroblastoma derived
NB	Neuroblastoma

NEUROD2	Neurogenic differentiation factor 2
NLS	Nuclear localization signal
NMR	Nuclear magnetic resonance
NPC	Neural precursor cell
NTC	No template control
P	Post-natal day
PCR	polymerase chain reaction
PFA	Paraformaldehyde
PP	Pre-plate
Rbfox1	RNA-Binding Fox1
RGCs	Radial glial cells
RNA	Ribonucleic Acid
rpm	Revolutions per minute
RRM	RNA recognition motif
RT	Room temperature
RT-qPCR	Real Time Quantitative PCR
siRNAs	Small interfering RNAs
SNPs	Single-nucleotide polymorphism
SNV	Single-nucleotide variant
SSC	The Simons Simplex Collection
SVZ	Subventricular zone
SP	Subplate
TCF4	Transcription factor 4
UIF	Upstream intronic flanking
UPL	Universal Probe Library
UTR	Untranslated region
VZ	Ventricular zone
ºC	Celsius
%	Percent

Contents

1. Introduction

1.1 Autism Spectrum Disorder (ASD)

The term autism was used for the first time in 1943 by Leo Kanner to describe a very distinctive trait of “enclosure in one’s self” shared by a cohort of eleven children. Since then, great advances have been achieved in understanding the psychopathology underlying this complex disorder (Antonio M. Persico, 2013). Autism spectrum disorders (ASD) are a group of neurodevelopmental disorders that include autism, Asperger’s syndrome, childhood disintegrative disorder and pervasive developmental disorder not otherwise specified. ASD has an estimated prevalence of 1 in 150 children, with a prevalence four times higher in males than females (Christa Lese Martin 2007). Disorders within the spectrum are characterized by impairment of social interaction and verbal and nonverbal communication, as well as by limited interests, accompanied by repetitive behaviors. These symptoms manifest themselves during the first 3 years of life and remain for the rest of life (Tiffany D. Rogers, 2013).

ASD has been recognized as a neuropsychiatric disorder with the greatest genetic component, with a monozygotic twin concordance rate between 80-95%, a noticeable sibling recurrence risk of 5-6% for full-blown autistic disorder and approximately 15-25% for broad ASD (Angelica Ronald, 2006; Paul Lichtenstein, 2010, Sven Sandin, 2014). Additionally, the presence of mild autistic traits in many first-degree relatives of patients with autism has been reported (Antonio M. Persico, 2013). Most of the genetic findings in ASD have occurred in the last decade, outstanding most of the other neuropsychiatric disorders. Consequently causative mutations could be identified in 10–20% of all ASD cases (Daniel.H. Geschwind, 2011).

Some of the well-known syndromic disorders (genetic or genomic disorders) can display autistic features in their clinical presentation, such as fragile X syndrome (*FRM1)*, tuberous sclerosis (*TSC1* and *TSC2)*, neurofibromatosis, untreated phenylketonuria, Angelman, Cornelia de Lange or Down syndrome. In some studies, autistic patients having gene-disrupting mutations in genes associated with the fragile X protein, FRMP, were identified, reinforcing the links between autism and synaptic plasticity (Ivan Iossifov, 2012). Moreover, compared to controls (healthy siblings) an increased frequency of copy number variants (CNV) was identified in the ASD population.

More recently, it has become evident that CNVs location and their functional relevance may play a more important role in terms of pathogenicity than mean CNVs, number and size. Notably, many CNVs found in ASD patients have been found also in patients with other psychopathologies, especially intellectual disability and schizophrenia. Actually, two studies analyzing large dataset have unveiled highly heterogeneous de *novo* CNVs affecting several genes and supposedly accounting for less than 10% of all ASD cases (Stephan J. Sanders, 2011; Dan Levy, 2011).

Several ASD causative mutations have been identified in genes encoding proteins involved in synapse formation, maturation and stabilization, including neuroligins, SHANK and neurexin proteins. For this reason, ASDs were initially considered disorders of synaptic function (Synaptopathies) (Antonio M. Persico, 2013).

The Neuroligins family consists of *NLGN1, NLGN2, NLGN3, NLGN4X,* and *NLGN5* genes, however, only mutations in *NLGN3, NLGN4*, and *NLGN4Y* genes have been linked to autism. Nevertheless, the frequency of mutations in the *NLGN* gene among idiopathic ASD patients is very low, accounting for less than one percent of the ASD cases. The *SHANK* gene family consists of three members, *SHANK1, SHANK2* and *SHANK3*, which encode scaffolding proteins required for the proper formation and function of neuronal synapses. *SHANK3* is predominantly expressed in the

cerebral cortex and cerebellum, localized at excitatory synapses where it binds to neuroligins in post-synaptic boutons. However, mutations in the *SHANK3* locus in ASD patients accounts for only 0.85% of the ASD cases (Antonio M. Persico, 2013). The third group involved in the autism-related synaptic network are the neurexins, encoded by three highly conserved genes, *NRXN1, NRXN2* and *NRXN3*. Neurexins are mediators for neurotransmitter release by linking calcium (Ca^{2+}) channels to synaptic vesicle exocytosis (Antonio M. Persico, 2013). Several studies have reported rare sequence variants or CNVs affecting the *NRXN1* locus. In fact, truncating mutation in *NRXN1* and *NRXN2* have been linked to ID (F.R. Zahir, 2008; Anna C. Need, 2009), ASD and schizophrenia (Anna C. Need, 2009; Julie Gauthier). In addition, rare deletions in the *NRXN3* locus have been found in four ASD patients three of which were inherited from either subclinical or apparently healthy parents (Andrea K. Vaags, 2012).

Mutations in chromatin architecture genes have been also identified in ASD patients (Antonio M. Persico, 2013). DNA methylation is the major epigenetic modification of eukaryotic genomes playing an essential role in mammalian development. Methyl-CpG binding protein 2 (MeCP2), is a transcriptional repressor involved in chromatin remodeling and in the modulation of RNA splicing, and is required for correct brain function and development. In fact, loss of MECP2 has been shown to delay neuronal maturation and synaptogenesis, (Maria Chahrour, 2007) and *de novo* loss-of-function mutations cause Rett syndrome in approximately 70% of affected females, whereas they are lethal in males (Ruthie E. Amir, 1999). In addition, *MECP2* mutations have also been found in non-syndromic autistic girls. (Antonio M. Persico, 2013).

The phosphatase and tensin homolog (*PTEN*) gene, located on chromosome 10q23, harbors mutations associated with a broad spectrum of disorders, including Cowden syndrome (CS), Bannayan–Riley–Ruvalcaba syndrome, Proteus syndrome, and Lhermitte–Duclos disease

(Gideon M Blumenthal, 2008). *PTEN* is a tumor suppressor gene which stimulates cell-cycle arrest in G1 and apoptosis (Antonio M. Persico, 2013). Patients with autism carrying *PTEN* mutations are characterized by severe to extreme macrocephaly. In some ASD patients the overgrowth starts prenatally, whereas in others macrocephaly occurs only postnatally (Eric Courchesne, 2007). The incidence of *PTEN de novo* mutations in macrocephalic ASD patients has been estimated at 4.7% of all ASD patients (C. Lintas 2008).

Genetic evidence suggests that at least some ASD cases may result from abnormal Ca^{2+} homeostasis during neurodevelopment (Jocelyn F Krey, 2007). Moreover, several genetic studies have identified autism-related genes involved either directly or indirectly in controlling intracellular Ca^{2+} levels, such as *CACNA1C, CACNA1F, CACNA1H, KCNMA1* and *SCN2A* (Antonio M. Persico, 2013). These genes encode for ion channels, receptors, and Ca^{2+}- regulated signaling proteins, often crucial for a correct CNS development. For example, gain-of-function mutations in the L-type voltage-gated Ca^{2+} channel Cav1.2 (*CACNA1C*) cause Timothy syndrome, a multisystem disorder including mental retardation and autism (Igor Splawski, 2004). Similarly, mutations in the L-type voltage-gated Ca^{2+} channel Cav1.4 (*CACNA1F*) cause the incomplete form of X-linked congenital stationary night blindness (*CSNB2*), and gain-of-function mutations *in CACNA1F* cause CSNB2 frequently accompanied by cognitive impairment and either autism or epilepsy (Ariana Hemara-Wahanui, 2005). Additionally, mutations and chromosomal abnormalities indirectly increasing cytosolic or intracellular Ca^{2+} levels have been associated with autism. A study identified a balanced translocation disrupting one copy of the *KCNMA1* gene, in a boy with autism (Frédéric Laumonnier, 2006). Another study conducted in one ASD patient identified a R1902C mutation in the *SCN2A* gene, resulting in a decreased binding affinity for

calmodulin, destabilizing the inactivation gate and promoting sustained channel activity during depolarization (L.A. Weiss, 2003).

Biochemical parameters linked to mitochondrial function are frequently abnormal in autism. However, mitochondrial dysfunction appears secondary to the pathophysiology underlying ASD in most of the cases. Only in rare cases mutations in mitochondrial DNA (mtDNA) or in nuclear DNA (nDNA) were found involved in mitochondrial functions in ASD patients (Antonio M. Persico, 2013). In fact, a comprehensive study carried out in 1298 autistic patients failed to provide any evidence of common contributions by mtDNA variation or heteroplasmy to ASD (Athena Hadjixenofontos, 2013).

Nevertheless, the genetic causes of the majority of the non-syndromic ASDs remain still unexplained. Rare variants may have strong effects on the phenotype, however, one must remember that each gene is associated with other genes forming part of a complex network. The effect of a mutation in a gene can be neutralized by a different gene, but it can also be amplified. Another added factor to this puzzle are the environmental factors. Importantly, within the framework of a polygenic disease, by definition no single gene variant would be expected to be associated with the disease in each and every sample, as common variants conferring autism vulnerability are predicted to vary widely from patient to patient. All these factors together, make the search for ASD candidate genes more complex. (Antonio M. Persico, 2013).

About ten years ago genome-wide association studies (GWAS) emerged as the gold standard method for the unbiased search of common variants highly contributing to a complex disease, like ASD (Lauren A. Weiss, 2009). While several studies have shown that rare structural variants (deletions/duplications or point mutations) can have substantial effects on disease risk, GWAS have failed in identifying any common variant repeatedly associated with autism in multiple

studies. Associations that reach (fully or nearly) strict genome wide significance levels in one study typically do not replicate in other GWAS, (Antonio M. Persico, 2013).

Since 2005, next-generation sequencing (NGS) technologies have improved as fast as high-throughput and cost-effective approaches, aiming to fulfil medical sciences and research demands (Bahareh Rabbani, 2012). Whole-exome sequencing (WES) was introduced less than ten years ago aiming to identify rare or novel genetic defects from genetic disorders. Particularly, ASD is a model disease to apply WES, due to the fact that multiple loci are involved in its development with relatively weak genotype–phenotype correlation. Several groups joined forces and carried out whole-exome sequencing studies of Autistic patients from The Simons Simplex Collection (SSC), which collects the data of 3000 families with an autistic child and their healthy siblings (Stephan J. Sanders, 2012; Benjamin M. Neale, 2012; Brian J. O'Roak, 2012). Data from Simplex families are particularly interesting, since only one child is affected and consequently it is highly likely to be caused by a *de novo* mutation. Further studies have been published by alliances not only in the US, but also in Europe (Silvia de Rubeis, 2014). The combination of large DNA data sets of affected people and their families, and the recent development of high throughput sequencing has led to the identification of rare *de novo* mutations in genes associated with ASD. The identification of these genes has driven the research to focus on earlier events, such as the cell division of the neural precursor cells and the subsequent migration of cells into certain layers of the developing cerebral cortex. This is supported by the phenotypes of different knockout mice that carry mutations in high-confidence ASD candidate genes identified in several recent whole-exome sequencing (Gaurav Kaushik, 2016).

1.2 The Rbfox family proteins

Alternative splicing of pre-mRNAs is considered to be a major source of proteomic complexity in metazoans and a key mechanism of gene regulation. Many alternative splicing events are tissue-specific and/or cell-type dependent. This mechanism plays an important role in the central nervous system (CNS), where it affects neuronal development and controls mature brain functions (Lauren T Gehman, 2011).

Developmental and tissue-specific alternative splicing is mediated by *cis*-acting elements in the pre-mRNA and by corresponding *trans*-acting protein factors that bind these elements to influence adjacent spliceosome assembly. One interesting group of *trans*-acting regulators is the Fox family of splicing factors, which are related to the *feminizing on X* (Fox) gene product of C. *elegans.* (Jonathan Hodgkin, 1994). The Rbfox family includes a highly evolutionary conserved group of RNA-binding proteins, which regulate alternative splicing in a tissue-specific manner. Each of these proteins contains an evolutionary highly conserved RNA recognition motif (RRM) which specifically recognizes the (U)GCAUG sequence in alternatively spliced exons or in flanking introns, and either promotes or represses inclusion of the target exons.

The RRM is highly evolutionary conserved, being identical in mouse RBFOX1 and RBFOX2, almost identical (97%) in RBFOX3 and only slightly diverged from the evolutionarily distant *Drosophila* (94% identity) and *Caenorhabditis elegans* (77% identity) proteins (John G. Conboy 2016) (Figure 1).

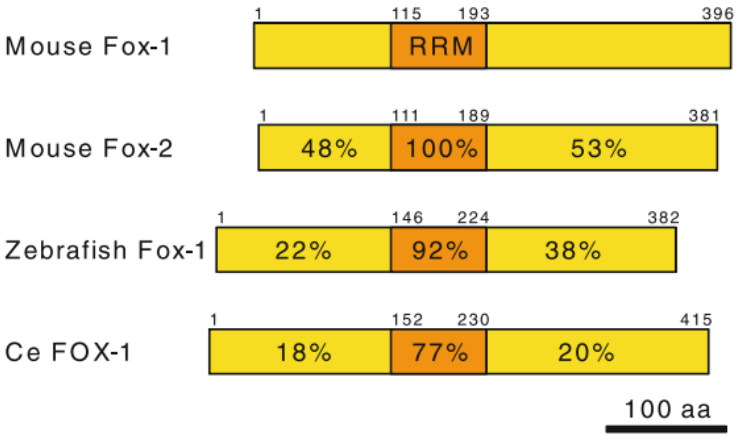

Figure 1. Schematic illustration of the domain structure of mouse RBFOX1 (Fox-1) and RBFOX2 (Fox-2), zebrafish Fox-1/A2bp1l, and C. *elegans* FOX-1. RRM domain is shown in orange. Identities of amino acid sequences of each domain compared to mouse Fox-1 are indicated. Amino acid positions are indicated. Adopted from Hidehito Kuroyanagi, 2009.

The solution structure of the mammalian RRM domain was solved by nuclear magnetic resonance (NMR) spectroscopy and adopts the typical β1α1β2β3α2β4 fold of an RRM (Sigrid D. Auweter, 2006; Christophe Maris, 2004). Its unusual packing, through an unusual molecular mechanism mediates an exceptionally high affinity and specificity for the recognition sequence (U)GCAUG. (U)GCAUG motifs are located at strategic regulatory points in the transcriptome, such as introns flanking tissue-specific alternative exons, 3' untranslated regions (UTRs), in mRNAs and pre-microRNA hairpins (Sigrid D. Auweter, 2006).

Mammals have three different Rbfox paralogs: Rbfox1 (Fox-1, Ataxin2-binding protein 1, A2BP1), Rbfox2 (Fox-2, RNA-binding motif 9, RBM9), and Rbfox3 (Fox-3, hexaribonucleotide-binding protein 3, HRNBP3, NeuN) (Andrey Damianov, 2010). *Rbfox1* is expressed in neurons and both skeletal and cardiac muscle cells. *Rbfox2* is also expressed in neurons and muscle but has a broader expression pattern, being observed in stem cells, hematopoietic cells, and in the whole

embryo (Jason G. Underwood, 2005). *Rbfox3* has only been observed in neurons (Tim-Rasmus Kiehl, 2001; Kee K. Kim, 2009; Ji-Ann Lee, 2016).

The Rbfox family, although having many splicing isoforms themselves, they all have the same identical RRM domain which resides in the middle portion of the protein (Figure 2) and their function absolutely relies on the intact RRM domain.

A nuclear localization signal (NLS), with a consensus protein sequence of RF(A/T)PY (Figure 2), was identified in the C-terminus of the RBFOX1 and RBFOX2 proteins, concluding that the C-terminal portion is indispensable for this protein function (Shingo Nakahata, 2005). Nevertheless, recently, a new NLS has been identified in the N-terminus of the RBFOX2 protein (Manuel Wenzel, 2016).

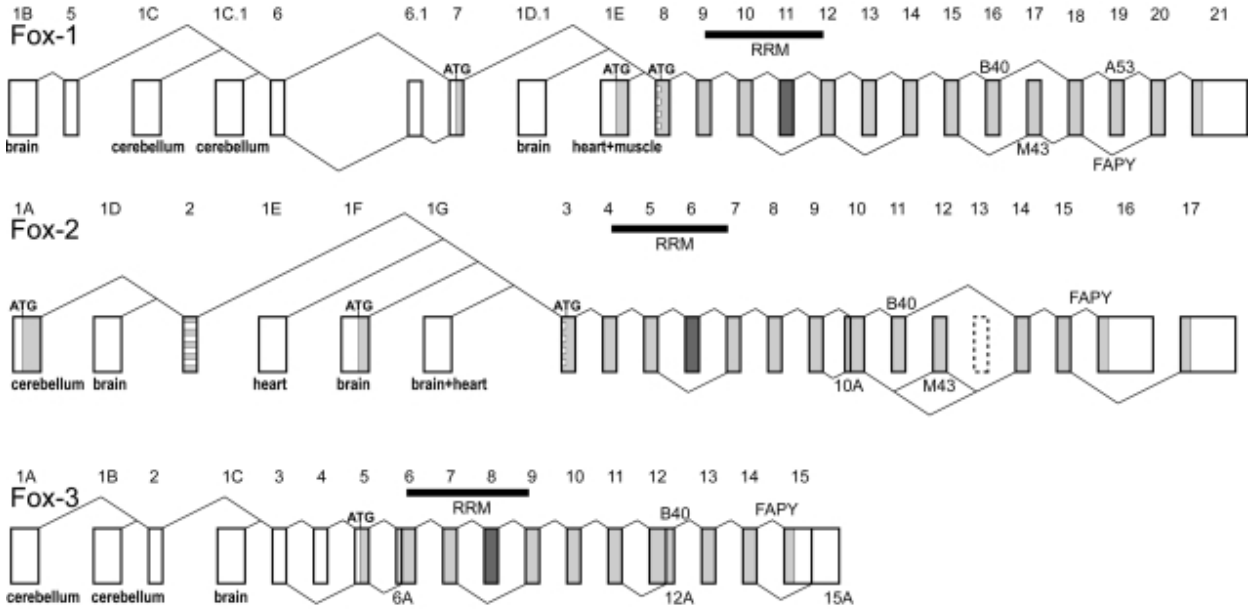

Figure 2. Organization of Rbfox family genes. Diagram of the mouse Rbfox genes, where is shown that *Rbfox2* and *Rbfox3* are also encoded by large complex genes with many of the same features as *Rbfox1.* Exons are shown as boxes. Coding exons are indicated in light grey, and the alternative in-frame start codons are also indicated. The dark-gray box represents the alternative exon encoding the second half of

the RRM domain which give rise to FoxΔRRM. Exons 1C.1 and 1D.1 of *Rbfox1* derive from mouse-specific promoters. Alternative exons B40, M43, and A53 and the FAPY C-terminal splice isoforms are also indicated. Fox-2 exon 13 (dashed box) is seen in human but not found in mice. The tissue specificity of the mouse Rbfox first exons is indicated below. (Adopted from Andrey Damianov, 2010).

Rbfox proteins typically act as splicing activators when bound downstream of an alternative exon, or as repressors when bound upstream (Hidehito Kuroyanagi, 2009; Jason G. Underwood 2005) (Figure 3). However, exons can contain Rbfox elements upstream, downstream, and within the exon itself, and it is often not possible to predict the direction of Rbfox dependent splicing regulation (Zhen Zhi Tang, 2009).

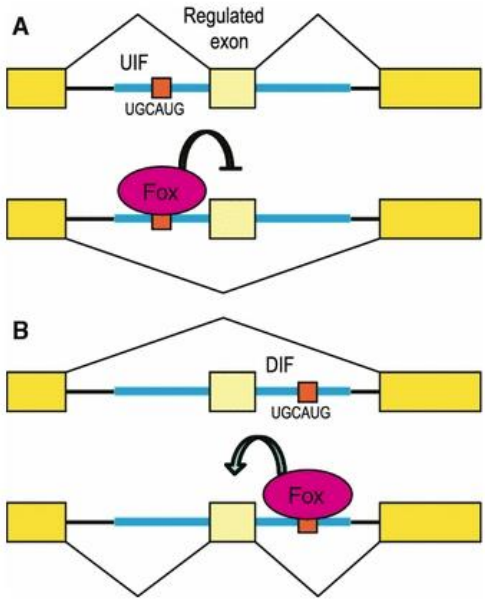

Figure 3. Schematic illustration of alternative splicing regulation by the Rbfox family proteins. a) Rbfox proteins repress exon inclusion by binding to (U)GCAUG element(s) in the upstream intronic flanking (UIF) region. b) Rbfox proteins enhances exon inclusion by binding to the (U)GCAUG element(s) in the downstream intronic flanking (DIF) region. Boxes indicate exons and horizontal lines indicate introns. Blue

horizontal lines indicate the UIF and DIF regions. Orange boxes indicate (U)GCAUG elements. (Adopted from Hidehito Kuroyanagi, 2009).

Mammalian Rbfox genes are highly complex, using multiple promoters, alternative exons, and alternative splice sites to produce complex sets of proteins differing in the N- and C-terminal domains and in their subcellular distributions. How these multiple Rbfox paralogs and isoforms vary in activity is not clear yet (Shingo Nakahata, 2005; Ji-Ann Lee, 2009). Multiple promoters of *Rbfox1* and *Rbfox2* presumably drive their expression in different cellular contexts, but their tissue specificity is not well characterized. The fact that the expression is driven by alternative promoters may also change the N-terminal residues of the proteins and presumably their activity.

1.2.1 Rbfox1

RBFOX1 encodes a highly versatile RNA binding protein that plays an important role in RNA metabolism during development of organisms from nematodes and insects to mammals (Hidehito Kuroyanagi, 2009). RBFOX1 is a neuron-specific splicing factor that exerts both, positive and negative regulatory effects on alternative splicing. In addition, RBFOX1 protein interacts with binding sites in the 3'UTRs of its target genes and regulates gene expression post-transcriptionally (Andrey Damianov, 2010).

1.2.1.1 The link between RBFOX1 and ASD

Given the different functions of Rbfox proteins in regulating alternative splicing and gene expression, and taking into account the phenotypes observed in animal models, one might expect defects in Rbfox networks to be associated with human diseases (John G. Conboy 2016). In fact, a gene co-expression network analysis of post mortem cerebral cortex from individuals with ASD identified *RBFOX1* as a hub gene in a neuronal module associated with ASD. Notably, reduced expression of *RBFOX1* in a subset of ASD patient brains was shown to correlate with altered splicing of its predicted target exons and massive splicing changes were detected in 48 ASD-susceptibility genes (Irina Voineagu, 2011). Furthermore, fluorescence *in situ* hybridization (FISH), array comparative genomic hybridization (aCGH) and genome-wide linkage studies (GWAS) have demonstrated that the *RBFOX1* gene is associated with ASD (Christa Lese Martin, 2007) and other neurodevelopmental and neuro-psychiatric disorders such as mental retardation and epilepsy (Kavita Bhalla, 2004; Fady M. Mikhail, 2011; Richard F. Wintle, 2011), attention deficit hyperactivity disorder (J. Elia, 2010), bipolar disorder and schizophrenia (H. Le-Niculescu, 2009).

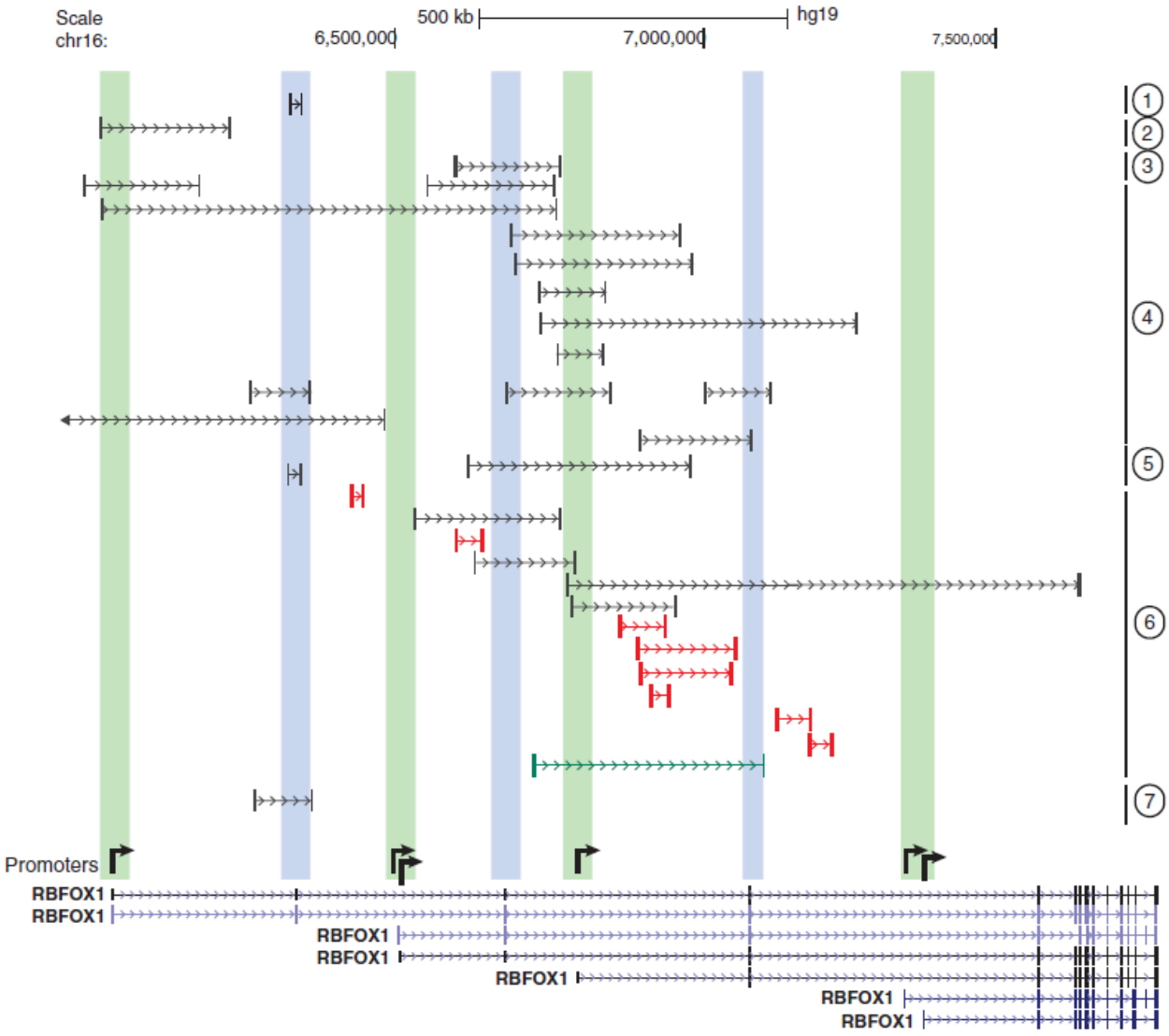

Figure 4. *RBFOX1* deletions associated with neurodevelopmental disorders in humans. At the bottom part of the image, below the Rbfox1 annotations are arrows depicting presumed promoter locations. Green bars indicate deletions that span promoters; blue bars indicate deletions that span internal exons likely to be translated; red lines indicate deletions apparently in introns only. Numbers at the right margin indicate the relevant citations for deletions as follows: (group 1, L. K. Davis, 2012); (group 2, Jonathan Sebat, 2007); (group 3, Natalie M. Gallant, 2011); (group 4, Dennis Lal, 2015); (group 5; Dennis Lal, 2013); (group 6, Wei-Wei Zhao, 2013); (group 7, Manuela Fanciulli, 2014). (Adopted from John G. Conboy 2016).

Several studies associated mutations in *RBFOX1* with ASD. A study in two different patients, one with mental retardation and the second one with epilepsy, showed two *de novo* chromosome 16 translocations disrupting the *RBFOX1* gene. The patient with mental retardation showed a translocation between chromosome 1 and 16, t(1:16), and the patient with epilepsy had a translocation with three different breakpoints t(14:16)(q32;p13.3) inv 16(p13.3 p12.1) (Kavita Bhalla, 2004).

A cytogenetic and FISH study of the *RBFOX1* gene identified a balanced *de novo* translocation between the short arms of the chromosome 15 and 16 in a female patient with autism, epilepsy and general developmental delay, along with a small deletion spanning exon 1 and intron 1 of the *RBFOX1* gene (Christa Lese Martin, 2007).

A study performed in 8 patients with different neurodevelopmental disorders, using array CGH, identified a patient carrying a 353 kb intragenic deletion in the *RBFOX1* gene, encompassing two exons, exons 3 and 4 (Fady M. Mikhail, 2011).

Another study was able to identify 12 out of 14 patients carrying deletions/duplications in the *RBFOX1* gene with all 14 patients presenting neurodevelopmental or neuropsychiatric disorders (Wei-Wei Zhao, 2013).

A study conducted in patients with developmental coordination disorder, a disorder often co-occurring with ASD, attention-deficit hyperactivity disorder (ADHD), intellectual disability or schizophrenia, identified a patient with a 300 kb deletion in the *RBFOX1* gene (Stephen J. Mosca, 2016).

1.2.1.2 The *Rbfox1* gene

RBFOX1 is encoded by an extremely large gene (1.7 Mb of DNA in human and 1.5 Mb in mouse), which is located on human chromosome 16p13.2 (Figure 5).

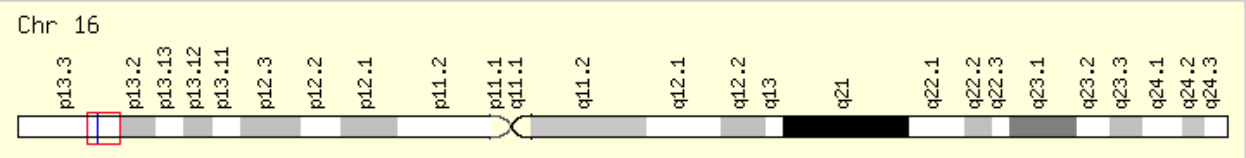

Figure 5. Genomic location of the *RBFOX1* gene in human. *RBFOX1* cytogenetic locus is showed with a red box. Chromosomal bands drawn according to Ensembl and locations according to GeneLoc. (Image adopted from www.genecards.org).

The murine *Rbfox1* gene is expressed in all brain regions that are also affected in human ASD patients. Moreover, the 5' region of the human *RBFOX1* gene is conserved in the mouse (Jason G. Underwood, 2005; Elizabeth A.D. Hammock, 2011). *Rbfox1* has multiple transcription start sites at alternative first exons spanning approximately 1.3 mb (Andrey Damianov, 2010). This is often described as the '5 UTR', however, it contains three different exons, of 63, 48, and 42 nucleotides, that are conserved in human but not in mouse. Notably, these exons maintain an open reading frame, that in principle can be translated into RBFOX1 proteins with alternative N-terminal domains (transcript classes Ib and II in Figure 6) (John G. Conboy 2016). In the downstream coding region of the gene, alternative splicing events produce a diversity of proteins by modulating inclusion of exons, and generating active vs inactive RRM domains, brain and muscle-specific protein isoforms, (Shingo Nakahata, 2005) and also exons that change the C-terminal reading frame, expressing or not the nuclear localization signal ((John G. Conboy 2016; Hidehito Kuroyanagi, 2009).

The alternative 3' end, which is also highly conserved in mammals, can encode two additional C-termini (John G. Conboy 2016). All together these transcriptional and posttranscriptional processes span the family of the RBFOX1 protein isoforms summarized in Figure 6.

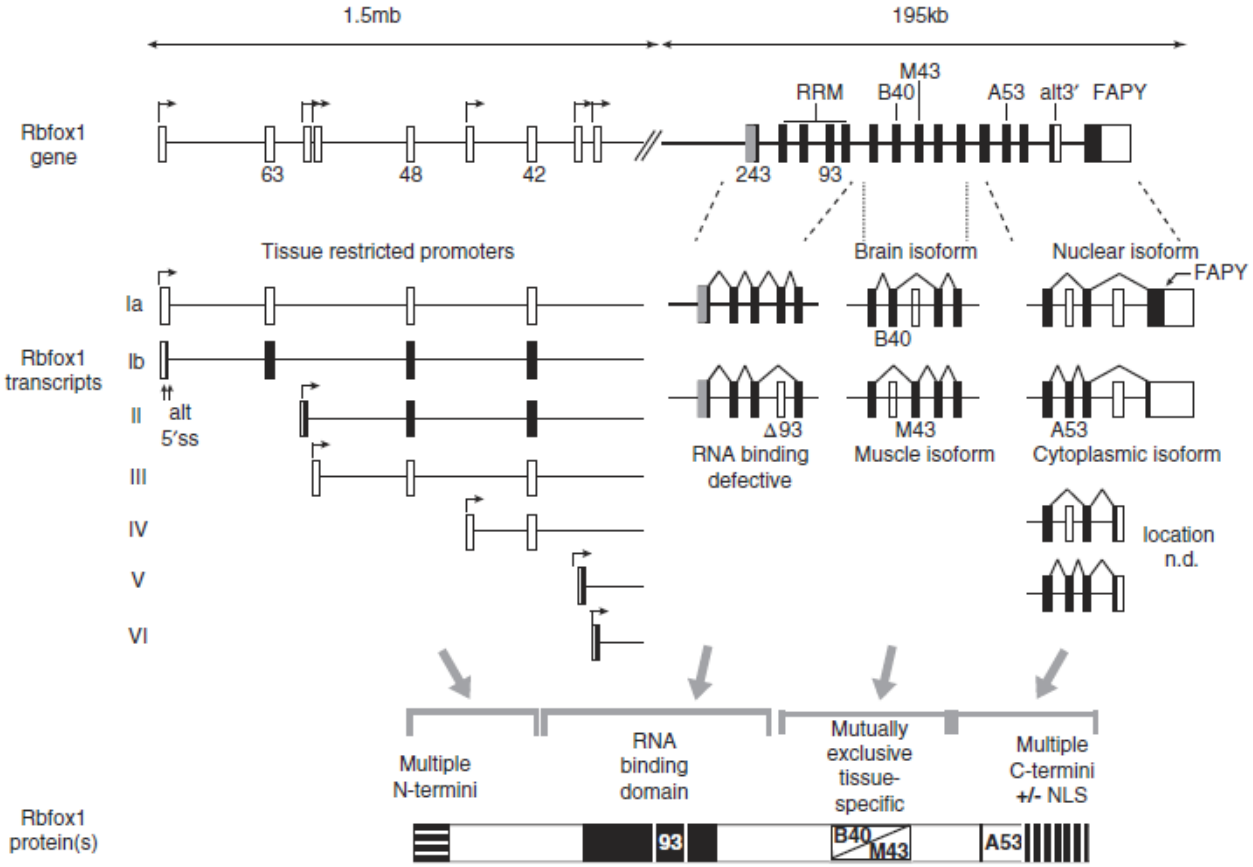

Figure 6. *Rbfox1* gene architecture and proteins. In the long 5' region, multiple promoters driving *Rbfox1* expression provide several independent proteins. In the RRM region, the 93 nucleotides exon is deleted to generate isoforms with non-functional RRMs. Mutually exclusive exons B40 and M43 are differentially spliced to generate tissue-specific protein isoforms. In the 3' region, inclusion of exon A53, designated as exon 19 in mouse, shifts the translational reading frame of the downstream exons and results in loss of the NLS. Alternative C-terminal reading frames are generated by inclusion or exclusion of A53. n.d., not determined. White boxes indicate untranslated sequence; black boxes indicate translated sequences; grey boxes indicate alternative N-terminal sequences predicted by reading frame analysis (Adopted from John G. Conboy 2016).

1.2.1.3 Regulation of *Rbfox1* expression

Rbfox1 is transcriptionally regulated during development and differentiation of skeletal and cardiac muscle, as well as in various neuronal regions. Some of the promoters are tissue-specific but little is known concerning their regulation (Andrey Damianov 2010; Shingo Nakahata, 2005). Presumably the long 5'region is populated with multiple enhancers sensitive to developmental and environmental input. However, specific enhancers neither have been identified nor functionally studied yet (Andrey Damianov 2010).

Alternative splicing events within Rbfox1 pre-mRNAs are also subject to auto-regulation and/or cross-regulation. As described in some studies, (Andrey Damianov 2010) *Rbfox1* (and also *Rbfox2*) contains a 93 nucleotides exon encoding a part of the RRM domain. The introns flanking this exon contain UGCAUG motifs, which can be bound by all three mammalian Rbfox paralogs inducing exon skipping. This skipping event leads to the synthesis of a dominant negative RBFOX1 isoform that cannot bind RNA (FoxΔRRM) but antagonizes splicing enhancer activity of the full length protein (Andrey Damianov 2010).

In addition, the alternative 3' terminal exon in *Rbfox1* has a highly conserved UGCAUG located upstream, which makes it a good for auto-regulation (Andrey Damianov 2010).

Other studies identified an environmentally-responsive splicing switch, involving the A53 exon, where extracellular stimuli, such as depolarization or CaM kinase signaling, lead to changes in the relative rate of nuclear/cytoplasmic isoforms of RBFOX1. Neuronal depolarization induces repression of exon A53 splicing, therefore increasing the nuclear RBFOX1. (Ji-Ann Lee, 2009; Shingo Nakahata, 2005).

Some existing evidence of an additional 'post-splicing' regulation at which the availability of the RBFOX1 protein level can be modulated are known. Recent discoveries, supported by behavioral, molecular, cellular, and genetic data suggest that miR-980 represses *Rbfox1* expression via interaction with 3' UTR motifs, and may trigger downstream changes in Rbfox1-regulated splicing networks to impact specific memory phenotypes. Additionally, there is also evidence that Rbfox1 mRNA can be regulated via other RNA binding proteins **l**arge **a**ssembly of **s**plicing **r**egulators (LASR). In this complex Rbfox can be recruited to RNA indirectly, for example through the binding of other components including hnRNP M proteins (heterogeneous nuclear ribonucleoproteins), which allow the cross-link to RNA and exhibit splicing enhancer activity in the absence of UGCAUG motifs (Andrey Damianov 2016; Tugba Guven-Ozkan, 2016).

1.2.1.4 RBFOX1 transcript isoforms

As previously mentioned, the *Rbfox1* gene, via alternative promoter and alternative pre-mRNA splicing, encodes multiple protein isoforms with different subcellular localization and different affinities to interact with regulatory co-factors.

Four different RBFOX1 transcript isoforms have been described: (named after their first exon) the neuron specific isoforms 1B, 1C and 1D and the heart and muscle specific isoform 1E (Andrey Daminanov, 2010).

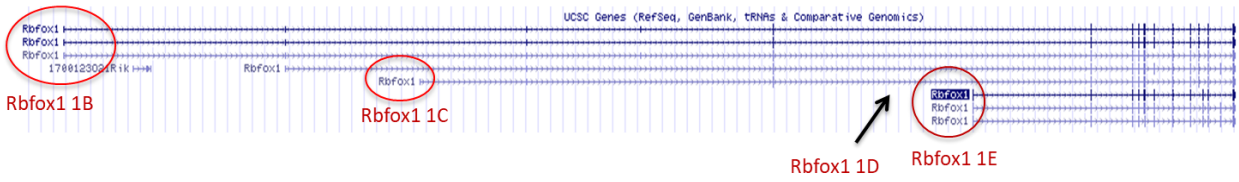

Figure 7. Scheme of the mouse RBFOX1 transcript isoforms. RBFOX1 1B, RBFOX1 1C and RBFOX1 1E are encircled in red. RBFOX1 1D is the putative RBFOX1 transcript (Andrey Damianov, 2010). RBFOX1 1B, RBFOX1 1C and RBFOX1 1D are brain-specific, whereasRBFOX1 1E is expressed in heart and muscle. (Modified from UCSC Genome browser).

The skipping of the mouse exon 19 (human A53) generates an Rbfox1 mRNA encoding for a protein with a NLS in the C terminus, expressed in the nucleus. In contrast, the inclusion of the mouse exon 19 (human A53) encodes for an RBFOX1 protein lacking of a NLS that localizes in the cytoplasm. Therefore, the primary structures of the nuclear and cytoplasmic isoforms are different in their C' termini.

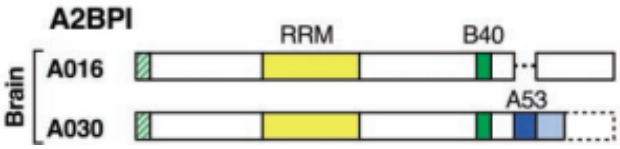

Figure 8. Scheme of the brain-specific *RBFOX1* isoforms. RBFOX1 (A016), skipped A53 exon, therefore it has de nuclear localization. RBFOX1 (A030), has the A53 exon, which causes a shift in the translational reading frame of the downstream exons resulting in a loss of the NLS and therefore presenting a cytoplasmic localization. (Adopted from Shingo Nakahata, 2005).

1.2.1.5 The RBFOX1 protein

Several *in vivo* and *in vitro* studies have been carried out to understand the brain specific functions of RBFOX1. Since neuronal migration is essential for corticogenesis, the role of the two different RBFOX1 isoforms has been examined during mouse corticogenesis *in vivo* and in *in vitro* (Nanako Hamada, 2016; Ji-Ann Lee, 2016; Nanako Hamada, 2015).

A study of the nuclear RBFOX1 isoform demonstrated an essential role of this protein during corticogenesis (A2BP1-A016). A knockdown of the nuclear RBFOX1 isoform, carried out via *in utero* electroporation, resulted in defects in radial migration and terminal translocation of cortical neurons, due to an impaired nucleokinesis (Nanako Hamada, 2016). Additionally, changes in the synapse network formation and regulation of axon growth and dendritic arborization were observed (Nanako Hamada, 2016).

In the same study, electrophysiology analysis of the nuclear RBFOX1-deficient neurons was carried out, showing, significant defects in cell membrane and synaptic properties, suggesting an essential role of the nuclear RBFOX1 in synapse functions. All together, these results concluded that an impairment of the nuclear RBFOX1 function may induce both, structural and functional defects in the cerebral cortex (Nanako Hamada, 2016).

A similar study was conducted analyzing the function of the cytoplasmic RBFOX1 (A2BP1-A030) *in vivo*, showing defects in radial migration, terminal translocation of the cortical neurons, axon elongation to the contralateral cortex, and dendritic arborization formation during corticogenesis. These results showed a functional impairment of the cytoskeleton system in the RBFOX1-deficient neurons, suggesting that cytoplasmic RBFOX1 serves as a regulator for spine

morphology and dynamics, while appeared not to be involved in neuronal proliferation (Nanako Hamada, 2015).

Remarkably, the phenotypes observed in neuronal migration and morphology comparing these two studies, were similar, but not identical (Nanako Hamada, 2015; Nanako Hamada, 2016).

Other studies in which both nuclear and cytoplasmic isoforms were knocked out (KO) have been carried out (Lauren T Gehman, 2011; Ji-Ann Lee, 2016). Interestingly, *Rbfox1* KO mice showed susceptibility to seizures, increased neuronal excitability in the dentate gyrus and altered synaptic transmission, but did not show any evident morphological alterations in the cerebral cortex. Nevertheless, an increased expression of *Rbfox2* was observed, probably compensating for the loss of Rbfox1, whereas the expression of *Rbfox2* in the nuclear *Rbfox1* knockdown was comparable to the controls, a fact that may be due to a compensatory effect avoidance in the RNAi (Hamada N., 2016).

1.2.1.5.1 Splicing functions of the RBFOX1 protein

The main studied function of RBFOX1 is the splicing activity through the binding to the UGCAUG motifs. Alternative splicing has a crucial role in the generation of biological complexity, and its misregulation is often involved in human disease (John G. Conboy, 2016).

UGCAUG motifs are highly enriched and evolutionarily conserved in proximal introns within 200–300 nucleotides of tissue-specific alternative exons, but are less common/conserved near non-tissue-specific alternative exons and constitutive exons. As mentioned before, genome-wide mapping of RBFOX1 binding sites in the brain transcriptome have revealed approximately 1059 direct RBFOX1 target alternative splicing events, half of which show dynamic changes during

brain development. These data suggest a major role of RBFOX1 in the splicing program (John G. Conboy, 2016).

Generally, RBFOX1 motifs located downstream of the alternatively-spliced exon, enhances splicing, leading to the inclusion of the exon, while motifs located upstream, tend to inhibit splicing. This conclusion is supported by bioinformatics studies (Yoseph Barash, 2010; Sebastien M. Weyn-Vanhentenryck, 2014) and experimental data as well (Yui Jin, 2003). Nevertheless, the exact molecular mechanisms for position-dependent effects on exon splicing are not well understood yet (John G. Conboy, 2016).

Approximately between 10^5 - 10^6 UGCAUG hexamers reside in the human transcriptome, however, not all of them are functional. Functional sites tend to reside in highly conserved regions with specific sequences and folding in specific secondary structures, indicating that the neighborhood matters (Andrey Damianov, 2016).

A study documenting the coordination between RBFOX1 and SUP-12 in the splicing regulation occurs in the fibroblast growth factor receptor pre-mRNA in C. *elegans*, concluding that co-regulation of tissue-specific splicing, through cooperative binding of multiple factors, provides a greater regulatory flexibility than would have a simple interaction of RBFOX1 alone with its motifs. (Hidehito Kuroyanagi, 2007).

Co-regulatory networks involving RBFOX1 proteins in tissue-specific splicing, have been characterized in mammalian tissues as well (Chaolin Zhang 2010). A study performed in mouse brain, concluded that about 15% of the exons in the NOVA-regulated splicing network have UGCAUG motifs in the flanking introns. Additionally, experimental analysis confirmed that NOVA and RBFOX1 synergistically regulate Gabgr2 exon 9 (Chaolin Zhang 2010).

Another study performed with the human embryonic muscle cell line HFN, showed a co-regulatory network of splicing events sharing control between RBFOX1 and MBNL1 (Roscoe Klinck, 2014).

All of these studies concluded that RBFOX1 can either synergize with or antagonize activity of the co-regulators, providing considerable flexibility to the networks (John G. Conboy, 2016).

1.2.1.5.2 Non-splicing functions of the RBFOX1 protein

Pre-mRNA splicing is the main studied function of the RBFOX1 protein, but recent work has shown that RBFOX1 is involved in other RNA regulatory processes.

The discovery of the cytoplasmic RBFOX1 isoform and the strong enrichment of UGCAUG motifs in 3' UTRs of transcripts, suggested that RBFOX1 protein may have non-splicing functions (John G. Conboy, 2016). Recently, a regulation in the processing of some microRNA in the nucleus has been reported to go through RBFOX1 (Kee K. Kim, 2014; (Yu Chen, 2016).

One study identified transcriptome-wide targets of RBFOX3 in neuronally differentiated P19 cells and mouse brain using Photoactivatable-Ribonucleoside-Enhanced Crosslinking and Immunoprecipitation (PAR-CLIP). PAR-CLIP analysis revealed diverse RBFOX3 targets including primary-microRNAs (pri-miRNAs) which lack the UGCAUG motif. RBFOX3 was shown to positively regulate processing pre-miR-15a, while negatively regulating other pre-miRNA processing events, for example pre-miR-485. (Kee K. Kim, 2014). Selected isoforms of RBFOX1 and RBFOX2 exhibited similar regulation of these two representative pre-miRNAs when exogenously expressed in P19 cells, although with a weaker activity than Rbfox3.

Another study focused on two miRNAs, miR-20b and miR-107, which contain essential GCAUG motifs in the terminal loops of their primary transcripts (Yu Chen, 2016). The binding of these miRNA to RBFOX1 and RBFOX2 was shown to inhibit processing of the pri-microRNAs to pre-microRNAs, reduce expression of the mature microRNAs, and increase expression of targets which would normally be downregulated by these microRNAs.

These studies showed that Rbfox family members are involved in different physiological events, like regulation of miRNA biogenesis (John G. Conboy, 2016).

It is also well documented that the cytoplasmic RBFOX1 isoform regulates mRNA stability of developmentally important genes, from Drosophila to human (Arnaldo Carreira-Rosario, 2016; Ji-Ann Lee, 2016; John G. Conboy, 2016).

A study performed in Drosophila, analyzing the effects of an isoform-specific knockdown and their subsequent rescue experiments, showed that mRNAs with GCAUG motifs in their 3'UTR, including transcripts encoding the RBP Pumilio, are targets of repression by the cytoplasmic but not the nuclear Rbfox1 protein (Arnaldo Carreira-Rosario, 2016).

More recently, functional studies of the different RBFOX1 transcript isoforms in mouse hippocampal neurons implicated cytoplasmic RBFOX1 isoform in regulating expression of synaptic and autism-related genes through effects on mRNA abundance. A study of the nuclear and cytoplasmic RBFOX1 function was performed, where total *Rbfox1* was knocked down, and rescued the phenotype either with the nuclear or the cytoplasmic RBFOX1. Notably, a rescue in the splicing changes was observed with the nuclear RBFOX1, whereas a rescue in mRNA levels was observed only with the cytoplasmic RBFOX1 (Ji-Ann Lee, 2016). A difference between where the different isoforms were bound was also observed. The nuclear RBFOX1 protein isoform was

predominantly bound to introns in nascent RNA, while the cytoplasmic form was observed more predominantly in the 3'UTRs, indicating that in addition to regulating alternative splicing, RBFOX1 regulates mRNA and protein abundance. These results suggested that this regulation occurs by direct RNA binding to (U) GCAUG sites in the 3' UTR, highlighting the importance of cytoplasmic RNA metabolism for cortical development (Ji-Ann Lee, 2016).

1.3 Candidate transcription factors

One of the main goals of this thesis was to identify transcription factors that regulate *Rbfox1* expression. The candidate transcription factors belong to the basic Helix-Loop-Helix (bHLH) protein family. Proteins containing the bHLH motif are known to be involved in a diverse range of cellular processes including proliferation, differentiation and morphogenesis. bHLH proteins can bind DNA as homodimers, but heterodimerization with other bHLH proteins has been shown to dramatically increase DNA binding efficiency (Edward V. Prochownik, 1993).

1.3.1 The basic Helix-Loop-Helix (bHLH) protein family

The bHLH family is organized into seven functional classes according to expression, dimerization capability, and DNA-binding specificity (Mark Eben Massari, 2000).

The class I (also known as E-proteins) are related to the Drosophila daughterless gene. Humans express three of them: TCF4 (E2-2), TCF3 (E2A) and TCF12 (HEB), each of them encoding two major isoforms. E-proteins are widely expressed in different tissues and are able to form stable homo- and heterodimers with other bHLH proteins that bind to E-boxes with the consensus

sequence ‘CANNTG’ in genomic DNA. The class I bHLH proteins can heterodimerize with class II (ASCL1 and ATOH1), class V (ID proteins), and class VI (HES1) members of the bHLH family.

The Class II HLH proteins, which include members such as MyoD, myogenin, Atonal, NeuroD/BETA2, and the achaete-scute complex, show a tissue-restricted pattern of expression and are potent inducers of cell type specification (Nicolas Bertrand, 2002). With few exceptions, to efficiently bind DNA they must form homodimers and preferentially heterodimerize with the E proteins. Class I-class II heterodimers can bind both canonical and non-canonical E-box sites (Mark Eben Massari, 2000).

Class III HLH proteins include the Myc family of transcription factors, TFE3, SREBP-1, and the microphthalmia-associated transcription factor, Mi. Proteins of this class contain a Leucine Zipper(LZ) adjacent to the HLH motif.

Class IV HLH proteins define a family of molecules, including Mad, Max, and Mxi, which are capable of dimerizing with the Myc proteins or with one another.

Class V (ID proteins) and class VI (HES1) transcription factors are characterized by their inhibitory or repressive activities. The ID proteins are orthologous to the *Drosophila extramacrochaetae* protein and lack the basic region of the bHLH sequence, rendering them unable to bind DNA. They heterodimerize with E-proteins and sequester them into inactive complexes that limit their availability for class II transcription factors. In conclusion, ID proteins inhibit the activity of the bHLH transcription factor network, affecting cell proliferation and differentiation. The hairy and enhancer of split (HES) proteins are unique as they contain a proline residue in their basic region. This unique structure enables them to bind N-boxes (consensus sequence ‘CACNAG’) rather than

E-boxes. They also heterodimerize with class I factors and repress their transcriptional activity. HES proteins play a central role in maintaining progenitor cells in an undifferentiated state.

Finally, the class VII proteins contain Per–ARNT–Sim (PAS) domains that sense oxygen tension, redox potential, light, and some other stimuli (Mark P. Forrest, 2014).

1.3.2 c-MYC (Mouse myelocytomatosis oncogene)

c-Myc encodes for a nuclear protein, MYC, that acts as a key regulator of mammalian cell proliferation and apoptosis. This transcription factor belongs to the helix-loop-helix/ leucine zipper (HLH/LZ) family (Class III) of proteins. It has been shown that high expression levels of *c-Myc* often correlate with cell proliferation and apoptosis, and manipulation of c-MYC function strongly affects both processes in a large number of experimental systems (Bruno Amati, 1994).

C-MYC must heterodimerize with MAX to accomplish its functions as a transcription factor. This specific heterodimerization occurs through the b-HLH-LZ domains and acts as an activator of the transcription (Marie-Eve Beaulieu, 2012). Together with its heterodimeric partner MAX, c-MYC binds to the E-box sequence CACGTG and CACATG elements (Laurie Desbarats, 1996; A .J. Walhout, 1998; F. Fisher, 1993).

One study found that homo- and heterodimeric complexes of these proteins bind to the CACGTG sequence in free DNA with similar affinities, however they demonstrated that MAX-MAX homodimers and c-MYC-MAX heterodimers can activate transcription, but on the contrary, c-MYC homodimers are biologically inactive (Daniel S. Wechsler, 1994; Bruno Amati, 1994).

1.3.3 MAX (MYC Associated Factor X)

In contrast to c-MYC, the transcription factor MAX, is capable of forming homodimers or heterodimers with related proteins, like MAD proteins, MXI-1, MNT and ROX, which function as antagonists of c-MYC. Together with c-MYC and MAX, these proteins form the group of bHLH-LZ. It is believed that MAX is the main protein of this group of transcription factors and via dimerization with other members facilitates the formation of complexes with different physiological effects. MAX-MAX homodimers bind to the same DNA elements as MYC-MAX heterodimers but fail to activate transcription. Thereby, MAX homodimers are transcription repressors in a passive manner (Laurie Desbarats, 1996). It has been shown that several c-MYC responsive genes contain E-box elements for c-MYC-MAX binding at relatively distal position downstream of the transcription start site. Furthermore, the elements bound by c-MYC-MAX are often found in pairs and bound to E-box sequences CACGTG and CACATG (A. J. Walhout, 1998; G. J. Kato, 1992).

1.3.4 MYCN (v-myc myelocytomatosis viral related oncogene, neuroblastoma derived)

MYCN is one member of a family of oncogenic transcription factors that also include c-MYC and MYCL. These proteins bind DNA in a sequence specific manner in order to regulate normal growth and differentiation during development (Derek M. Murphy, 2009).

High level genomic amplification of the *MYCN* gene occurs in approximately 20 to 25% of neuroblastoma (NB), a highly genetically heterogeneous childhood cancer derived from precursor cells of the sympathetic nervous system. *MYCN* amplification is the single most

important prognostic indicator of poor clinical outcome. Patients with *MYCN* amplified neuroblastoma tumors have less than a 30% chance of 5-year survival (Garrett M. Brodeur, 1984).

Using a MYCN ChIP-chip studies on NB cell lines it was possible to identify the E-box DNA sequence CATGTG motif as the predominant binding site for MYCN. This study was performed using a set of microarrays containing all annotated human gene promoter regions, as well as a custom tiling array covering selected miRNA loci and intergenic regions (Derek M. Murphy, 2009).

1.3.5 NEUROD2 (Neurogenic differentiation factor 2)

The NEUROD2 transcription factor belongs to the neuronal class II bHLH family of transcription factors, and regulates neuronal differentiation upon binding to an E-box motif defined as CANNTG. Some genome-wide studies have shown a preference of NEUROD2 to CATCTG (Efil Bayam, 2015) and CAGATG over CAGCTG (Abraham P. Fong, 2012).

NeuroD2 is expressed within a wide temporal window (from embryonic day 10.5 throughout adulthood) outside of the proliferative zones and constitutes a potential regulator of critical aspects of differentiation and/or maintenance of different types of cortical excitatory neurons.

On one hand, several studies investigating the consequences of NEUROD2 loss-of-function in mice, have demonstrated that NEUROD2 is required for commissural axon pathfinding of layer II/III callosal projection neurons, formation of cortical somatosensory maps within layer IV granular neurons and maturation of dendrites and synapses in the hippocampus (Gulayse Ince-Dunn, 2006).

On the other hand, studies investigating a NEUROD2 gain-of-function have demonstrated that misexpression of NeuroD2 in ventral telencephalon progenitors is sufficient to prevent their

normal GABAergic differentiation (Laurent Roybon, 2010). Although, NeuroD2 controls the execution of a wide range of functions during development, its target genes during cortex development are largely unknown. A genome-wide ChIP-seq study of *NeuroD2* targets during mid-embryogenesis (E14.5) identified a large number of genes with prominent roles in radial migration, layer-specific differentiation and axon pathfinding. Amongst all the target genes identified, multiple putative NEUROD2 binding sites were identified in the 5'UTR and intronic regions of *Rbfox1* (Efil Bayam, 2015).

1.3.6 KLF7 (Krüppel Like Factor 7)

Given its broad, low-level expression in adult tissues, Krüppel-like factor 7 (KLF7) was initially termed ubiquitous Krüppel-like factor (UKLF), nonetheless, this transcription factor is unique since its expression is strictly restricted within the nervous system during development and peripheral nervous system, being strongly active in postmitotic neuroblasts of the developing nervous system.

KLF7 belongs to the large family of KLF transcription factors, which comprises at least 17 members. Krüppel-like factors are defined by their conserved C-terminal DNA-binding domains, each consisting of three Cys2His2 type of zinc fingers, which recognize G-rich sequences such as CCCCGCCCC (Lei Lei, 2001).

KLF7 is required for neuronal morphogenesis and axon guidance in selected regions of the nervous system, including hippocampus, olfactory bulbs and cortex, as well as in neuronal cell cultures (Massimiliano Caiazzo, 2010; Massimiliano Caiazzo, 2011). Loss of *Klf7* in mice leads to neonatal lethality, with 98.5% of pups dying within 3 days of birth. *Klf7* null mice have hypoplastic

olfactory bulbs, with defects of axonal projection in the olfactory and visual systems, cerebral cortex, and hippocampus, as well as abnormalities of dendritic organization (Friedrich Laub, 2005).

1.3.7 TCF4 (Transcription factor 4)

Transcription factor 4 (Tcf4 alias ITF2, E2-2, ME2 or SEF2) is a conserved member of the basic helix–loop–helix (bHLH) family of transcription factors, binding to the consensus E-box DNA sequences CANNTG. It has been shown that TCF4 binds specifically to the DNA sequence CACCTG (Mari Sepp, 2011) and CAAGTG (Mari Sepp, 2012), which are also present in the *RBFOX1* promoter 1C region. *TCF4* was one of the first genes to reach genome-wide significance in large-scale genetic association studies of schizophrenia (Hreinn Stefansson, 2009) and is one of the most promising risk genes.

Very interesting is the fact that, common TCF4 variants are also associated with increased risk of Fuchs' corneal endothelial dystrophy (FECD) and primary sclerosing cholangitis (PSC), whereas rare TCF4 mutations cause Pitt–Hopkins syndrome (PTHS), a genetic disorder characterized by ID, distinctive facial features, developmental delay, and autonomic dysfunction (Marc P. Forrest, 2014).

Recently, a new role for TCF4 as a neuronal-activity-regulated transcription factor has been described, offering a novel perspective on the association of TCF4 with cognitive disorders. A TCF4-controlled transcription in primary cortical neurons was demonstrated to be induced by neuronal activity and protein kinase A, supporting the hypotheses that dysregulation of

neuronal-activity-dependent signaling plays a significant part in the etiology of neuropsychiatric and neurodevelopmental disorders (Mari Sepp, 2017).

In humans, *TCF4* is located on chromosome 18q21.2 and is predicted to encode at least 18 different proteins with unique N-terminal sequences (Mari Sepp, 2011). Several alternatively spliced *TCF4* variants have also been documented, expanding the potential repertoire of distinct TCF4 isoforms in humans. However, only two major TCF4 isoforms, TCF4-A and TCF4-B have been extensively studied.

Isoform TCF4-B is the full-length protein, and like the other E-proteins, has two activation domains (AD1 and AD2) that are thought to modulate transcriptional activity, and a nuclear localization signal (NLS) that controls subcellular localization.

In contrast, TCF4-A protein isoform lacks AD1 and the NLS, and is thought to traffic to the nucleus when heterodimerized with another bHLH transcription factor (Figure 12). The N-terminal region of the bHLH domain contains a highly conserved group of positively charged amino acids that make up the basic region that interacts with DNA (Mari Sepp, 2011).

TCF4, together with TCF3/E2A and TCF12/HEB, belongs to the family of E-proteins that are homologous to Drosophila protein Da (Daughterless). TCF4 is highly expressed in the nervous system and is known to heterodimerize with several bHLH transcription factors that play important roles in the development of the nervous system, e.g. ATOH1 (atonal homolog 1, alias MATH1), ASCL1 (achaete–scute complex homolog 1, alias MASH1), NEUROD1 (neurogenic differentiation 1, alias BETA2) and NEUROD2 (alias NDRF) (Mari Sepp, 2012).

Homozygous *Tcf4* knockout (*Tcf4*$^{-/-}$) mice die within 24 h of birth indicating that TCF4 is a crucial transcription factor required for normal developmental. *Tcf4*$^{-/-}$ mice have no important

anatomical defects; however, detailed analysis of their hindbrain has shown that these mice have disrupted pontine nucleus development. *Tcf4* deletion in mice causes a reduction in the number of neurons forming the pontine nucleus and an accumulation of ectopic neurons outside this region that fail to migrate to their correct location. Importantly, these deficits are highly specific to Tcf4, as the development of this hindbrain nucleus in other E-protein knockout mice (*Tcf3*$^{-/-}$ and *Tcf12*$^{-/-}$) is normal (Adriano Flora, 2007).

1.4 Purpose of the thesis

Neuropathological studies suggest that dysplasia of specific brain regions and defects in neurogenesis or in neuronal migration might cause ASD. Recently, the alternative splicing regulator *RBFOX1* has been identified as a hub in a neuronal module associated with ASD. The encoding gene contains a large noncoding part in its 5' end with four alternative promoters. These four promoters drive the expression of the different Rbfox1 transcripts, which differ in their 5'UTR but not in their coding exons. Rare deletions in the 5' region of the human *RBFOX1* gene were found in autism patients. The detected deletions include *RBFOX1* intronic sequences as well as isoform specific 5'UTR exons and likely interfere with transcriptional regulation of individual Rbfox1 transcript isoforms. However, the pathogenic potential of the respective deletions is still unclear. This is due to a lack of understanding of *RBFOX1* transcriptional regulation and of a suitable animal model. The mouse is a suitable system to study transcriptional regulation of *RBFOX1* because the 5'-region of the human *RBFOX1* gene is conserved in the mouse.

Based on this information, the main goal of this thesis was to study the complex regulatory mechanisms of *Rbfox1* expression. To this end, primary cortical neurons from E14.5 embryos and RNA from different brain sub-regions were isolated and subjected to various expression and functional analysis to investigate:

- The *Rbfox1* transcript-specific expression levels in the developing mouse brain, as well as in different brain regions of juvenile mice (6 weeks-old).
- The activity of the different brain-specific *Rbfox1* promoters via luciferase assays.
- Identification of transcription factors that drive the *Rbfox1* expression in cortical neurons.

2. Materials and Methods

2.1 Materials

2.1.1 Reagents

Table 1. Reagents used and their manufacturer.

	Manufacturer
Ethanol (100 %)	AppliChem, Darmstadt, Germany
Isopropanol	Roth, Karlsruhe , Germany
TRIzol	Thermo Fisher Scientific, Rockford, IL, USA
Chloroform	Roth, Karlsruhe , Germany
Elution buffer	Agilent Technologies, Waldbronn, Germany
RNA later	Thermo Fisher Scientific, Rockford, IL, USA
ABsolute qPCR ROX Mix	Thermo Fisher Scientific, Rockford, IL, USA
Universal ProbeLibrary	Roche Diagnostics GmbH, Indianapolis (USA)
SYBR®Premix Ex Taq™ II, ROX plus	Takara Clontech, Japan
6x DNA Loading Dye	Thermo Fisher Scientific, Rockford, IL, USA
Digoxygenin NT Mix	Roche Diagnostics GmbH, Indianapolis (USA)
STOP RNase inhibitor RX	5Prime, Hilden, Germany
RQ1 RNase-Free DNase	Promega GmbH, Germany
Glycogen	Roche Diagnostics GmbH, Indianapolis (USA)
Sodium Acetate	Roth, Karlsruhe , Germany
Xylol	Roth, Karlsruhe , Germany
Proteinase K, PCR grade	Roche Diagnostics GmbH, Indianapolis (USA)
Paraformaldehyde	Roth, Karlsruhe , Germany

Triethanolamin	Sigma-Aldrich, Munich, Germany
Formamide	Roth, Karlsruhe , Germany
Tris	Roth, Karlsruhe , Germany
Natrium Chloride	Roth, Karlsruhe , Germany
Disodium salt dehydrate p.A (EDTA)	Roth, Karlsruhe , Germany
SDS (Sodium dodecyl sulfate) ultra-pure	Roth, Karlsruhe , Germany
PBS Tablets	Gibco Life Technologies, Carlsbad, CA, USA
Tween® 20	Roth, Karlsruhe , Germany
Dextran sulfate	Sigma-Aldrich, Munich, Germany
Denhardt's Solution	Thermo Fisher Scientific, Rockford, IL, USA
Ribonucleic acid from baker's yeast	Sigma-Aldrich, Munich, Germany
Acetic Anhydride	Sigma-Aldrich, Munich, Germany
RNase A	Roche Diagnostics GmbH, Indianapolis (USA)
Sheep Serum	Sigma-Aldrich, Munich, Germany
Blocking reagent	Roche Diagnostics GmbH, Indianapolis (USA)
Anti-Digoxigenin AP	Roche Diagnostics GmbH, Indianapolis (USA)
Maleic Acid	SERVA Electrophoresis GmbH, Germany
NaOH lentils	Roth, Karlsruhe , Germany
Magnesium Chloride	Roth, Karlsruhe , Germany
HCl 32%	Roth, Karlsruhe , Germany
BM Purple	Roche Diagnostics GmbH, Indianapolis (USA)
Kaiser's Glycerol Gelatine	Merck KGaA, Darmstadt, Germany
Agarose	AppliChem, Darmstadt, Germany
GeneRuler™ 1 kb DNA Ladder	Thermo Fisher Scientific, Rockford, IL, USA
GeneRuler™ 100 bp DNA Ladder	Thermo Fisher Scientific, Rockford, IL, USA

10x Buffer T4 DNA Ligase with 10mA ATP	New England Biolabs GmbH, Frankfurt am Main, Germany
Agar-Agar	Roth, Karlsruhe , Germany
Ampicillin	AppliChem, Darmstadt, Germany
Yeast extract	Roth, Karlsruhe , Germany
Trypton	Roth, Karlsruhe , Germany
NEBuffer 3.1	New England Biolabs GmbH, Frankfurt am Main, Germany
CutSmart Buffer	New England Biolabs GmbH, Frankfurt am Main, Germany
Lipofectamine® 2000 Transfection Reagent	Thermo Fisher Scientific, Rockford, IL, USA
Lipofectamine® 3000 Transfection Reagent	Thermo Fisher Scientific, Rockford, IL, USA
Luciferase Assay Lysis Buffer (5x)	Promega GmbH, Germany
Water (Aqua ad iniectabilia)	B. Braun Biotech, Melsungen, Germany
Triton® X-100	Roth, Karlsruhe , Germany
gly2-Mercaptoethanol	Roth, Karlsruhe , Germany
Glycerin	Roth, Karlsruhe , Germany
HCl 37%	Roth, Karlsruhe , Germany
Magnesium sulfate	Roth, Karlsruhe , Germany
Luciferin	Sigma-Aldrich, Munich, Germany
Magnesiumacetat	Roth, Karlsruhe , Germany
Natriumcitrat	Roth, Karlsruhe , Germany
Millipore Wasser ELGA labwater classic	ELGA, Buckinghamshire (UK)
Ready-to-use Mouse Embryo Brain E.15 Paraffin Sections	ZYAGEN Labotaries, San Diego (USA)

5x siRNA Buffer	Dharmacon, GE healthcare, Buckinghamshire (UK)

2.1.2 Cell culture

Table 2. Reagents used in the cell culture and their manufacturer.

	Manufacturer
B27-Supplement with vitamin A	Gibco Life Technologies, Carlsbad, CA, USA
DMEM	Gibco Life Technologies, Carlsbad, CA, USA
DMEM high Glucose	Gibco Life Technologies, Carlsbad, CA, USA
DPBS	Gibco Life Technologies, Carlsbad, CA, USA
GlutaMAX™	Gibco Life Technologies, Carlsbad, CA, USA
Neurobasal® Medium	Gibco Life Technologies, Carlsbad, CA, USA
Poly-L-Ornithine	Sigma-Aldrich, Munich, Germany
Natural Mouse Laminin	Sigma-Aldrich, Munich, Germany
Trypsin-EDTA (0.05%), phenol red	Gibco Life Technologies, Carlsbad, CA, USA
FBS	Gibco Life Technologies, Carlsbad, CA, USA
Trypan blue	Roth, Karlsruhe, Germany
Opti-MEM® I Reduced Serum Medium	Gibco Life Technologies, Carlsbad, CA, USA

2.1.3 Solutions and Buffers

Table 3. Buffers and solutions used to prepare the self-made competent E.coli bacteria.

Table 3.1. Stock solutions for S.O.B medium.

	Stock	***grams***	***dH_2O***
NaCl	5 M	14.61	50 ml
$MgCl_2$	1 M	4.76	50 ml
$MgSO_4$	1 M	6	50 ml
NaOH	5 M	10	50 ml

Table 3.2. S.O.B medium.

	Volume (500 ml)
Trypton	10 g
Yeast	2.5 g
NaCl	1 ml
KCl (1M)	1.25 ml
$MgCl_2$	5 ml
dH_2O	to 500 ml; pH = 7 with 5 M NaOH
Autoclave	
$MgSO_4$	5 ml (added after autoclaving)
Store at 4ºC	

Table 3.3. Stock solution for Tfb I.

	Stock	***Grams***	***dH_2O***
KOAc	3 M	29.44	100 ml
KCl	3 M	22.37	100 ml
$CaCl_2$	1 M	11.1	100 ml

Table 3.4. Tfb I Buffer.

	Concentration	***Volume (200 ml)***
KaAC	**30 mM**	2 ml
$MnCl_2$	**50 mM**	1.97g
KCl	**100 mM**	6.6 ml
$CaCl_2$	**10 mM**	2 ml
Glycerin	**15%**	30 ml

Tfb1 Buffer was made up to 200 ml with Millipore H2O, adjusting the pH to 5.8 with 20% acetic acid. Tfb1 buffer was sterile-filtered and then stored at 4ºC

Table 3.5. Stock solution for Tfb II Buffer.

	Stock	***grams***	***dH_2O***	
NaMOPS	1 M	2.09	10 ml	pH = 7

Table 3.6. Tfb II Buffer.

	Concentration	***Volume (200 ml)***
NaMOPS	10 mM	2 ml
$CaCl_2$	75 mM	15 ml
KCl	10 mM	0.6 ml
Glycerin	15%	30 ml

Tfb II Buffer was prepared up to 200 ml with Millipore H2O. The buffer was sterile-filtered and stored at 4ºC afterwards.

Table 4. Media and solutions used in the cell culture and their composition.

Cell culture solutions	***Composition***
Primary cortical neurons culture medium	48 ml Neurobasal media 1ml B-27 supplement with vitamin A 500 µl GlutaMax
Primary cortical neurons STOP medium	DMEM high glucose 20% FBS

Table 5. Buffers and solutions used in the *in situ* hybridization experiment and their composition.

In sity hybridization	***Composition***
PFA	50ml of 20% Paraformaldehyde stock thawed at 70ºC + 200ml PBS/PBT
PBT	1L Milipore water 2 PBS tablets 1ml Tween20
Proteinase K solution	400µl Proteinase K stock solution in 200ml PBS *Proteinase K stock solution:* 10mg/ml in Millipore water.
TAE	3ml Triethanolamin 400µl Acetic Anhydride 197ml DEPC / Millipore water Mix strongly until well combined NOTE: Mix the solution directly in to the cuvette and mix using a very small fish. Add the Acetic Anhydride drop by drop.
Hyb-Mix (variant)	50% Formamid 10mM Tris 1M pH 7.5 600mM NaCl 1mM EDTA pH 8 0.25% SDS 10% Dextran Sulfat 1x Denhardt's

	200µg/ml yeast RNA (stored at -20)
TNE	2ml 0.5M EDTA (1mM) 100ml 5M NaCl (500mM) 10ml Tris 1M pH 7.5 (10mM) Add Millipore water up to 1000ml
RNAse solution	100µl RNAse stock solution in 200ml TNE *RNAse stock solution:* 10 mg/ml RNAse in Millipore water
Heat inactivated sheep serum	Incubate the sheep serum at 56ºC for 30 minutes (water bath). Aliquot them and store at -20
20x SSC	175.3g NaCl 88.2g Natrium Citrate Adjust pH 4.5 using HCl 1M Add Millipore water up to 1000ml
MABT	23.2g Maleic Acid 17.5g NaCl (150mM) 1800ml water Add 20-30 NaOH lentils (between 2 or 3 spoonful) →Shake until is combined →Adjust pH 7.5 using 10M NaOH or 32% HCl Add 10ml Tween20 (0.05%) Add Millipore water up to 2000ml
NTMT	4ml %M NaCl (100mM) 20ml 1M Tris pH 9.5 (100mM) 20ml 0.5M MgCl (50mM)

	2ml Tween20 Add Millipore water up to 200ml
1M Tris pH 7.5	60.5 g Tris add 400 ml Millipore water Adjust pH= 6.8 with HCl Add Millipore water up to 500 ml
1M Tris pH 9.5	60.5 g Tris add 400 ml Millipore water Adjust pH= 9.5 with HCl Add Millipore water up to 500 ml
10 % SDS	10 g SDS Up to 100 ml Millipore water and heat to 90ºC

Table 6. Buffers and solutions used in the in the luciferase assay and their composition.

Luciferase Assay	***Composition***
TRIS-P 100mM (stock solution)	0.61g TRIS 50ml Millipore water pH=7.8 with Phosphaic Acid
Magnesium Sulfate 100mM (stock solution)	0.6g $MgSO_4$ 50ml Millipore water
ATP 2mM (stock solution)	1g ATP 100mM 18.15ml Millipore water pH=7.8 with NaOH

Luciferin (stock solution)	10 mg Luciferin 33ml Millipore water
Firefly Luciferase reaction mix	25mM Tris-P pH 7.8 (12.5 ml of the Stock solution) 10mM $MgSO_4$ (5 ml of the Stock solution) 2mM ATP pH 7.5 (1 ml of the Stock solution) 50µM Luciferin (1 ml of the Stock solution) Add water up to 50ml (30.5ml)

Table 7. Buffers and solutions used and their composition.

Others	***Composition***
4 % PFA	4g of PFA in 100 ml of Millipore (60ºC) with 10 M NaOH and aliquot Store at -20 ° C
50x TAE Buffer	242 g Tris 18.6 g EDTA 57.1 ml Acetic acid (100 %) ad 1 L Millipore
2% Agarose gel	8g Agarose 400 ml 1x TAE Puffer heat up in the microwave until dissolved 6 µl EtBr
Agar plates	10g Trypton 5g yeast extract

	5g NaCl 15g Agar-Agar 1L Millipore water. Autoclave Add Ampicillin to a final concentration of 50µg/ml
LB medium (lysogenic broth)	10g Trypton 5g yeast extract 5g NaCl 1L Millipore water. Autoclave Add Ampicillin to a final concentration of 50µg/ml

2.1.4 Kits

Table 8. Kits used and their manufacturer.

	Manufacturer
High Pure RNA Isolation Kit	Roche Diagnostics GmbH, Indianapolis (USA)
RevertAid First Strand cDNA Synthesis Kit	Thermo Fisher Scientific, Rockford, IL USA)
High Pure PCR Product Purification Kit	Roche Diagnostics GmbH, Indianapolis (USA)
Agarose GelExtract Mini Kit	5Prime, Hilden (Germany)
EndoFree Plasmid Maxi Kit	Qiagen, Venlo (Netherlands)
MinElute Gel Extraction Kit	Qiagen, Venlo (Netherlands
Renilla Luciferase Assay System	Promega GmbH, Germany
QuikChange II XL Site-Directed Mutagenesis Kit	Agilent Technologies, Waldbronn, Germany
QuikChange Multi Site-Directed Mutagenesis Kit	Agilent Technologies, Waldbronn, Germany
P3 Primary Cell 4D-Nucleofector X Kit	Lonza BioResearch, Cologne GmbH, Germany

Qubit® Protein Assay Kit	Thermo Fisher Scientific, Rockford, IL, USA

2.1.5 Primers

All the primers used throughout the doctoral thesis were ordered via Sigma-Aldrich.

Table 9. Primers used in the *Rbfox1* expression analysis.

RT-qPCR primers	*Primer Sequence (5'-3')*	*Probe (Roche)*
Rbfox1 all transcripts-UPL_F	GACCCCTACCACCACACACT	19
Rbfox1 all transcripts-UPL_R	TCTTGGCATCGGTCAAGG	
Rbfox1-1B-UPL-F	GTTGCCTCTGGTGGATGCTG	68
Rbfox1-1B-UPL-R	TGAGCTGTTTCCTAGAACTCCTG	
Rbfox1-1C-UPL-F	CGGATCAGAATCCGGACCT	58
Rbfox1-1C-UPL-R	CTTTGATATCCTACCCTGTGTAA	
Rbfox1-1D-UPL-F	GCCTTGACTTTTATGTACTTACAGCAG	11
Rbfox1-1D-UPL-R	ATAAGGCTGAGCCATTGTGTC	
Gapdh-UPL-F	TGCTGAGTATGTCGTGGAGTCT	157
Gapdh-UPL-R	TTGGCTCCACCCTTCAAGT	

Table 10. Primers to generate the *Rbfox1* probes used in the *in situ* hybridization experiment.

PCR primers	***Primer Sequence (5'-3')***
Rbfox1_Probe_all transcripts_F	AGACCACTGTCCCTGACCAC
Rbfox1_Probe_all transcripts_R	CATTTGTCGGAGGTCTGGAT
Rbfox1_Probe_T1_F	TTAGGAGTGATCCGGACCTT
Rbfox1_Probe_T1_R	CTAGAACTCCTGGCGAGCTT
Sequencing primers	**Primer Sequence (5'-3')**
M13 forward	GTTTTCCCAGTCACGAC
M13 Reverse	CAGGAAACAGCTATGAC

Table 11. Primers to generate the wild type and the mutated *Rbfox1* promoters construct.

PCR primers	***Primer Sequence (5'-3')***
Rbfox1_Prom1_KpnI_F	ACTGGGTACCAGACGCCTGGCTCTTGATAA
Rbfox1_Prom1_HindIII_R	ACTGAAGCTTTCCTCCTGGATTCCTCAGTT
Rbfox1_Prom2_XhoI_F	ACTGCTCGAGTACCTCGTGGGGGATATGAA
Rbfox1_Prom2_ext_BglII_R	ACTGAGATCTCATCTTCTTTGCAAAATCCAG
Rbfox1_Prom4_XhoI_F	ACTGCTCGAGAGACTGTAGTTTTTTCCAGT
Rbfox1_Prom4_BglII_R	ACTGAGATCTCCGATTATCTAACTCACACA
Promoter1_c1658t_a1659t_R	TACTCAGGTCACACTACCATGAATTGCTTACATAGTTTGCACTG
Promoter 1_ c1658t_a1659t_F	CAGTGCAAACTATGTAAGCAATTCATGGTAGTGTGACCTGAGTA
Promoter1_c2865t_a2866t_R	GCTGTCCCCTCCAGAAACGAGCTGAGCGACTC
Promoter 1_c2865t_a2866t_F	GAGTCGCTCAGCTCGTTTCTGGAGGGGACAGC
Promoter1_c2378t_a2379t_R	GCGAGAAAAATGTGTGCATGAATGTGTGTGTCTCTCTGTG

Promoter1_c2378t_a2379t_F	CACAGAGAGACACACACATTCATGCACACATTTTTCTCGC
Promoter1_c2815t_a2816t_c2817t_R	CGCGAGGCGCACGCAAAGGTCCTGTGGCTGG
Promoter 1_c2815t_a2816t_c2817t_F	CCAGCCACAGGACCTTTGCGTGCGCCTCGCG
Promoter 2_c332t_a333t_F	CATCAGTTTGCTCACTTTCTTAGTGCTTGGCAAAGGGGGT
Promoter 2_c332t_a333t_R	ACCCCCTTTGCCAAGCACTAAGAAAGTGAGCAAACTGATG
Promoter 2_c194t_a195t_F	CATTGCTCCTGAGTTAAAATTGGTTGTTTAGTGAGGACTCTGG
Promoter 2_c194t_a195t_R	CCAGAGTCCTCACTAAACAACCAATTTTAACTCAGGAGCAATG
Promoter 2_c236t_a237t_F	GGGACTGTGCAAGGTGCCCTATTCTGTTTTGTGGTACATATTT
Promoter 2_c236t_a237t_R	AAATATGTACCACAAAACAGAATAGGGCACCTTGCACAGTCCC
Promoter 2_c564t_a565t_R	AGCCACCAGCAGGAATTCAAGGCCTTGAACAAGCGA
Promoter 2_c564t_a565t_F	TCGCTTGTTCAAGGCCTTGAATTCCTGCTGGTGGCT
Promoter 2_c652t_a653t_c654t_F	TAGAATCATTGGCATTGCTAGTTTGTGGGTACCATTCTCTGCTGC
Promoter2_c652t_a653t_c654t_R	GCAGCAGAGAATGGTACCCACAAACTAGCAATGCCAATGATTCTA
Promoter 2c278t_a279t_c280t_F	AAGAACAAGGGAAGAGATTTGTGCTGGGGGGGGGGTG
Promoter2_c278t_a279t_c280t_R	CACCCCCCCCCCAGCACAAATCTCTTCCCTTGTTCTT
Sequencing primers	**Primer Sequence (5'-3')**
pGL4_reverse	AATGTTTTTGGCATCTTCCA
Rbfox1_Prom1_forward_1	GTGCCAGAGATAGGGACCAC
Rbfox1_Prom1_forward_2	GAGAGGAGAGAAGGGAGGAAA
Rbfox1_Prom1_forward_3	CAAACCCACTTTGGGAAGAG
Rbfox1_Prom1_forward_4	CTCTTCTTATCGCGCCAGAC
Rbfox1_Prom1_reverse_1	TCTGCTATCCACAACCATCAA
Rbfox1_Prom1_reverse_2	CCCCCTTCCCTCTCTTTTCT
Rbfox1_Prom1_reverse_3	TTCCTAAAGTGCACAAGGGG
Rbfox1_Prom1_reverse_4	ACTCACTGGTGGTTTCTCGG

Rbfox1-Prom2-forward1	ACGTGGGTACCATTCTCTGC
Rbfox1-Prom2-reverse1	TCCTGCTCCCTCTCTTGCTA
RVprimer3	CTAGCAAAATAGGCTGTCCC
Rbfox1-Prom4-Forward-2	GCAAAGGACTCACAAAGCGT
Rbfox1-Prom4-Forward-3	TTACCCCTTGTGGGAATCAA
Rbfox1-Prom4-Forward-4	CCCAGCTGAGCAGTCTTGTT
Rbfox1-Prom4-Forward-5	TACTTCCCTGCCTCTCCAAG
Rbfox1-Prom4-Reverse-2	CACTTTGCAAACCCACTCCT
Rbfox1-Prom4-Reverse-3	TGGATTTCGTTAGTCTTTATGCAA
Rbfox1-Prom4-Reverse-4	TAAAATCCTTCGAGGGGAGG
Rbfox1-Prom4-Reverse-5	TCCTCCCTGGCTCTCCTC

Table 12. Primers used in the transcription factors knockdown experiments.

RT-qPCR primers	*Primer Sequence (5'-3')*
c-Myc qPCR Forward	GGACACGCTGACGAAAGTG
c-Myc qPCR Reverse	AGGCGAAGCAGCTCTATTTCT
NeuroD2 qPCR Forward	TCCTCTCTGAGGCACCATGCT
NeuroD2 qPCR Reverse	TGGCGAACTTGGGCACG
Klf7 qPCR Forward	ACAAGTGCTCATGGGAAGGA
Klf7 qPCR Reverse	CTGGAGAAACACCTGTCGCA
Mycn qPCR Forward	TGAGCGACTCAGATGATGAGG
Mycn qPCr Reverse	AGTGGTTACCGCCTTGTTGT
Max qPCR Forward	GGTTTCAATCTGCGGCTGAC
Max qPCR Reverse	CGGGATGCCTTCTCTCCTTG

Tcf4 qPCR Forward	GCAGGGATCTTGGGTCACAT
Tcf4 qPCR Reverse	GAGACTCTGCTGGTGGCAA
Bcas2 Forward	CAACCGATTGAATTACTCAGCA
Bcas2 Reverse	ACACATTCTTGCCATGCAGT

2.1.6 Vectors

Table 13. Vectors used in the course of the doctoral thesis and their manufacturer.

	Manufacturer
pGEM®-T Easy Vector System I	Promega GmbH, Germany
pGL4.10 [luc2]	Promega GmbH, Germany
pRL-TK	Promega GmbH, Germany

2.1.7 Bacteria

Table 14. Bacteria used and their manufacturer.

	Manufacturer
One Shot Top10 Chemically Competent E.coli	Thermo Fisher Scientific, Rockford, IL, USA
self-made competent E. coli	See Molecular Biology methods

2.1.8 Enzymes

Table 15. Enzymes used and their manufacturer.

	Manufacturer
SpeI-HF	New England Biolabs GmbH, Frankfurt am Main, Germany
SphI-HF	New England Biolabs GmbH, Frankfurt am Main, Germany
FastStart™ High Fidelity PCR System	Roche Diagnostics GmbH, Indianapolis (USA)
T4 DNA Ligase	New England Biolabs GmbH, Frankfurt am Main, Germany
SP6 RNA Polymerase	Roche Diagnostics GmbH, Indianapolis (USA)
T7 RNA Polymerase	Roche Diagnostics GmbH, Indianapolis (USA)
PrimeSTAR® GXL DNA Polymerase	Takara Clontech, Japan
KpnI-HF	New England Biolabs GmbH, Frankfurt am Main, Germany
HindIII-HF®	New England Biolabs GmbH, Frankfurt am Main, Germany
XhoI	New England Biolabs GmbH, Frankfurt am Main, Germany
Bgl II-HF	New England Biolabs GmbH, Frankfurt am Main, Germany
Taq DNA Polymerase	AXON Labortechnik, Kaiserslautern, Germany
EcoRI-HF®	New England Biolabs GmbH, Frankfurt am Main, Germany

2.1.9 Cells

Primary cortical neurons were used, as a cell model, for most of the experiments. They were always prepared fresh at the beginning of the experiment and cultured as described in the section Cell Biology methods. Neural precursor cells and P19 cells were also used for expression analysis.

2.1.10 Small interfering RNA

Table 16. Small interfering RNA (siRNA) used and their manufacturer.

ON-TARGETplus siRNA	*Manufacturer*
ON-TARGETplus Mouse Myc (17869) siRNA-SMARTpool	Dharmacon, GE healthcare, Buckinghamshire (UK)
ON-TARGETplus Mouse NeuroD2(18013) siRNA-SMARTpool	Dharmacon, GE healthcare, Buckinghamshire (UK)
ON-TARGETplus Mouse Klf7 (93691) siRNA-SMARTpool	Dharmacon, GE healthcare, Buckinghamshire (UK)
ON-TARGETplus Mouse Mycn (18109) siRNA-SMARTpool	Dharmacon, GE healthcare, Buckinghamshire (UK)
ON-TARGETplus Mouse Max (17187) siRNA-SMARTpool	Dharmacon, GE healthcare, Buckinghamshire (UK)
ON-TARGETplus Mouse Tcf4 (21413) siRNA-SMARTpool	Dharmacon, GE healthcare, Buckinghamshire (UK)
ON-TARGETplus Non-targeting siRNA-SMARTpool	Dharmacon, GE healthcare, Buckinghamshire (UK)

2.1.11 Mice

Table 17. Mice used to carry out the experiments and their origin.

	Origin
NMRI	Janvier Labs, Le Genest-Saint-Isle (France)
C57BL/6	Translational-Animal Research Center (TARC)

2.1.12 Consumables

Table 18. List of consumables used in the course of the doctoral thesis.

	Manufacturer
6-well cell culture plates	Greiner Bio-One, Frickenhausen, Germany
24-well cell culture plates	Greiner Bio-One, Frickenhausen, Germany
cell culture plates	Greiner Bio-One, Frickenhausen, Germany
Petri dishes	Greiner Bio-One, Frickenhausen,
Coverslips Menzel-Gläser 24x60mm	VWR, Darmstadt, Germany
15 ml Falcon	Greiner Bio-One, Frickenhausen, Germany
50 ml Falcon	Greiner Bio-One, Frickenhausen, Germany
qPCR plates	Thermo Scientific, UK
ABsolute^{TM} QPCR Seal	ThermoScientific, Massachusetts (USA)
Filter Tips 10 µl	StarLab, Hamburg, Germany
Filter Tips 20 µl,	StarLab, Hamburg, Germany
Filter Tips 200 µl	StarLab, Hamburg, Germany
Filter Tips 1000 µl	StarLab, Hamburg, Germany

Reaction tubes 5 ml	Eppendorf, Hamburg, Germany
Reaction tubes 2 ml	Eppendorf, Hamburg, Germany
Reaction tubes 1.5 ml	Eppendorf, Hamburg, Germany
Serological pipettes 25 ml	Greiner Bio-One, Frickenhausen, Germany
Serological pipettes 10 ml	Greiner Bio-One, Frickenhausen, Germany
Serological pipettes 5 ml	Greiner Bio-One, Frickenhausen, Germany
Serological pipettes 2.5 ml	Greiner Bio-One, Frickenhausen, Germany

2.1.13 Laboratory equipment

Table 19. Laboratory equipment and devices used in the course of the doctoral thesis.

Device	*Manufacturer*
Binocular SZH10 Research Stereo	Olympus, Japan
Microscope EVOS XL	Life Technologies, Carlsbad, CA, USA
Gel chamber PerfectBlue™ Gel System Mini L	VWR, Darmstadt, Germany
Gel chamber PerfectBlue™ Gel System Mini M	VWR, Darmstadt, Germany
Gel chamber PerfectBlue™ Gel System Mini S	VWR, Darmstadt, Germany
Thermoblock Thriller® 1,5ml	VWR, Darmstadt, Germany
Thermoblock, Thriller® 2,0ml	VWR, Darmstadt, Germany
Incubator Certomat®H Heater	B. Braun Biotech, Melsungen, Germany
Incubator Certomat®R Shaker	B. Braun Biotech, Melsungen, Germany
Inverted microscope, Axiovert 25	Zeiss, Oberkochen, Germany

Mini-Incubator INCU-Line	VWR, Darmstadt, Germany
Minicentrifuge neolab 3-Speed	NeoLab Migge Laborbedarf-Vertriebs GmbH, Heidelberg, Germany
NanoDrop 1000 Spectrophotometer	ThermoScientific, Massachusetts (USA)
Electrophoresis Power Supply peqlab EV215	VWR, Darmstadt, Germany
Slide warmer	VWR, Darmstadt, Germany
pH-meter Sartorius pH Meter PB-11	Sartorius AG, Göttingen, Germany
Pipette boy accu-jet®	Brand GmbH & CO KG, Wertheim , Germany
Qubit® 2.0 Fluorimeter	ThermoScientific, Massachusetts (USA)
Vortex REAX 2000	Heidolph Instruments, Schwabach, Germany
Roller Mixer SRT9D Stuart®	Bibby Scientific Limited, Staffordshire (UK)
Sterile bench hood, Heraeus, Herasafe	ThermoScientific, Massachusetts (USA)
Thermocycler Mastercycler Gradient	Eppendorf, Wesseling-Berzdorf, Germany
Thermocycler MJ Research PTC-200	Bio-Rad, Munich, Germany
Thermocycler Advanced Primus 96 Peqlab	PEQLAB, Erlangen, Germany
UV Transilluminator Intas Gel iX Imager	Intas-Science-Imaging Instruments GmbH, Göttingen, Germany
Scale Scout™ pro	Ohaus Europe GmbH, Nänikon , Switzerland
Water bath WNB 7	Memmert GmbH + Co. KG, Schwabach (DE)
Cell culture incubator CO2-Inkubator Serie CB	BINDER GmbH, Tuttlingen (DE)
Centrifuge Megafuge, Heraeus, 16R Centrifuge	ThermoScientific, Massachusetts (USA)
Centrifuge Microfuge® 16	Beckman Coulter GmbH, Krefeld, Germany

Centrifuge Peqlab PerfectSpin 24R Refrigerated	PEQLAB, Erlangen, Germany
Avanti J-26 XP Centrifuge	Beckman Coulter®
JLA-16.250 centifruge rotor	Beckman Coulter®
M220 Focused-Ultrasonicator	Covaris Inc., Massachusetts (USA)
4D-Nucleofector Core Unit	Lonza BioResearch, Cologne GmbH, Germany
4D-Nucleofector X Unit	Lonza BioResearch, Cologne GmbH, Germany
4D-Nucleofector Y Unit	Lonza BioResearch, Cologne GmbH, Germany
Nanodrop™ Spectrophotometer ND-1000	ThermoScientific, Massachusetts (USA)
Research® plus 100-1000 µl pipettes	Eppendorf, Hamburg (Gerrmany)
Research® plus 20-200 µl pipettes	Eppendorf, Hamburg (Gerrmany)
Research® plus 2-20 µl pipettes	Eppendorf, Hamburg (Gerrmany)
Research® plus 0.5–10 µL pipettes	Eppendorf, Hamburg (Gerrmany)
Centro XS^3 LB 960 Microplate Luminometer	Berthold Technologies GmbH & Co. KG, Bad Wildbad, (Germany)

2.1.14 Software and Databases

2.1.14.1 Programs

Table 20. Programs used and their manufacturer.

Program	*Manufacturer / Publication*
Serial Cloner 2.6	http://serialbasics.free.fr/Serial_Cloner.html
GraphPad Prism 7.00	GraphPad Software, San Diego, CA
Intas Science Imaging GDS 2013	www.intas.de

StepOne® Software v2.3	Life Technologies, Carlsbad, CA, USA
LinRegPCR: analysis of real-time PCR data	Version 7.5. Amsterdam, the Netherlands. Department of Anatomy and Embryology, Academic Medical Centre, 2004.

2.1.14.2 Online Tools

Table 21. Online tools and their URL.

	URL
Universal ProbeLibrary Assay Design Center	qpcr.probefinder.com
Bisearch	http://bisearch.enzim.hu/
Primer3	http://bioinfo.ut.ee/primer3-0.4.0/primer3/
Reverse complement	http://www.bioinformatics.org/sms/rev_comp.html
Ensembl Genome browser	http://www.ensembl.org/index.html
Double Digest Finder	https://www.neb.com/tools-and-resources/interactive-tools/double-digest-finder
GenePaint	www.genepaint.org
Allen Brain Atlas: Mouse Brain	mouse.brain-map.org
Addgene	www.addgene.org
Nucleotide	NCBI
QuikChange Primer Design	www.genomics.agilent.com
Pubmed	NCBI
UCSC Genome Browser	genome.ucsc.edu

2.2 Methods

2.2.1 Cell Biology methods

All the experiments carried out with eukaryotic cells were performed under sterile conditions. Incubation of the cells was carried out in the incubator at 37ºC and 8% CO_2 (see Laboratory equipment section).

2.2.1.1 Coating plates and cell culture dishes

To enable adhesion of the cells, plates and cell culture dishes were coated with both poly-L-ornithine and laminin (see Cell culture section).

Plates and dishes were filled with a sufficient amount of a 0.1 mg/ml poly-L-ornithine solution and incubated for 30 minutes at 37º C. Afterwards, they were washed three times with DPBS and a sufficient amount of 2.5 µg/ml laminin solution was added, incubated for 60 minutes at 37ºC and after washing 3 times with DPBS, they were ready to use. Alternatively, plates or dishes could be sealed with parafilm and stored at 4ºC until further use. Before seeding cells, the plates and dishes were washed three times with PBS and filled with the suitable medium, and stored in the incubator for proper equilibration until use.

2.2.1.2 Isolation of primary cortical neurons

Both, the expression analysis of the Rbfox1 transcripts and the transcription factor knockdown experiments were carried out using primary cortical neurons as a cell model. Primary cortical neurons were prepared freshly for each experiment, directly from the cerebral cortex of embryos at embryonic day 14.5.

Tubes and solutions for the mouse preparation

For the isolation of primary cortical neurons, either 6-well plates or 24-well plates were coated with L poly-Ornithine and natural mouse Laminin (see chapter 2.2.1.1).

Two 50 ml Falcons were filled with 70% EtOH for sterilization and DPBS for washing the utensils. In addition, three 50 ml Falcons were filled with DMEM. Two of them were kept at room temperature, while the third was stored on ice. In addition, trypsin-EDTA, stop medium, DMEM and freshly prepared culture medium were warmed up to 37ºC in a water bath before the preparation (see Table 3).

Mouse preparation

An E14.5 pregnant mouse was sacrificed by cervical dislocation. The abdominal region was first disinfected with 70% ethanol and dried gently with a tissue. A V-shape cut was done with scissors in the direction of the head. Mouse embryos were released by folding back the resulting skin flap. Embryos were carefully lifted from the belly cavity of the mother, the connection to the mother was severed and transferred to a petri dish filled with pre-heated DMEM. The yolk sac was opened and the embryos were removed and decapitated with scissors. The following steps were performed under a binocular. For each embryo, the brain was released by separating the face from the rear head with the help of two curved tweezers and opening up the cranium. The isolated brains were transferred to a petri dish with fresh DMEM. The hindbrain was dissected out from the rest of the brain and the two hemispheres were separated. Then the cerebral membranes were removed and the cortex was isolated and transferred into a Falcon filled with DMEM on ice (Figure 9).

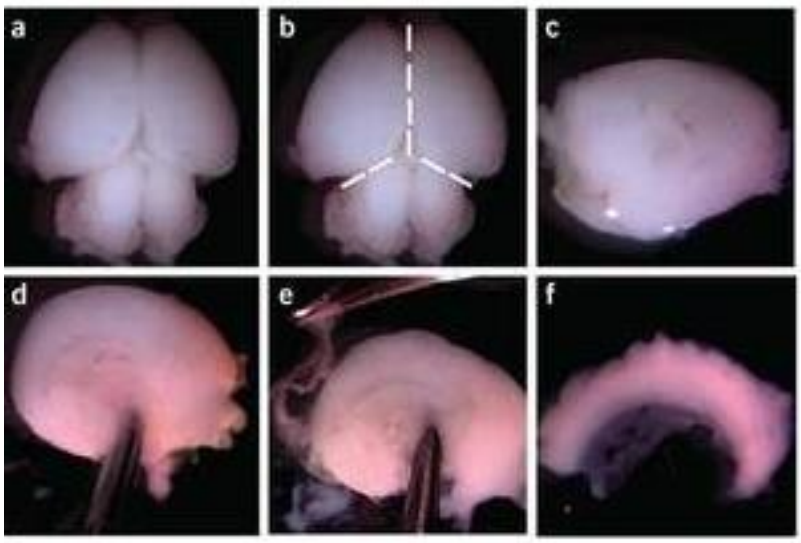

Figure 9. Steps for dissection of the cortex from the intact brain. (a) Place the brain dorsal side up in DMEM medium. (b) Separate the hindbrain region and make a sagittal incision to separate the two hemispheres. (c) Place each hemisphere's cortex side down and remove any noncortical forebrain. Tissue. (d) Hold the hemisphere in place using forceps. (e) Remove the meningeal tissue with another pair of forceps (f) Dissect out the cortex. (Adopted from www.nature.com).

Isolation of primary cortical neurons

Once all the cortices were isolated, DMEM was carefully aspirated from the 50 ml Falcon. Pre-heated trypsin-EDTA (0.5 ml per brain) was added and the cortices were incubated for exactly 6 minutes at 37ºC. The digestion was then stopped with 15 ml of stop medium (see Table 3) and the cell suspension was centrifuged for 3 minutes at 1000 rpm. The supernatant was discarded and the cell pellet was washed with 40 ml of DMEM and centrifuged again for 3 minutes at 1000rpm. This washing step was repeated a second time. DMEM was aspirated with suction and the cell pellet was carefully resuspended in 1 ml of culture medium (see Table 3). Then 4 ml of

culture medium were added and mixed with the cell suspension. Cells were counted (see section 2.2.1.3) and the suitable amount of cells was seeded in 24-well plates or 6-well plates. Primary cortical neurons were cultured at 37ºC and 8% CO_2.

2.2.1.3 Cell number determination

In order to seed a specific number of cells to be able reproduce an experiment under the same conditions, cells need to be counted. Cell number was determined using a Neubauer counting chamber (Figure 10). Cells were first detached from the culture dish with Trypsin-EDTA and resuspended in culture media, similar to the passaging (see section 2.2.1.5). To count them, 20 µl of the cell suspension were mixed with 40 µl of trypan blue. 10 µl of the mixture was then transferred to a Neubauer counting chamber. Cells in four small squares were counted (Figure 11) and the cell number was calculated according to the following formula:

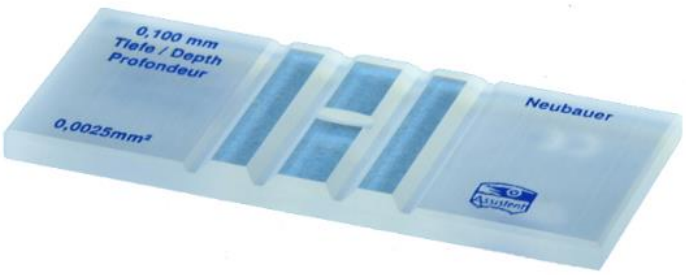

Figure 10. Neubauer chamber used to count the cells. (Adopted from www.laboratoryinfo.com)

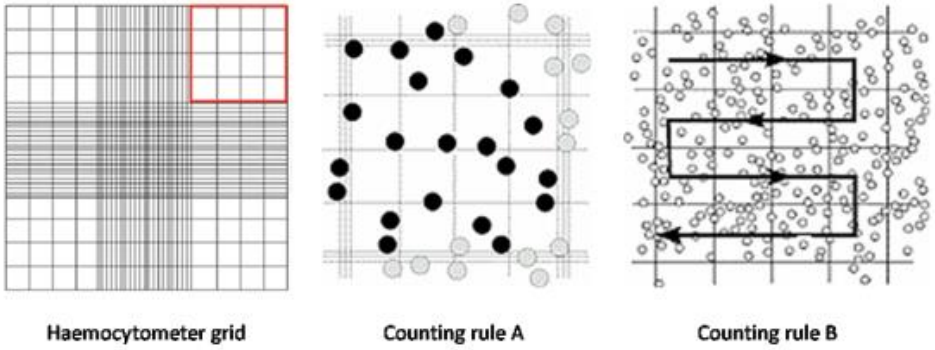

Figure 11. Scheme of how to use a Neubauer chamber to count the cells. (Modified from rnai-screening-wiki.dkfz.de).

According to the chemical formula c1 x V1 = c2 x V2 which determines the cell count/ml the following derivation results:

Counted cells x 2 (dilution factor) = cells in Eppendorf

(Cells in Eppendorf x constant* x volume) / (desired cell number) = total volume

* Constant of the counting chamber: 10 000

Depending on the experiment performed, cells were seeded in 6-well plates or 24-well plates, previously coated and equilibrated. 6-well plates were used to knockdown the transcription factors and subsequently analyze the effect on the *Rbfox1* expression (see section 2.2.5). 24-well plate were used to carry out the luciferase assays and study the expression of the different Rbfox1 regulatory regions (section 2.2.4).

2.2.1.4 Culture of primary cortical neurons

Primary cortical neurons were cultured up to four days before harvesting. Cell number was determined as described in section 2.2.1.3. $4x10^5$ cells per well were seeded in 24-well plates to perform the luciferase assays. $4x10^6$ cells per well were seeded in 6-well plates to knockdown the studied transcription factors and subsequently analyze the effect on *Rbfox1* expression.

2.2.1.5 Cell harvesting

To analyze the changes in *Rbfox1* expression upon transcription factors knockdown cells were harvested as follow:

Culture medium was aspirated by suction and cells were washed once with DPBS. DPBS was aspirated and fresh DPBS was pipetted onto the cells again. Cells were removed then from the surface with a cell scraper, transferred to a 15 ml Falcon and centrifuged for 5 minutes at 1000 rpm. The supernatant was removed and the necessary amount of RNA-later was added. Cell pellet was resuspended and stored at -20ºC until further use.

Primary cortical neurons used to perform the luciferase assay and study the expression of the three different Rbfox1 transcripts, were harvested as described in section 2.2.4.10.

2.2.2 Molecular Biology methods

2.2.2.1 Expression analysis of the *Rbfox1* gene

The expression analysis of the *Rbfox1* gene was performed in both, the developing and the juvenile murine brain. For the embryonic analysis the cerebral cortex of mice embryos was isolated for RNA extraction at different embryonic stages: E13.5, E15.5, E17.5 and P0.

To study *Rbfox1* expression levels in different brain regions in juvenile mice, 6 weeks old male C57BL/6 mice were sacrificed via cervical dislocation. Brains were soaked in RNA later for one week before cerebral sections were prepared. Total RNA was extracted using the Trizol/Phenol-Chloroform method described above.

2.2.2.1.1 Isolation of total RNA from mouse brain tissue

The isolation of the total RNA was performed using TRIzol according to the manufacturer's protocol. The isolation of the RNA took place under a fume hood and in an RNAse-free environment.

1ml TRIzol was added to the tissue, homogenized with the help of a mortar and incubated for five minutes at room temperature. After adding 200µl of chloroform, the solution was shaken vigorously until it appeared pinkish-milky, after which it was incubated for two minutes at room temperature. The solution was centrifuged at 12,000g and 4°C to have a two phase separation. The upper colorless aqueous phase was transferred to a new reaction tube with 500 µl of ice-cold isopropanol in it. The liquid was mixed gently and incubated for 10 minutes at room temperature. Afterwards, the tubes were centrifuged at 12,000g and 4ºC for 15 minutes to have a pellet. The supernatant was discarded and the pellet was washed with 1 ml of 70% ethanol and centrifuged at 12,000g and 4°C for five minutes. This washing step was repeated once again

before the pellet was air dried. If the pellet appeared glassy, it was dissolved in 10-100µl of Elution Buffer (Agilent), depending on the pellet size. Until further use, the RNA sample was stored at -80 ° C.

2.2.2.1.2 Reverse transcription from total RNA of mouse brain tissue

1µg of total RNA isolated from the tissue was used as a template for the reverse transcription using random hexamer primer and an RNA-dependent DNA polymerase. For the reverse transcription, the protocol described in the RevertAidTM First Strand cDNA Synthesis Kit was followed. The cDNA was stored at -20 ° C until further use.

2.2.2.1.3 Real Time Quantitative PCR (RT-qPCR)

RT-qPCR allows the determination of the relative mRNA amount of a target gene in a treated sample compared to a control sample. RT-qPCR reactions were performed to study the expression levels of the different Rbfox1 transcripts: *Rbfox1 transcript 1B, Rbfox1 transcript 1C, Rbfox1 transcript 1D* and *Rbfox1 all transcripts isoforms.* In order to study the expression of each transcript individually the Universal ProbeLibrary system technology (UPL) was used. The UPL system is based on the hydrolysis of short probes, which are labeled at the 5' end with fluorescein (FAM) and at the 3' end with a dark quencher dye. For this analysis Rbfox1 transcript-specific primers were designed and used with a suitable Universal ProbeLibrary probe (Table 9) and Absolute qPCR ROX mix and run on an ABI StepOnePlus^{TM} Real-Time PCR System. All cDNA samples were measured in triplicates, with a single “no template control (NTC)” for each. As internal control to assess the integrity of the different RNAs and to confirm the success of the reverse-transcription reaction, primers for the housekeeping gene *Gapdh* (glyceraldehyde

phosphate dehydrogenase) were employed in the amplification reaction. Primer efficiencies were calculated with the software LinRegPCR (see section Programs). Relative expression was calculated using the equation published by Pfaffl et al which adjusts for the primer efficiency (Michael W. Pfaffl, 2001).

The RT-qPCR reactions were run in 96-well optical reaction plates using the following conditions (Table 24).

Table 22. Cycling conditions for the RT-qPCR

	Temperature	***Time***	***Number of cycles***
Enzyme activation	95 ºC	15 minutes	1 cycle
Denaturation	95 ºC	15 seconds	40 cycles
Annealing / extension	60 ºC	60 seconds	

Table 23. RT-qPCR reaction solution per well

	Volume	***Final concentration***
Absolute qPCR ROX mix	6.3µl	1X
Probe (10µM) (Roche)	0.1 µl	80 nM
Primer Forward+Reverse (10µM)	1 µl	800 nM
Template (cDNA)	2.5 µl	0.8 ng/µl
H2O (Braun)	2.6 µl	
Final volume	12.5 µl	

2.2.2.1.4 *Rbfox1* expression analysis in different cell lines

Rbfox1 expression was analyzed in several cell lines aiming to find the most suitable cell model and transfection host for a successful experiment.

A transcript-specific analysis of the *Rbfox1* gene, and also the total *Rbfox1* expression, was carried out in P19 cells, neural precursor cells (NPC) and primary cortical neurons after 4 days and 7 days in culture (Figure 12).

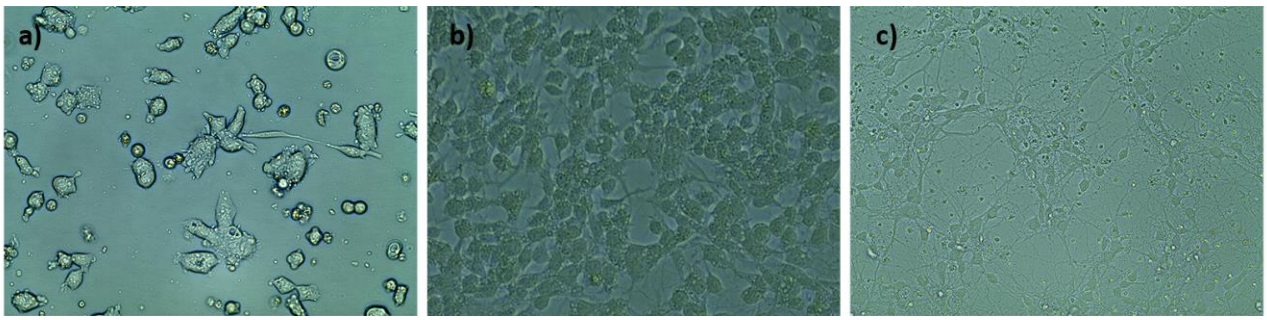

Figure 12. Different cell lines used for *Rbfox1* expression analysis. a) P19 cells under 40x objective. b) Neural Precursor cells under 20x. c) Primary cortical neurons after 6 days in culture under de 20x objective.

Cells were prepared and cultured as described in sections 2.1.2. RNA isolation was performed with the High Pure RNA isolation Kit (see section Kits) following the given protocol. 1000 ng of total RNA isolated from the cells was used as a template for the reverse transcription using random hexamer primers and an RNA-dependent DNA polymerase. For the reverse transcription, the protocol described in the RevertAid™ First Strand cDNA Synthesis Kit was followed (see section Kits). The cDNA was stored at -20 ° C until further use.

2.2.2.1.4.1 Real Time Quantitative PCR (RT-qPCR)

RT-qPCR reactions were performed to study the expression levels of total *Rbfox1*, *Rbfox1 1B, Rbfox1 1C* and *Rbfox1 1D* in P19 cells, NPC and primary cortical neurons after 4 days and 7 days in culture. RT-qPCR were run on an ABI StepOnePlus™ Real-Time PCR System. All cDNA samples were measured in triplicates, with a single "no template control (NTC)" for each. As internal control to assess the integrity of the different RNAs and to confirm the success of the reverse-transcription reaction, primers for the housekeeping gene *Bcas2* were employed in the amplification reaction (Table 12).

The RT-qPCR reactions were run in 96-well optical reaction plates using the following conditions (Tables 24 and 25) with a melting curve analysis to assess whether the intercalating dye qPCR assays produced single specific products. For each target gene, all the primers were designed to span an exon-exon junction (Table 9).

Table 24. RT-qPCR reaction solution per well

	Volume	***Final concentration***
SYBR® Premix Ex Taq™ II	5 µl	1X
Primer Forward+Reverse (10µM)	0.4 µl	400nM
Template (cDNA)	2 µl	1 ng/µl
H2O (Braun)	2.6 µl	
Final volume	10 µl	

Table 25. Cycling conditions for the RT-qPCR

	Temperature	*Time*	*Number of cycles*
Holding Stage	95 ºC	30 seconds	1 cycle
Cycling stage	94 ºC	15 seconds	40 cycles
	60 ºC	60 seconds	
	72 ºC	30 seconds	
Melt curve stage	60 ºC	15 seconds	1 cycle
	95ºC	15 seconds	1 cycle
	20ºC	10 seconds	1 cycle

2.2.2.2 *In situ* hybridization experiment

2.2.2.2.1 Generation of the Digoxigenin-Labeled cRNA probes

Supplementing the expression analysis of the different *Rbfox1* transcripts a transcript-specific *in situ* hybridization (ISH) experiment was carried out. The principle of ISH is the specific annealing of a labeled probe to complementary sequences of a target nucleic acid (DNA or mRNA) in a fixed specimen, followed by detection and visualization of the nucleic acid hybrids by cytological methods. This technique allows to identify specific expression patterns of those target genes (mRNA) in the course of either embryonic development or in distinct tissues.

2.2.2.2.1.1 Amplification of the target sequence by PCR

Cortical cDNA from 6 weeks-old mouse and transcript-specific primers (Table 10) were used to amplify the target sequence of the *Rbfox1* transcript 1B and *Rbfox1* all transcripts isoforms. Primers to generate the *Rbfox1 1B* probe bind to the first exon, and the ones used to generate

the probe that detected all transcripts isoforms bound to exon 6, which is common in all transcript isoforms.

Table 26. Cycling conditions for the PCR

	Temperature	*Time*	*Number of cycles*
Initial denaturation	95 ºC	2 minutes	1 cycle
Denaturation	95 ºC	30 seconds	35 cycles
Annealing	60 ºC	30 seconds	
Elongation	72 ºC	2 minutes	
Final elongation	72 ºC	5 minutes	1 cycle
Storage	4 ºC	∞	

Table 27. PCR reaction solution per well

	Volume	*Final concentration*
Cortex cDNA		200 ng
FastStart High fidelity reaction buffer 10x	2.5µl	1.8 mM $MgCl_2$
dNTPs	0.5µl	200µM (of each dNTP)
Forward primer (10 µM)	1µl	0.4 µM
Reverse primer (10 µM)	1µl	0.4 µM
FastStart High fidelity Enzyme Blend	0.2µl	2.5 U/reaction
H2O (Braun)	Up to 25µl	

The success of the target amplification was assessed in a 1.5% agarose gel.

2.2.2.2.1.2 Ligation

PCR products and the linearized plasmid pGEM-T Easy vector were linked to each other with a ligation reaction (Table 30). The ligation reaction was carried out in a 1:3 ratio and ran at 16ºC overnight. Table 28 shows an example of a ligation reaction, each of those were calculated individually using the online tool ligation calculator from Düsseldorf University (section online tools).

Table 28. Example of a ligation reaction between pGEM-T easy and an insert.

	Volume
10x Buffer for T4 DNA Ligase (10mA ATP)	1µl
pGEM-T easy backbone	100 ng
Insert	Xµl
T4 DNA Ligase	1µl
H2O (Braun)	5µl

2.2.2.2.1.3 Preparation of chemically competent *E. coli*

For the preparation of chemically competent bacteria, 250 µl of S.O.C medium was added to E. *coli* TOP10 while kept on ice. Bacteria were incubated for 30 minutes at 37ºC shaking. Subsequently, 10 µl, 20 µl, 30 µl, 40 µl and 50 µl of the suspension were stroke out on agar plates without antibiotic. Plates were incubated overnight at 37ºC. On the following day, a single colony was picked and transferred to 15 ml of LB medium without antibiotic and incubated overnight at 37ºC. Optical density of the suspension was determined the next day at 550 nm. For this purpose, 1 ml of LB medium and 1 ml of the suspension were transferred into cuvettes and measured. An

OD550 = 0.05 in 200 ml S.O.B. medium should be achieved. The amount to be used was calculated and transferred to 200 ml of S.O.B. medium (see Tables 3.1 and 3.2) and incubated at 37ºC. The OD550 was measured after 60 minutes, 80 minutes, 90 minutes and on, until an OD550 of 0.5 was reached. Subsequently, the suspension solution was divided into four 50 ml falcons and centrifuged for 8 minutes at 2500 rpm and 4ºC. All subsequent steps were performed on ice. Supernatants were removed and the cell pellets resuspended in 30 ml of Tfb I (see Tables 3.3 and 3.4) and centrifuged at 2000 rpm and 4ºC for 6 minutes. Supernatants were decanted and the cell pellets resuspended in 4 ml Tfb II (see Tables 3.5 and 3.6) and mixed carefully. Cell suspension was aliquoted in 50 µl aliquots and pre-cooled to -80 ° C. Aliquots were stored at -80ºC until further use.

2.2.2.2.1.4 Transformation

The method of transformation was used to increase the number of plasmid constructs. During the transformation, the plasmid is taken up and amplified by competent Escherichia *coli* bacteria. Some bacteria possess a natural competence and absorb DNA without external effects. Other bacteria, such as the *Darmbacterium Escherichia coli (E. coli),* do not have this natural competence. These bacteria must be artificially initiated. The heat shock method with *E. coli* bacteria (see section Bacteria) was used to capture and replicate a plasmid with an integrated insert. For the transformation, the ligated product was pipetted in 50µl of *E. coli* cells and incubated on ice for 30 minutes. The heat shock was carried out in a water bath at 42ºC for 90 seconds. Cells were then cooled down on ice for two minutes, and 250µl LB medium without antibiotic was added (see table 7). Cells were incubated for one hour at 37ºC shaking in the incubator. Thereafter, 200µl of the reaction was spread on an agar plate containing ampicillin

and incubated overnight at 37ºC. Ampicillin was used as a selection method, since only the plasmid contained the resistance gene against ampicillin. Therefore, only the bacteria which had taken up the plasmid during the transformation and thus, had resistance to the antibiotic, grew on the agar plate.

The next day, five to ten colonies were picked per agar plate and transferred into 3 ml of LB medium with ampicillin with the lid loose to let the oxygen get in. Tubes were placed in the incubator at 37ºC shaking overnight.

2.2.2.2.1.5 Plasmid Isolation by Minipreparation

The next day, the plasmid was purified from the *E. coli* bacteria by minipreparation (miniprep). For this purpose, a protocol without columns was used with the buffers P1, P2 and P3 from the EndoFree® Plasmid Maxi Kit (section Kits). The method is based on the alkaline lysis of the bacteria, in which the cells are lysed and the DNA contained is released.

1.5 ml of the 3ml overnight culture was transferred into a 1.5ml eppendorf and centrifuged at 6000 rpm for five minutes. Supernatant was discarded and the pellet was resuspended in 100µl of P1 lysis buffer until all clumps were dissolved. The remaining 1.5 ml were left for later inoculation with fresh LB media to do the maxipreparation. Subsequently, 100µl of P2 buffer were added to the cell suspension and inverted several times. The buffer used contained NaOH-SDS and was mixed with RNase A. Phospholipids and protein components of the cell membrane were solubilized by the SDS. This leads to cell lysis and a release of the cell contents. NaOH denatures the chromosomal and plasmid DNA as well as proteins. RNase A is used to degrade disturbing RNA. The optimal lysis time of five minutes at RT should not be exceeded as this leads

to irreversible denaturation of the plasmid DNA. After the incubation time, 100µl of ice-cooled P3 buffer were pipetted onto the lysate. The lysate was neutralized by the acidic potassium acetate present in the P3 buffer. After an incubation time of five minutes at RT, the mixture was centrifuged for 10 minutes at 13,000 rpm. The supernatant was transferred to a new 1.5ml reaction tube containing 1 ml of 100% EtOH and centrifuged at 13,000 rpm for 10 minutes to precipitate the plasmid DNA. The supernatant was discarded and the visible pellet was washed with 150µl of 70% EtOH by centrifugation at 13,000 rpm for five minutes. After centrifugation, the entire supernatant was removed. With the lid of the reaction tube open, the pellet was dried at 50ºC in the heating block for a few minutes to completely remove the EtOH. The pellet was dissolved in 50µl of water and stored at -20 ° C.

2.2.2.2.1.6 Plasmid control PCR reaction

A PCR was carried out to clarify whether the ligation reaction was successful. M13 primers, which bind to the pGEM-T easy backbone upstream and downstream to the multiple cloning site, were used (Table 10). If the plasmid was empty a PCR product of 240 bp was amplified and if the ligation and transformation was successful, the PCR product was 240 bp+ insert length.

Table 29. PCR reaction solution per well

	Volume	***Final concentration***
DNA template (miniprep)		1µl
FastStart High fidelity reaction buffer 10x	2.5µl	1.8 mM $MgCl_2$
dNTPs	0.5µl	200µM (of each dNTP)
Forward primer (10 µM)	1µl	0.4 µM

Reverse primer (10 µM)	1µl	0.4 µM
FastStart High fidelity Enzyme Blend	0.2µl	2.5 U/reaction
H2O (Braun)	Up to 25µl	

Table 30. Cycling conditions for the control PCR

	Temperature	***Time***	***Number of cycles***
Initial denaturation	95 ºC	2 minutes	1 cycle
Denaturation	95 ºC	30 seconds	30 cycles
Annealing	55 ºC	30 seconds	
Elongation	72 ºC	60 seconds	
Final elongation	72 ºC	2 minutes	1 cycle
Storage	4 ºC	∞	

2.2.2.2.1.7 Sequencing

The purified constructs containing the insert were sequenced by the company GATC Biotech to check for possible errors.

For the sequencing of the Rbfox1 transcript 1B and Rbfox1 all transcript isoforms, the primers from table 10 were used and the tubes were labelled with barcodes of the LightRun Sequencing. Samples were prepared following the company instructions.

The sequences were subsequently analyzed for possible errors within the insert against the original sequence with the program "Serial Cloner" (see section Programs).

2.2.2.2.1.8 Plasmid Isolation by Maxipreparation

The 1.5µl saved from the 3ml overnight culture, which contained the plasmid with the sequence confirmed insert, was inoculated into 250 ml of fresh LB medium containing 50µg/ml Ampicillin and likewise incubated overnight at 37°C. The maxipreparation (maxiprep) differs from the miniprep essentially only in the quantity of the components used and the product produced. The method was also based on the principle of alkaline lysis and was performed with the EndoFree® Plasmid Maxi Kit following the manufacturer's indications (section Kits).

2.2.2.2.1.9 Plasmid linearization

The next step before converting the DNA to complementary RNA (cRNA), was to linearize the plasmid. Vectors used as transcription templates should be linearized by restriction enzyme digestion. Because transcription proceeds up to the end of the DNA template, linearization ensures that RNA transcripts of a defined length and sequence are generated. The restriction site does not need to be unique, and providing the promoter remains adjacent to the transcription template, the vector itself may be digested multiple times. It is also unnecessary to purify the promoter-insert sequence away from other fragments prior to transcription because only the fragment containing promoter sequence will serve as template. Restriction enzyme digestion should be followed by purification since contaminants in the digestion reaction may inhibit transcription.

10 µg of the DNA pGemT-easy/Rbfox1 transcript 1B and Rbfox1 all transcript isoforms were digested with either SpeI-HF or SphI-HF restriction enzyme depending on the direction of the insert within the plasmid (5'-3' or 3'-5'). The enzymatic reaction was run at 37ºC overnight. The

next day an aliquot was loaded on a 1.5 % agarose gel to analyze the success of the digestion. If the plasmid was not completely digested, about 5µl of the restriction enzyme was added and the reaction was run again at 37ºC overnight. After the linearization, the digested product was purified using the High Pure PCR Product Purification kit (section Kits).

Table 31. Example of the plasmid linearization reaction.

	Volume
DNA probe	10 µg
SpeI-HF / SphI-HF	5 µl
CutSmart Buffer	2 µl
H2O (Braun)	Up to 20 µl

2.2.2.2.1.10 *In vitro* transcription

In vitro transcription is a simple procedure that allows for template-directed synthesis of RNA molecules of any sequence, from short oligonucleotides to those of several kilobases, in µg to mg quantities. It is based on the engineering of a template that includes a bacteriophage promoter sequence (phage T7, SP6 or T3) upstream of the sequence of interest followed by transcription using the corresponding RNA polymerase. Many common plasmid cloning vectors contain two distinct promoters, one on each side of the multiple cloning site, allowing transcription of either strand of an inserted sequence. Such dual opposable promoter vectors include pGEM-t easy vector, the one used in this experiment. This dual opposable promoter vectors is what has

allowed us to synthesize the anti-sense (3'-5') cRNA probes to detect the mRNA in the brain and the sense (5'-3') probes, to be used as a control.

In the synthesis of cRNA, digoxigenylated (DIG) nucleotides were incorporated to make nonradioactive complementary RNA probes for the hybridization (table 32 and 33).

Table 32. *In vitro* transcription solution per reaction.

	Volume
Transcription buffer	2µl
Digoxygenin NT Mix	2µl
RNAse inhibitor	0.5µl
RNA polymerase (T7 / SP6)	2µl
Linearized plasmid	1µg
H_2O (Braun)	up to 20µl

Table 33. Cycling conditions for the in vitro transcription

RNA polymerase	***Incubation temperature***	
SP6	40ºC	Incubate 120 minutes.
T7	37ºC	Add 2µl of the T7/SP6 polymerase and incubate 120 minutes again

Afterwards, 1µl of the RNA probe were loaded on an agarose gel to confirm a successful in vitro transcription.

After the total incubation time of 4 hours, a DNA purification step was necessary to ensure there was no DNA left, which may contaminate our RNA probes. 2µl of DNAse were added to the sample and was incubated for 15 minutes at 37ºC.

Afterwards, 1µl of the RNA probe were loaded on an agarose gel to confirm a successful DNA-free probe.

The last step of the DIG-labelled RNA probes preparation was an RNA purification by Ethanol precipitation. This step was done in 1.5ml Eppendorf.

Table 34. RNA purification solution per reaction.

	Volume
H_2O (Braun)	Up to 100 µl
Ethanol 100%	300µl
Natrium acetate (3M, pH= 5.2)	10µl
Glycogen	1µl

Afterwards, tubes were placed at -20ºC (freezer) overnight. The next day, samples were centrifuged for 20 minutes at maximum speed and 4ºC. The supernatant was discarded. Pellet was washed twice with 200µl Ethanol 70% and centrifuged again for 10 minutes at maximum speed and 4ºC. Supernatant was discarded. Finally, pellet was resuspended in 20µl water. 1µl of the RNA probe was loaded on an agarose gel to confirm a successful RNA purification. Tubes were stored -80ºC for a later use.

2.2.2.2.2 *In situ* hybridization

6 weeks old male mice were sacrificed via cervical dislocation. Brains were extracted, soaked in formaldehyde and embedded in paraffin. Sagittal slices were used for the experiment (slides prepared by the Pathology Department of the Johannes Gutenberg University Medical Center). Commercial paraffin embryonic brain slices (E15) were used (Table 1).

The *in situ* hybridization experiments took place in three consecutive days and were performed as described below.

Day 1. Pre-hybridization

Every step of the experiment needs to be performed in an RNAse free environment. All solutions need to be prepared using DEPC or Millipore water. Every reagent, buffer or solutions was added as indicated below. Incubation times and temperatures are also indicated.

- Slides were warmed at 60ºC for 20 minutes
- Xylol, 10 minutes
- Xylol, 10 minutes
- Ethanol battery: 2x 100%, 75%, 50%, 25%, during 5 minutes
- PBT, 5 minutes
- PBT, 5 minutes
- 4% PFA (in PBT), 10 min (add the PFA directly on to the slide using a pipette)
- PBT, 2 minutes
- PBT, 5 minutes
- 4% PFA (in PBT), 5 minutes

- PBT, 5 minutes
- PBT, 5 minutes
- TAE (acetylation)
- PBT, 10 minutes
- PBT, 10 minutes
- Let dry the slides for 5-10 minutes

Pre-hybridization: 300µl Hyb-mix (variant) was added per slide (see table 5), with no coverslip. Slides were incubated in a wet chamber for 3 hours at 65ºC.

Probe preparation: 1µg RNA probe was used with the embryonic brain + 300µl Hyb-Mix; 6µg RNA probe was used for adult brain + 300µl Hyb-Mix. Probes were heated at 85ºC for 5 minutes to be ready to use.

300µl of the probe preparation was added to each slide, covered with coverslips and incubated in the wet chamber at 65ºC overnight.

Day 2. Antibody pre-incubation

Before starting the experiment water bath was set at 65ºC and at 37ºC.

- Wash the slides with 5xSSC to get rid of the coverslips (RT)
- 2xSSC / 50% Formamid, 65ºC, 30 minutes
- TNE, 37ºC, 10 minutes
- TNE + RNAse, 10 minutes

- TNE, 37ºC, 10 minutes
- 2xSSC, 65ºC, 30 minutes
- 0.2xSSC, 65ºC, 30 minutes
- 0.2xSSC, 65ºC, 30 minutes
- Cool down the slides at 4ºC
- MABT, 5 minutes
- MABT, 5 minutes
- Slides were incubated with 500µl of Blocking solution for 2 hours, at room temperature (with no coverslips) inside the wet chamber.
- Blocking solution was removed.
- 300µl of the antibody solution was added per slide, covered with coverslips, and incubated at 4ºC overnight (inside the wet chamber).

Blocking solution:

- MABT + 0.5% Blocking reagent.

Blocking reagent was warmed at 42ºC before use to make it liquid, and cooled down on ice.

- 10% sheep serum (heat inactivated).

Antibody solution:

- Anti-DIG-AP in blocking solution (1:2000).
- Antibody solution was incubated for 1-2 hours, at 4ºC with rotation.

Day 3. Color reaction

- Slides were washed with MABT to remove the coverslips (RT)
- MABT, 5 minutes
- MABT, 5 minutes
- MABT, 10 minutes
- MABT, 10 minutes
- NTMT, 10 minutes
- Slides were transferred into a dark chamber and covered with DM purple (3ml per slide). They were incubated until de color reaction is finished (from 2 hours to 4 days)

When the color reaction is finished:

- NTMT, 10 minutes
- PBS, 5 minutes
- 4% PFA (in PBS), 30 minutes
- PBS, 5 minutes
- PBS, 5 minutes
- Slides were washed very fast in Millipore water
- 200µl Kaiser's Glycerol Gelatin were added per slide and covered them with coverslips, avoiding bubbles formation.

The Kaiser's Glycerol Gelatin can be warmed at 42ºC to make it liquid and easier to manipulate.

See table 5 for all the solutions and buffers preparation.

2.2.2.3 Analysis of *Rbfox1* promoter's activity

To study the activity of the different regulatory regions in charge of driving the expression of the Rbfox1 transcripts in the brain, a luciferase assay was performed with promoter 1B, promoter 1C and promoter 1D. The three different promoter regions were amplified by PCR from genomic DNA of 6 weeks-old mouse cortex, using specially designed primers containing flanking restriction enzyme sites, to be finally cloned into the Luciferase reporter vector pGL4.10 [luc2] (see section Vectors). Luciferase reporter assay is commonly used as a tool to study the regulation of gene expression at the transcriptional level. Luciferases make up a class of oxidative enzymes found in several species that enable the organisms that express them to "bioluminesce" or emit light. The most famous one of these enzymes, and the one used in this study, is the firefly luciferase *(Photinus pyralis)* and Renilla luciferase reporter (*Renilla reniformis*)

This reaction is highly energetically efficient, meaning nearly all the energy put into the reaction is rapidly converted to light. This makes it extremely sensitive. Fireflies are able to emit light via a chemical reaction in which luciferin is converted to oxyluciferin by the luciferase enzyme. Some of the energy released by this reaction is in the form of light (Figure 13).

Firefly luciferase has been used as a sensitive reporter to study a wide range of biological responses. However the change of the expression of Firefly luciferase reporter can be due to a global effect instead of a specific effect. The accuracy of Firefly luciferase reporter can be improved by normalizing to a control reporter, such as Renilla luciferase reporter (*Renilla reniformis*, also known as sea pansy), in the same sample.

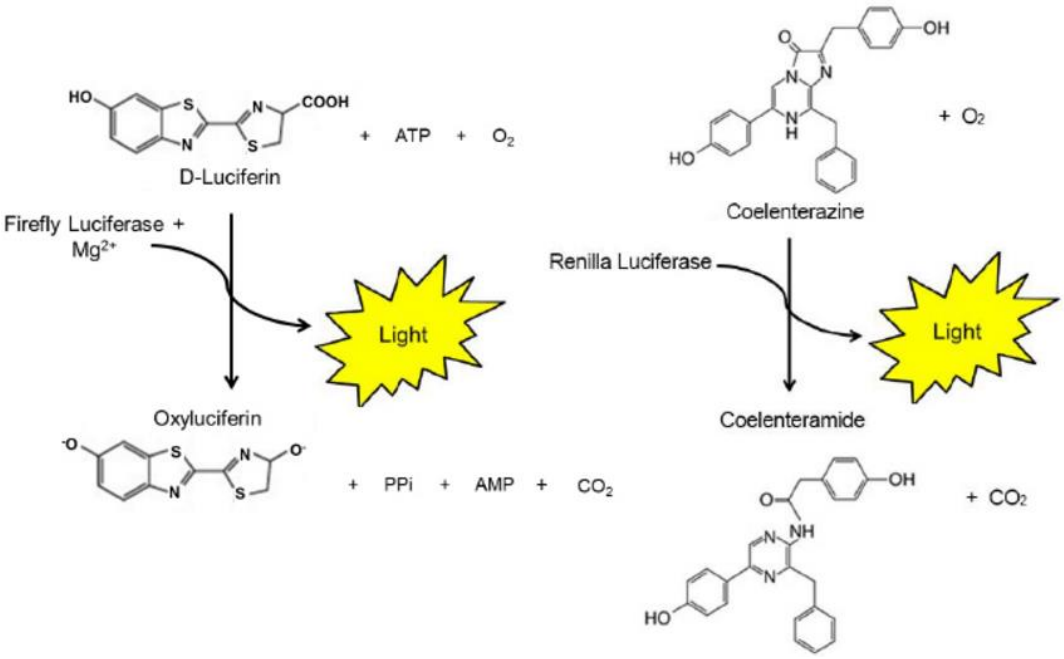

Figure 13. Bioluminescent reactions catalyzed by the firefly and Renilla luciferases. Adopted from (http://bpsbioscience.com/media/wysiwyg/dual2.jpg)

Primary cortical neurons were isolated, and transfected after 3 days in culture with both, the Rbfox1 promoter plasmid (firefly) and the Renilla reporter plasmid pRL-TK as a normalization reaction. Approximately 24 hours after transfection, cells were lysed and the luciferase activity was read on the Centro XS^3 LB 960 Microplate Luminometer (see section Laboratory equipment).

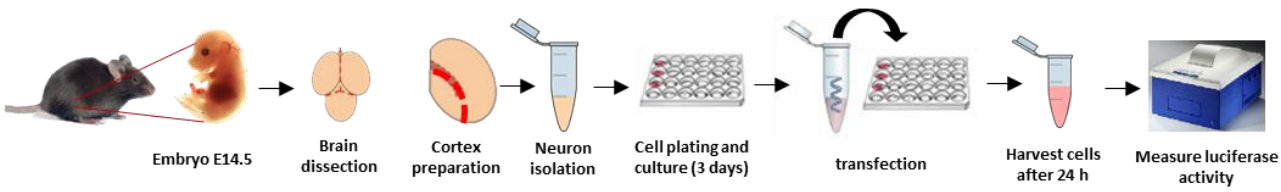

Figure 14. Workflow of the analysis of the *Rbfox1* promoter, from the embryos preparation to the luciferase activity measurement.

2.2.2.3.1 Amplification of the target sequence with PCR

2.2.2.3.1.1 Primer design

Primers used to amplify the regulatory regions of the three different Rbfox1 transcripts, promoter 1B, promoter 1C and promoter 1D, were generated using the online tool “Primer3” (Online tools). Afterwards, unspecific binding was checked using the online tool "BiSearch" (Online tools). In addition, primers were designed with flanking restriction enzymes sites, as well as a Kozak sequence (5'-GCCACCATG-3'), which contributes to the initiation of translation and thus increases translation efficiency. Primers with KpnI and HindIII restriction sites were designed to amplify the Promoter 1B region and XhoI and Bgl II for the promoter 1C and promoter 1D (Table 11).

Figure 15. Schematic representation of the primers designed. Flanking restriction enzyme sites (EcoRI, XhoI) and the Kozak sequence, used to amplify the target region of the *Rbfox1* promoter region are shown.

2.2.2.3.1.2 *Rbfox1* regulatory regions cloned

Regulatory regions of transcripts 1B and 1C aiming to be cloned, were selected using the UCSC Genome Browser. The selected sequence to be cloned was the one showing a high rate of transcription factors binding (Figure 16).

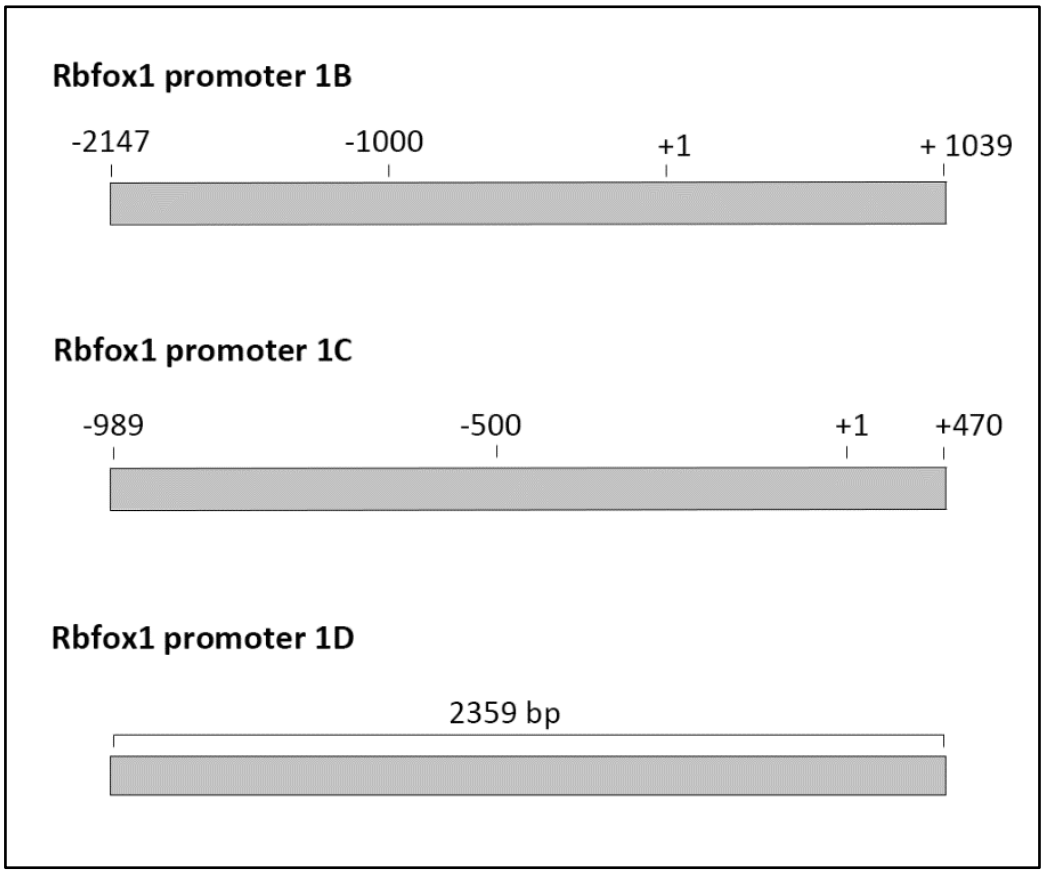

Figure 16. Schematic representation of the three *Rbfox1* regulatory regions cloned. Numbers indicate the length of the region cloned relative to the transcription start site.

In order to select the DNA sequence to be amplified for promoter 1D, as this transcript is not noted in the UCSC Genome Browser, the amplified target sequence was designed studying the Ref-seq data of the *Rbfox1* gene (Figure 17).

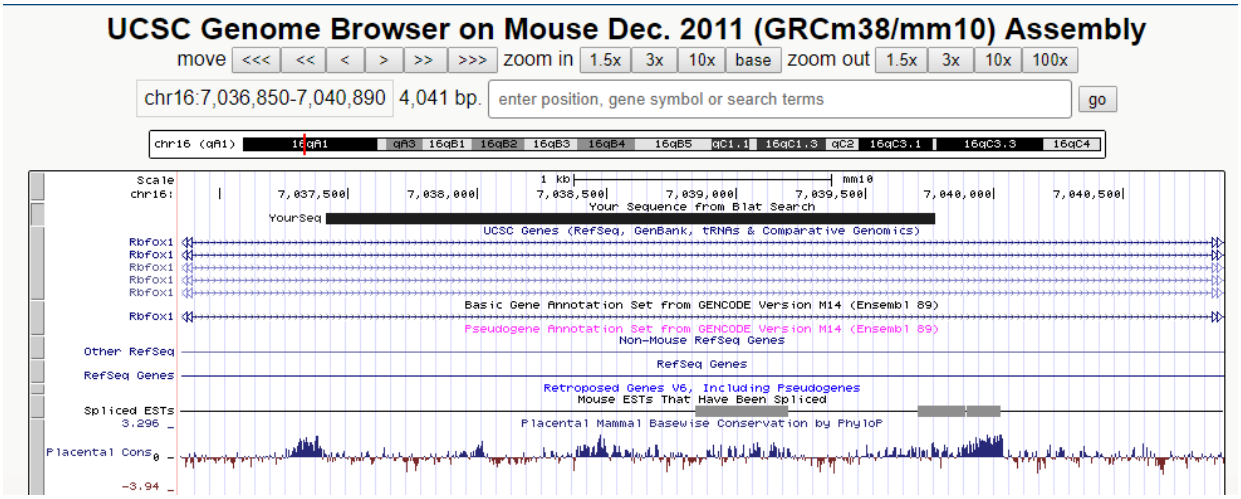

Figure 17. Position of the Promoter 1D. A blast of the promoter 1D sequence cloned against *Rbfox1* gene is shown in the figure (Black box). The position of the sequence within the gene as well as the Refseq data of the gene is displayed, showing an expression in that region with no exon described (Adopted from UCSC Genome Browser).

2.2.2.3.1.3 RT-PCR

Cortical genomic DNA from a 6 weeks-old mouse and the primers designed as described in the previous section (Table 11) were used to amplify the regulatory regions of the *Rbfox1 1B, Rbfox1 1C* and *Rbfox1 1D.*

Table 35. Cycling conditions for the PCR

	Temperature	***Time***	***Number of cycles***
Initial denaturation	94 ºC	1 minutes	1 cycle
Denaturation	94 ºC	15 seconds	35 cycles
Annealing	55 ºC	30 seconds	

Elongation	68 ºC	10 minutes	
Final elongation	72 ºC	10 minutes	1 cycle
Storage	4 ºC	∞	

Table 36. PCR reaction solution per well

	Volume	***Final concentration***
Cortex cDNA		200 ng
5X PrimeSTAR GXL reaction buffer	5µl	1X
dNTPs mixture (2.5mM each)	4 µl	200µM (of each dNTP)
Forward primer (5 µM)	0.5 µl	0.1 µM
Reverse primer (5 µM)	0.5 µl	0.1 µM
PrimeSTAR GXL DNA Polymerase	1 µl	0.625 U/ 25 µl
H2O (Braun)	Up to 25µl	

The success of the amplification was assessed by running a 1.5% agarose gel containing the amplified product.

2.2.2.3.2 Restriction enzyme digestion

Before the restriction enzyme digestion, the amplification product was cleaned up using the High Pure PCR Product Purification kit (section Kits).

Restriction enzyme digestion was used to cut the double-stranded DNA of the PCR product of the three different promoter regions (promoter 1B, promoter 1C and promoter 1D) and the target plasmid, the luciferase reporter vector pGL4.10 [luc2] (section Vectors) at the enzyme-specific

recognition sequences. The restriction enzymes used are endonucleases which produce mutually compatible 5' overhangs which were essential for the subsequent ligation (Table 37). For a reaction using two different enzymes, a suitable buffer must be used which produces a suitable environment for the optimal activity of both enzymes. This was determined using NEB's "Double Digest Finder" (Online tools).

Table 37. Restriction enzymes used and their recognition sequences for the *Rbfox1* promoter regions.

Promoter region	***Restriction enzyme***	***Recognition sequence***	***NEB buffer 1x***
Promoter 1B	KpnI-HF	5'...GGTAC↓C...3' 3'...C↓CATGG...5'	Cut Smart
	Hind III-HF	5'…A↓AGCTT...3' 3'...TTCGA↓A...5'	
Promoter 1C and Promoter 1D	XhoI	5'…C↓TCGAG...3' 3'...GAGCT↓C...5'	3.1
	Bgl II-HF	5'…A↓GATCT...3' 3'...TCTAG↓A...5'	

For the digestion reaction, 4µl of NEB buffer, 1µl of each of the correspondent restriction enzymes and 4µl of H_2O, were mixed with either 3µl of plasmid or 30µl of the PCR product, to a total volume of 40µl. The reaction tubes were incubated for two hours at 37ºC.

Subsequently, the High Pure PCR Product Purification Kit (see section Kits) was used to eliminate the enzymes and buffer leftovers.

2.2.2.3.3 Ligation

The compatible 5'-overhangs of the linearized pGL4.10 vector (section Vectors) and the amplified promoter 1B, promoter 1C and promoter 1D fragments were linked together by a ligation reaction as described in section 2.2.2.2.1.2.

2.2.2.3.4 Transformation

The method of transformation was used to increase the number of plasmid constructs produced by bacteria. Transformation was carried out as described in the section 2.2.2.2.1.4.

2.2.2.3.5 Plasmid isolation by Minipreparation

The next day, the plasmid was purified from the E. *coli* bacteria by minipreparation (miniprep). About ten colonies of each plate were picked and cultured in 3ml LB media with Ampicillin as a selection method. The purification of each plasmid was carried out as described in the Plasmid purification by minipreparation, section 2.2.2.2.1.5.

2.2.2.3.6 Restriction enzyme control digestion

A restriction enzyme control digestion was used to check whether the purified plasmids contained the correct insert. The control digestion for the luciferase reporter vector pGL4.10 containing the regulatory region of the three different *Rbfox1* transcripts was performed with the same endonucleases described in table 37 and 3µL of the miniprep. Restriction digestion was carried out as described in section 2.2.2.3.2.

2.2.2.3.7 Sequencing

Sequencing was carried out by the company GATC Biotech. Primers from Table 11 were used and the samples preparation was performed following the company instructions. Sequences were subsequently analyzed with the program "Serial Cloner" (section Online tools).

2.2.2.3.8 Plasmid Isolation by Maxipreparation

Maxiprep was performed with the EndoFree® Plasmid Maxi Kit following the manufacturer's indications (chapter 2.2.2.2.1.8).

2.2.2.3.9 Transfection reaction

Transfection is the process of deliberately introducing naked or purified DNA into eukaryotic cells. There are various methods of introducing foreign DNA into a eukaryotic cell; some of them rely on physical methods such as electroporation or cell squeezing, and others are reagent-based methods (lipids, calcium phosphate, etc...) or biological particles that are used as carriers (viruses). To evaluate the expression of the different *Rbfox1* promoters, a lipid-based method of transfection was used. The previously generated promoter 1B, promoter 1C and promoter 1D were transfected using Lipofectamine®2000 (section Reagents) into primary cortical neurons after 3 days in culture (chapter 2.2.1.4). The mechanism is based on the use of cationic lipid molecules called liposomes. Liposomes form DNA-lipid complexes with the negatively charged nucleic acid of the plasmid. These complexes are believed to be taken up by the cell through endocytosis and then released in the cytoplasm. Once in the cell, transfected DNA is translocated

to the nucleus to be expressed by a yet unknown mechanism, while RNA or antisense oligonucleotides skip the translocation step and remain in the cytoplasm.

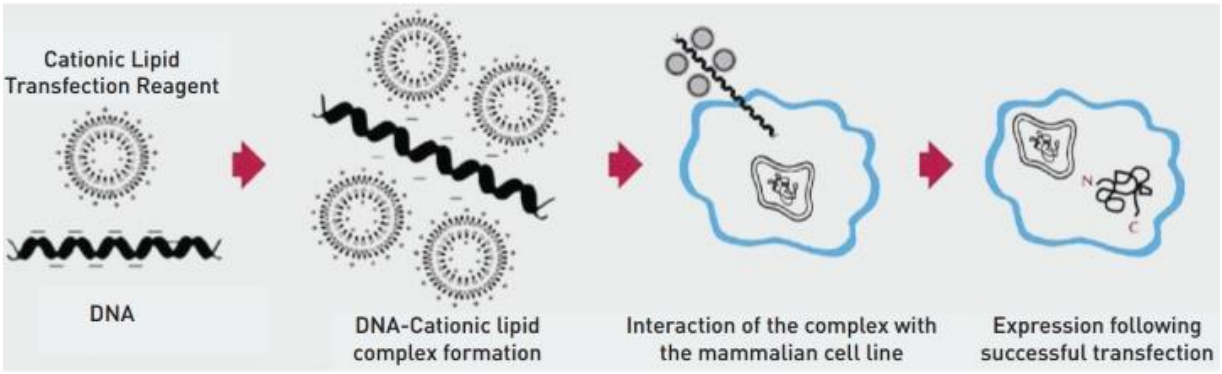

Figure 18: Mechanisms of cationic-lipid mediated delivery (Adopted from ThermoFischer Scientific).

$4x10^5$ primary cortical neurons were isolated from E14.5 embryos and seeded as described in section 2.2.1.2 in coated and subsequently equilibrated 24-well plates. After 3 days in culture cells were transfected with the generated plasmids. The plasmid DNA was diluted in Opti-MEM medium and then mixed with Lipofectamine®2000. In total, five plasmid constructs were transfected into primary cortical neurons: two different controls were used, a negative control which contained the promoter of the microRNA 302 (miR302) cloned into the pGL4 luciferase reporter vector and the empty pGL4.10 luciferase reporter vector. The *miR302* promoter is not active in neurons, therefore luciferase activity was expected to be low. The empty pGL4.10 luciferase reporter vector was transfected to analyze the background of the measurement. The three different promoter constructs were transfected: promoter 1B, promoter 1C and promoter 1D. All samples were transfected along with the renilla plasmid pRL-TK to normalize the results.

Table 38. Transfection scheme for a 24-well plate (one well).

	Mix 1	***Mix 2***
Plasmid DNA	4µg	
pRL-TK	1µg	
Opti-MEM	100µl	100µl
Lipofectamine 2000 reagent		3µl

Mix 1 and Mix 2 were prepared and incubated for 5 minutes at room temperature. 103µl of Mix 2 were transferred to Mix 1 and incubated 20 minutes at room temperature. Finally, around 210µl of the mix were pipetted into the well containing 2ml of the culture media. The transfected primary cortical neurons were incubated for 24 hours at 37ºC and 8% CO_2 content in an incubator.

2.2.2.3.10 Luciferase activity measurement

24 hours after transfection cells were harvested and both, firefly and renilla luciferase were measured. To measure the firefly activity a self-made buffer was used (Table 5) and the Renilla Luciferase Assay System (Promega) was used to measure the renilla activity. Renilla activity was measured following the manufacturer's recommendations (section kits).

Culture media was aspirated by suction and cells were washed with DPBS. Afterwards, 100µl of the Luciferase Assay Lysis Buffer 1X (provided with the kit) was added and the plates were shaken for 15 minutes at room temperature. Afterwards, the lysate was transferred to Eppendorf tubes

and the samples were centrifuged at 10,000rpm for 10 minutes at 4 ºC to pellet the cell debris. Supernatant were transferred to a new tube and the luciferase activity was measured.

2.2.2.3.11 Site-directed mutagenesis of the transcription factors binding sites

Mutations were introduced in the targeted E-box/C-Box of the previously generated *Rbfox1* promoters constructs, using the QuikChange II XL Site-Directed Mutagenesis Kit and following the manufacturer's recommendations (section Kits). This kit is specifically optimized for large, difficult constructs and allows site-specific mutation in virtually any double-stranded plasmid.

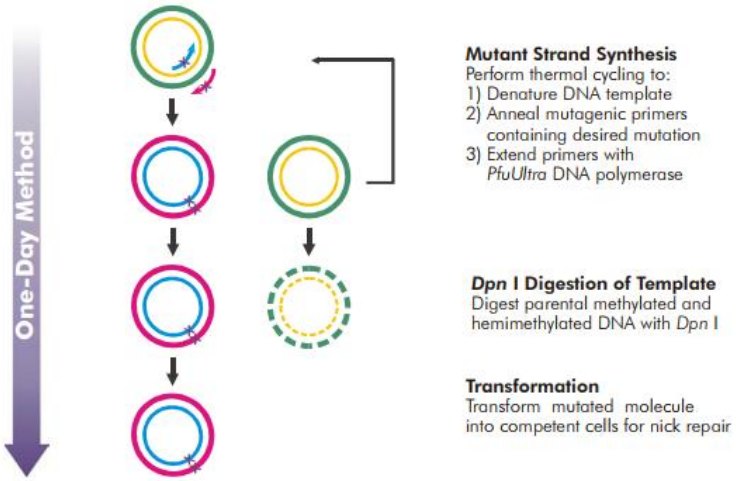

Figure 19. Workflow of directed-mutagenesis procedure. Overview of the three-step procedure carried out using the QuikChange II XL site-directed mutagenesis kit. (Adopted from www.agilent.com).

2.2.2.3.11.1 Mutagenic primer design

Primers used to introduce mutations into the transcription factors binding sites were generated using the online tool "QuikChange Primer Design" from Agilent Technologies (section online tools). Primers were designed to introduce a thymine in the position 1 and 2 of the E-box (Table 11).

2.2.2.3.11.2 Mutant Strand Synthesis Reaction

The synthesis of the mutant strand was carried out by a PCR following the manufacturer's recommendations.

Table 39. PCR reaction solution per well

	Volume	*Final concentration*
dsDNA Template		25 ng
Reaction buffer 10X	2.5 µl	1X
dNTPs mixture	0.5 µl	200µM
Forward primer (10 µM)	0.5 µl	0.1 µM
Reverse primer (10 µM)	0.5 µl	0.1 µM
QuikSolution	1.5 µl	
H2O (Braun)	Up to 25µl	
PfuUltra HF DNA polymerase	1 µl	

Table 40. Cycling conditions for the PCR

	Temperature	*Time*	*Number of cycles*
Initial denaturation	95 ºC	1 minutes	1 cycle
Denaturation	95 ºC	50 seconds	18 cycles
Annealing	60 ºC	50 seconds	
Elongation	68 ºC	10 minutes	
Final elongation	68 ºC	7 minutes	1 cycle
Storage	4 ºC	∞	

2.2.2.3.11.3 Dpn I Digestion of the Amplification Products

After the PCR 1 µl of the Dpn I restriction enzyme (10 U/µl) was added directly to each amplification reaction (enzyme provided with the kit). Gently mixed each reaction mixture and incubated them at 37°C for 1 hour to digest the parental DNA (Figure 19).

2.2.2.3.11.4 Transformation

Transformation was carried out following the manufacturer's recommendations. Very briefly:

For each sample an aliquot of 45 µl of the XL10-Gold ultracompetent cells (provided with the kit) were thawed on ice. 2 µl of β-Mercaptoethanol (β-ME) mix provided with the kit was added to the 45 µl of cells and incubated on ice for 10 minutes, swirling gently every 2 minutes. Subsequently, 2 µl of each Dpn I-treated DNA were transferred to the ultracompetent cells and incubated on ice for 30 minutes. In the meantime, the LB media was pre-heated at 42ºC in the water bath. Afterwards, the tubes were heat-shocked in a 42°C water bath for 30 seconds. After the heat-shock, the tubes were incubated on ice for 2 minutes before adding 500 µl of the pre-heated LB media into each reaction. The tubes were incubated at 37°C for 1 hour and shaking at 225–250 rpm. Eventually, 250 µl of each transformation reaction was plated in two agar plates containing Ampicillin antibiotic for selection and incubated overnight at 37ºC.

The next day, five to ten colonies of each plate were picked up and transferred into a tube containing 3 ml of LB medium with ampicillin with the lid loose to let the oxygen get in. Tubes were placed in the incubator at 37ºC shaking overnight.

The next day, plasmids were purified from the *E. coli* bacteria by miniprep (chapter 2.2.2.2.1.5) and sequenced (see chapter 2.2.2.2.1.7). The ones containing the sequences carrying the correct mutations were used for a maxiprep (see chapter 2.2.2.2.1.8).

2.2.2.4 Transcription factors knockdown

A knockdown of the transcription factors was carried out aiming to analyze the changes in Rbfox1 expression. The experiment was performed with primary cortical neurons as a cell model. Electroporation of the siRNA (see Small interfering RNA section) was carried out with the 4D-Nucleofector X unit (see Equipment section) following the manufacturer's recommendation. After 48 hours of transfection, cortical neurons were harvested and RNA extraction, cDNA synthesis and expression analysis via RT-qPCR was carried out as described in the previous sections.

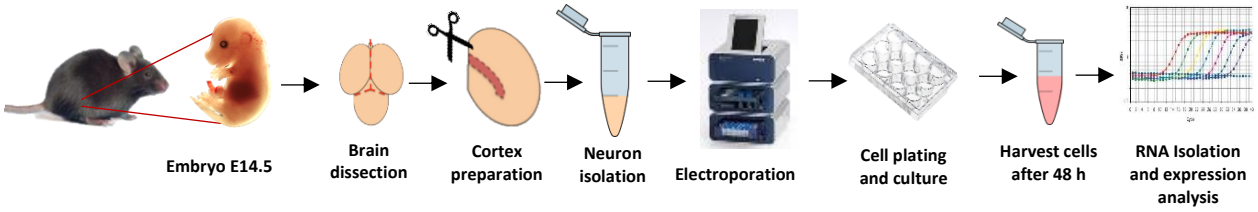

Figure 20: Workflow of the transcription factors knockdown experiment, from the embryos preparation to the expression analysis.

2.2.2.4.1 Transcription factors expression analysis

The first step, to design a successful experiment, was to perform expression analysis of the transcription factors in primary cortical neurons, after 4 days and 7 days in culture, and in P19 cells.

2.2.2.4.1.1 RNA isolation and Reverse transcription from total RNA of cells

Primary cortical neurons were prepared and cultured as previously described (see section Cell Culture). Cells were harvested after 4 days and 7 days in culture and stored in RNA later at -20ºC. RNA isolation was done with the High Pure RNA isolation Kit (section Kits) following the given protocol.

500 ng of total RNA isolated from the cells was used as a template for the reverse transcription using random hexamer primers and an RNA-dependent DNA polymerase. For the reverse transcription, the protocol described in the RevertAid™ First Strand cDNA Synthesis Kit was followed (section Kits). The cDNA was stored at -20 ° C until further use.

2.2.2.4.1.2 Real Time Quantitative PCR (RT-qPCR)

RT-qPCR reactions were performed to study the expression levels of c-Myc, NeuroD2, Klf7, Mycn, Max and Tcf4 in primary cortical neurons after 4 days and 7 days in culture, and determine the highest expression levels to decide to perform a transfection in suspension (at the moment of seeding the cells) or an adherent transfection (after some days in culture). The expression analysis was performed in P19 cells as well to use as a reference. RT-qPCR were run on an ABI

StepOnePlus™ Real-Time PCR System. All cDNA samples were measured in triplicates, with a single "no template control (NTC)" for each. As internal control to assess the integrity of the different RNAs and to confirm the success of the reverse-transcription reaction, primers for the housekeeping gene *Bcas2* were employed in the amplification reaction (Table 12).

The RT-qPCR reactions were run in 96-well optical reaction plates using the following conditions (Tables 41 and 42) with a melting curve analysis to assess whether the intercalating dye qPCR assays produced single specific products. For each target gene, all the primers were designed to span an exon-exon junction (Table 12).

Table 41. RT-qPCR reaction solution per well

	Volume	***Final concentration***
SYBR® Premix Ex Taq™ II	5 µl	1X
Primer Forward+Reverse (10µM)	0.4 µl	400nM
Template (cDNA)	2 µl	1 ng/µl
H2O (Braun)	2.6 µl	
Final volume	10 µl	

Table 42. Cycling conditions for the RT-qPCR

	Temperature	***Time***	***Number of cycles***
Holding Stage	95 ºC	30 seconds	1 cycle
Cycling stage	94 ºC	15 seconds	40 cycles
	60 ºC	60 seconds	
	72 ºC	30 seconds	

Melt curve stage	60 ºC	15 seconds	1 cycle
	95ºC	15 seconds	1 cycle
	20ºC	10 seconds	1 cycle

2.2.2.4.2 Electroporation program test

According to the manufacturer's recommendations a set of four pre-selected Nucleofector™ programs were tested with the P3 Primary Cell 4D-Nucleofector™ Kit (section Kits). The optimization was performed with the 100µl single Nucleocuvette™ Format. The electroporation was carried out with $4*10^6$ primary cortical neurons, 300nM NeuroD2 siRNA in 100µl Nucleofector solution following the manufacturer's recommendations.

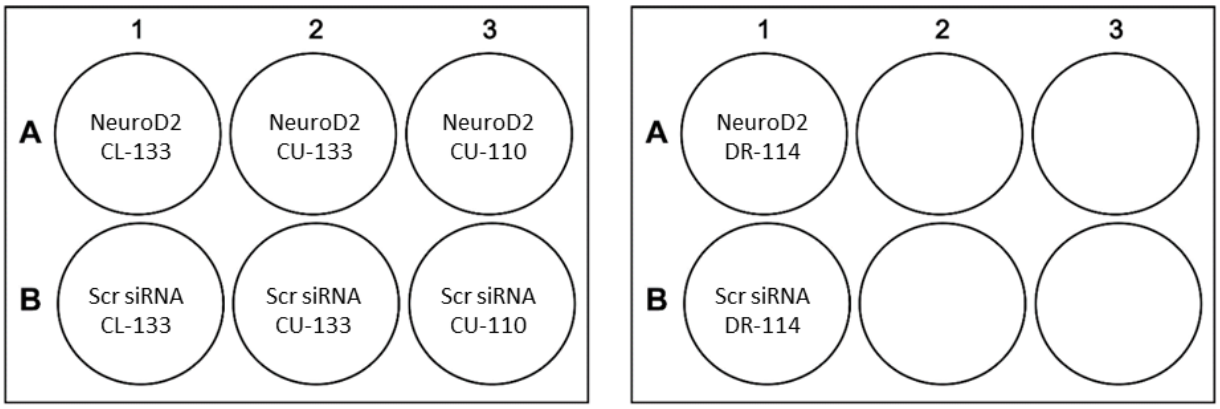

Figure 21: Scheme of the 6-well plates design for the electroporation program test. Four different programs were selected for the test. One well was electroporated with NeuroD2 siRNA, and another one with the pool of non-targeting siRNA for each selected program. The four programs were provided by the Nucleofector™.

Before the electroporation, two 6-well plates were coated with poly-L-ornithine and laminin (see section 2.2.1.1), followed by plate equilibration with the cell culture media (section Solutions and Buffers).

At the moment of the nucleofection, the entire supplement, provided with the kit, was added to the Nucleofector™ Solution, the 4D-Nucleofector™ System was started and the selected programs were uploaded for optimization: CL-133, CU-133, CU-110 and DR-114. An aliquot of culture medium was pre-warmed to 37°C for a later use.

300nM aliquots of NeuroD2 siRNA and non-targeting siRNA (21µl) were prepared in eppendorfs to be electroporated. Afterwards, cell density was counted and aliquots of $4*10^6$ primary cortical neurons were prepared in 15ml Falcons. Cell aliquots were centrifuged at 80xg for 5 minutes at room temperature. The supernatant was discarded completely and cell pellet was resuspended in 100µl 4DNucleofector™ Solution.

The cell solutions were quickly mixed with the siRNA and transferred into the Nucleocuvette™ Vessels. The Nucleocuvette™ Vessel were placed into the retainer of the 4D-Nucleofector™ X Unit with the lid closed. The Nucleofection™ Process was started by pressing the “Start” on the display of the 4D-Nucleofector™ Core Unit.

After each run was successfully completed, 100µl RPMI media was added to the cuvettes and they were placed into the incubator for 6 minutes at 37ºC for a recovery step. Afterwards, cells were resuspended with 500 µl pre-warmed medium and they were carefully plated and kept in the incubator (37ºC, 8% CO_2).

48 hours after the electroporation, cells were harvested (section 2.2.1.6) and the RNA isolation, reverse transcription and the expression analysis of the transcription factors was performed as described in section 2.2.2.4.1.

2.2.2.4.3 siRNA electroporation

The siRNA electroporation into primary cortical neurons to knockdown the transcription factors and analyze the changes in Rbfox1 expression levels was performed as described above (section 2.2.5.1) using the Nucleofector™ Program CU-133.

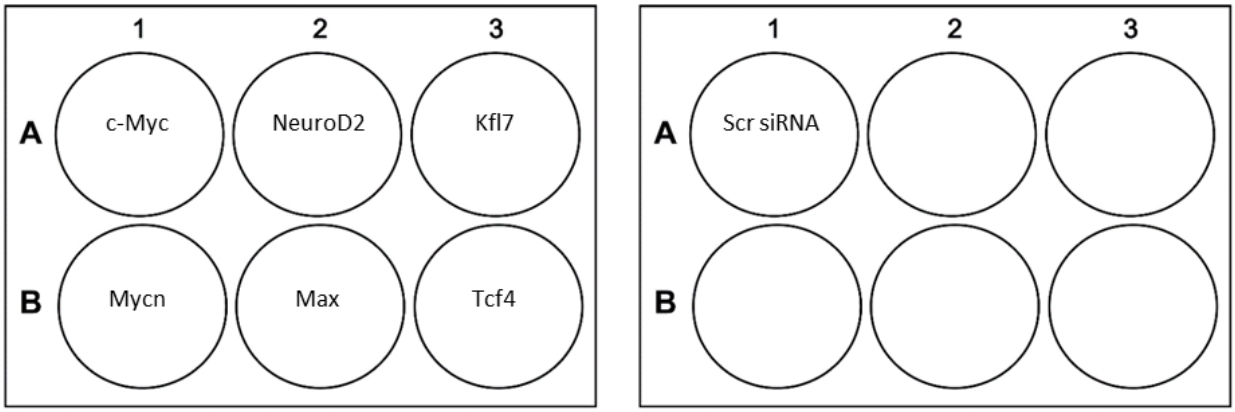

Figure 22. Designed of the plates for the siRNA electroporation. One well was electroporated with a pool of siRNA against the transcription factors (Table 16). Non-targeting siRNA was used as a control.

RNA isolation, reverse transcription and the RT-qPCR was performed as described in section 2.2.2.2.4.1.

3. Results

3.1 Expression analysis of the *Rbfox1* gene

RBFOX1 is an RNA-binding protein that regulates pre-mRNA splicing events in specific cell types including neurons. The encoding gene contains a large noncoding part in its 5' end with at least four alternative promoters, 1B, 1C, 1D (brain-specific) and 1E (muscle-specific). These promoters drive the expression of different *Rbfox1* transcripts, which differ in their 5'UTR but not in their coding exons (Figure 7 and Figure 23). CNVs that have been found in ASD patients or other neurodevelopmental disorders were typically located in the 5'-noncoding region of the *RBFOX1* gene and typically contained 5'-UTR exons and putative promoter or enhancer regions (Figure 4) of single *RBFOX1* transcript isoforms. Because these regions have not been functionally studied the CNV's impact on *RBFOX1* expression and their pathogenicity was unclear.

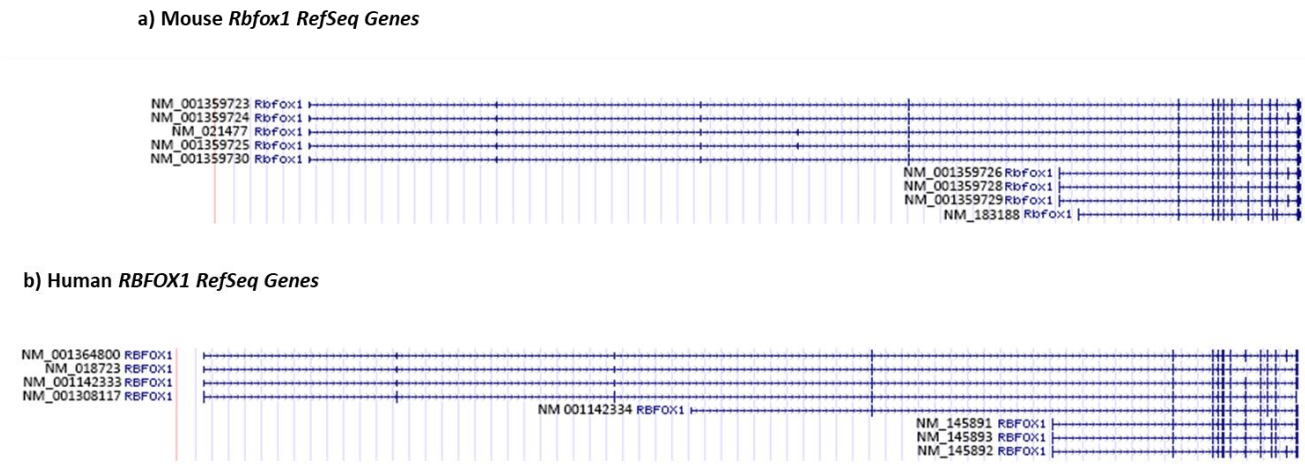

Figure 23. Comparison of the mouse *Rbfox1* and human *RBFOX1* gene. a) Mouse *Rbfox1* gene and all the transcripts annotated in the RefSeq database. b) Human *Rbfox1* gene and all the transcripts annotated in the RefSeq database. (Modified from UCSC Genome browser).

The goal of this thesis was to study the transcriptional regulation of the *Rbfox1* gene in the mouse brain and to identify transcription factors that bind to the *Rbfox1* promoters and regulate its expression. To better understand how this gene is transcriptionally regulated in the mouse cortex, an expression analysis of the three different brain-specific *Rbfox1* transcript isoforms was carried out. The overall structure of the *RBFOX1* gene is conserved between human and mouse (Figure 23). Therefore, the mouse was used as a model system.

3.1.1 *Rbfox1* expression analysis in mouse cortical development

As a first step, expression analysis of the different *Rbfox1* transcript isoforms during cortical development was carried out by RT-qPCR. For this purpose, transcript-specific primers were used in the RT-qPCR experiments (Table 11). In addition, a primer pair binding to exons 20 and 21, located in the 3'-part of the gene was used for comparison. This primer pair detects the majority of the Rbfox1 transcripts. A minor Rbfox1 transcript isoform containing an alternative 3' terminal exon was not covered by this primer pair. Due to the extensive alternative splicing in the *Rbfox1* gene it was not possible to design primers covering all transcript isoforms. The *Rbfox1* expression analysis was performed in cortex at different embryonic stages to study the expression pattern of the different transcripts during cortical development. Cerebral cortices of mouse embryos were isolated. RNA isolation and cDNA synthesis was carried out for the different samples, taken at different embryonic stages, starting at E13.5 (peak of neurogenesis) up to the moment of birth (P0). The analysis was performed with four biological replicates. Expression of the housekeeping gene *Gapdh* was used for normalization.

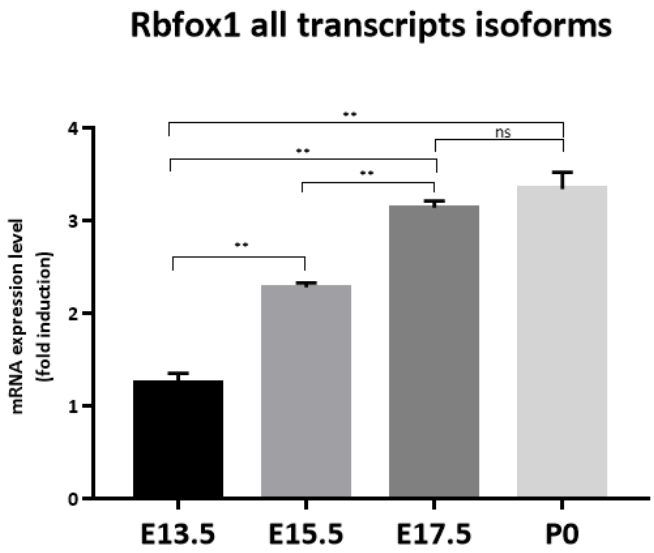

Figure 24. mRNA expression analysis of total *Rbfox1* in the cerebral cortex during embryonic development. Total *Rbfox1* expression levels during cortical development were analyzed with primers binding to exons 20 and 21 which the majority of transcript isoforms have in common. A significant upregulation of the total *Rbfox1* expression levels were observed during embryonic development in the cortex. N=4. Data are shown as the mean ± SEM. **p<0.01; Student's t-test; A paired two-tailed Student t test was used. Expression levels are shown as fold induction compared to E13.5 (peak of neurogenesis).

Expression analysis of the total *Rbfox1* levels showed a significant upregulation during cortical development, reaching the highest expression levels at the time of birth (P0). *Rbfox1* expression, relative to E13.5, revealed an increase of 1.8 fold at E15.5, 2.5 fold at E17.5 and 2.7 fold at P0. Additionally, a significant increase of 1.3 fold was observed between E15.5 and E17.5. (Figure 24).

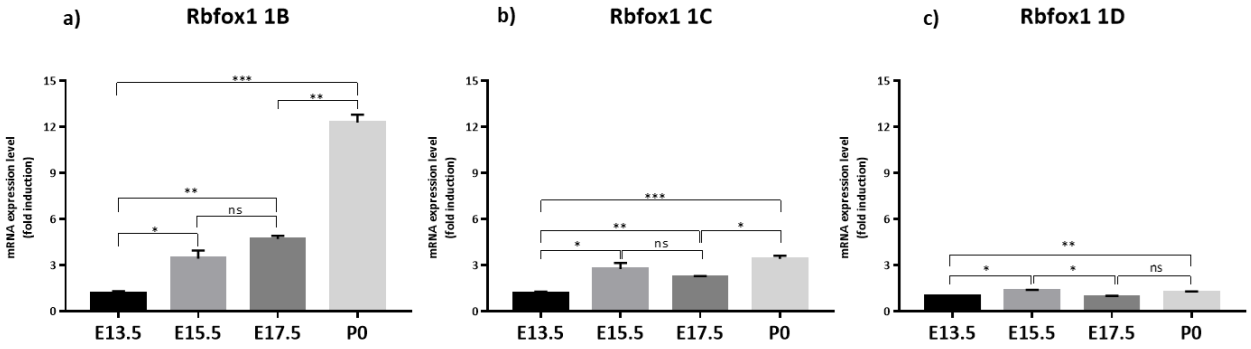

Figure 25. *Rbfox1* transcript-specific expression analysis in the cerebral cortex during embryonic development. a) mRNA expression analysis of the *Rbfox1* transcript 1B during cortical development. b) mRNA expression analysis of the *Rbfox1* transcript 1C during cortical development. c) mRNA expression analysis of the *Rbfox1* transcript 1D during cortical development. Data are shown as the mean ± SEM. n.s. not significant, *p < 0.05, **p<0.01, ***p<0.005; A paired two-tailed Student t test was used. Expression levels are shown as fold induction compared to E13.5 (peak of neurogenesis).

Transcript-specific *Rbfox1* expression analysis revealed a different expression pattern between the transcripts. A strong and significant upregulation of the Rbfox1 1B transcript was observed during cortical development, reaching the highest expression level at the time of birth (P0). Rbfox1 1B *e*xpression levels, relative to E13.5, revealed an increase of 2.9 fold at E15.5, 4 fold at E17.5 and 10.4-fold at P0 (Figure 25a).

Expression analysis of the Rbfox1 1C transcript revealed a slight upregulation of this transcript isoform during cortical development. Expression levels of Rbfox1 1C*,* relative to E13.5, revealed an increase of 2.4 fold at E15.5, 1.9 fold at E17.5 and 3 fold at P0 (Figure 25b).

Expression analysis of Rbfox1 1D transcript isoform showed more stable levels of this mRNA during cortical development. However, relative expression to E13.5 revealed a significant

increase of 1.3 fold between E13.5 and E15.5, and a 1.3 fold increase between E13.5 and P0 (Figure 25c).

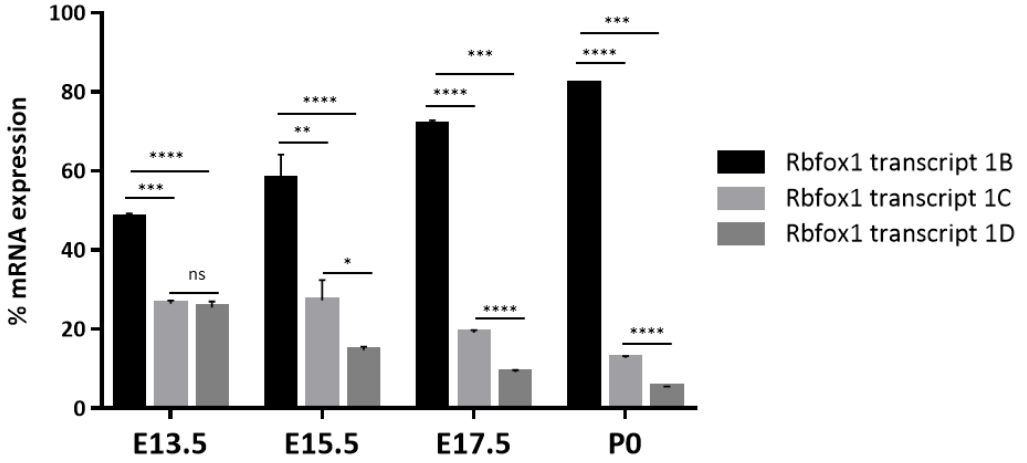

Figure 26. Direct comparison of the expression levels of the different *Rbfox1* transcript isoforms in the cerebral cortex at different embryonic stages. . The sum of expression of Rbfox1 1B, Rbfox1 1C and Rbfox1 D was set to 100%. A probe based RT-qPCR was carried out and primer efficiencies were considered in all calculations for generating reliable results when comparing different primer sets which each other. N=4. Data are shown as the mean ± SEM. n.s. not significant, *p < 0.05, ***p<0.005, ****p<0.001; Student t test was used.

Since we used probe-based qPCR assays we were able to compare the transcript levels of the different *Rbfox1* isoforms directly after correcting for differences in primer efficiencies (section Materials and Methods).

Percentage of expression of each *Rbfox1* transcript isoform was calculated, revealing that the Rbfox1 1B transcript was the highest contributor to the total *Rbfox1* expression during cerebral cortex development. Analysis confirmed that *Rbfox1* 1B expression is upregulated during cortical development, whereas Rbfox1 1D expression is downregulated (Figure 26).

At the peak of neurogenesis (E13.5), the Rbfox1 1B transcript isoform accounts for 48% of total *Rbfox1* expression. At that embryonic stage, Rbfox1 1C and Rbfox1 1D were expressed at similar levels, 26% and 25.5% respectively. At E15.5, approximately 58% of expression was observed with Rbfox1 1B, followed by Rbfox1 1C with a 27%, and Rbfox1 1D with a 15% expression. At E17.5, the Rbfox1 1B transcript isoform accounts for 72% of total Rbfox1, followed by Rbfox1 1C with a 19% expression, and Rbfox1 1D with a 9% expression rate. Lastly, P0 was identified as the embryonic stage where the Rbfox1 1B expression was the highest, 82%. 13% of expression was detected for Rbfox1 1C and a significantly lower expression rate was observed for Rbfox1 1D (5%) (Figure 26).

A transcript-specific *in situ* hybridization experiment was carried out to support the *Rbfox1* expression analysis data obtained with the RT-qPCR. Transcript-specific probes, complementary to the mRNA, were generated to perform this experiment. Riboprobes against Rbfox1 1B, Rbfox1 1C and Rbfox1 1D mRNA were aimed to be generated, but unfortunately, due to the great similarity between the different *Rbfox1* transcript isoforms it was impossible to generate a probe for each transcript with a high specificity. Only a probe to detect Rbfox1 1B transcript and another one to detect all the Rbfox1 isoforms were generated with a high specificity. Primers to generate the probe against Rbfox1 1B bound to the first exon (exon 1B), and the ones used to generate the probe to detect all transcripts isoforms bound to coding exon 6, which all transcript isoforms have in common.

The *in situ* hybridization experiments were performed with sections from embryonic (E15) brain.

The RNA *in situ* hybridization experiment with a riboprobe detecting total *Rbfox1* (all transcripts) gave a positive signal in the cortical plate of the cerebral cortex and spinal cord (Figure 27.d),

whereas Rbfox1 1B expression could only be detected in the cortical plate of the cerebral cortex (Figure 27a). A close-up of the cortical plate showed a strong signal with both, *Rbfox1* (all transcripts) and Rbfox1 1B (Figure 27b and 27e respectively). Sense probe generated against the total Rbfox1 mRNA was used as a negative control, giving no signal in the embryonic mouse brain (E15) (Figure 28).

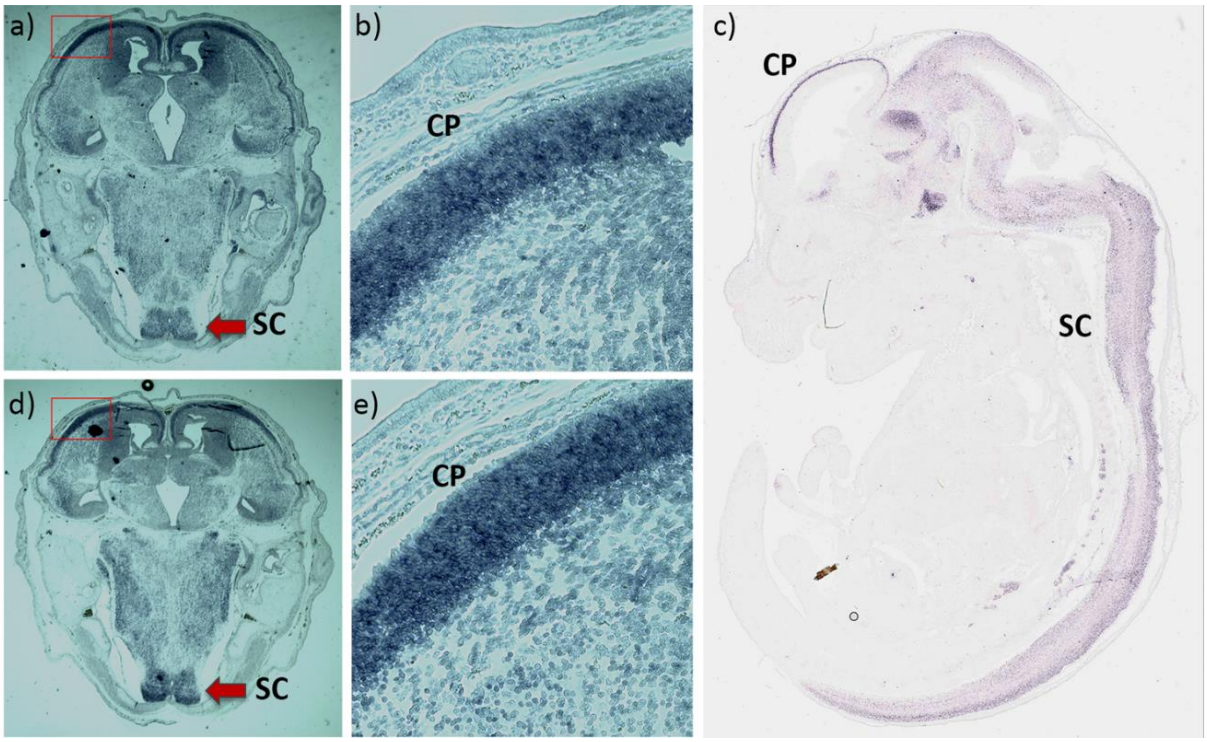

Figure 27. RNA *in situ* hybridization of Rbfox1 in the embryonic mouse brain (E15). a) RNA *in situ* hybridization experiment using a riboprobe against Rbfox1 1B, where strong signal was observed in the cortical plate and in the spinal cord. b) Close-up of the cerebral cortex showed a high expression of the Rbfox1 1B in the cortical plate (40X). c) Rbfox1 *In situ* hybridization experiment adopted from GenePaint, where strong signal was observed in the cortical plate and in the spinal cord. d) RNA *in situ* hybridization experiment using a riboprobe against Rbfox1 all transcripts isoforms, where a positive signal was observed in the cerebral cortex and spinal cord. d) Close up of the cerebral cortex where a high expression of the Rbfox1 all transcripts was observed in the cortical plate (40X). Red boxes indicate amplified regions. CP indicates cortical plate; SC indicates spinal cord.

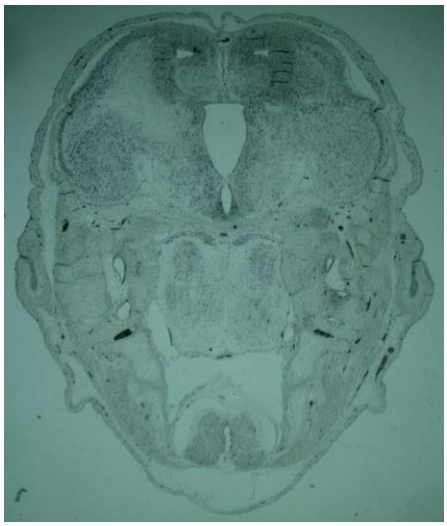

Figure 28. RNA *in situ* hybridization negative control for the embryonic mouse brain (E15). A sense Rbfox1 riboprobe was used as a negative control, showing no binding in the E15 embryonic brain.

Results obtained from RNA *in situ* hybridization experiment in mouse E15 brain correlate with the expression analysis data obtained with the RT-qPCR, where embryonic cortices were used to analyze the mRNA levels at different embryonic days. Additionally, our *in situ* hybridization results are validated by the Rbfox1 *In situ* hybridization experiment published on GenePaint (Figure 27c). The published experiment was carried out using an RNA probe against Rbfox1 1B*,* and expression was observed in the cortical plate and in the spinal cord (Figure 27c). Likewise, I have also detected expression of Rbfox1 1B in the same brain regions during embryonic development (Figures 27a and 27b).

3.1.2 *Rbfox1* expression analysis in the juvenile brain

*Rbfox1 t*ranscript-specific expression analysis in juvenile brain was carried out to elucidate the expression pattern of the different Rbfox1 transcripts in different brain regions. The analysis was performed with three different biological replicates. Expression of the housekeeping gene *Gapdh* was used for normalization.

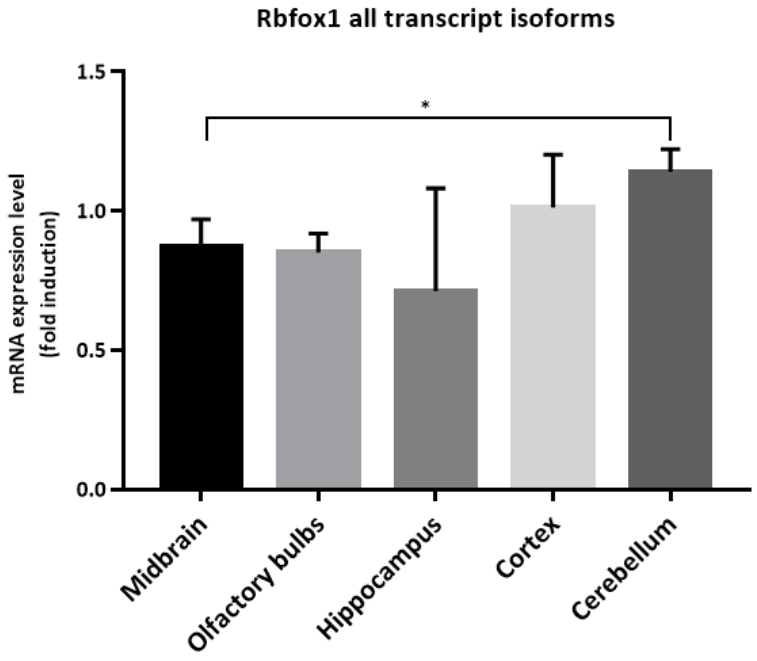

Figure 29. mRNA expression analysis of total *Rbfox1* in different brain regions in the juvenile mouse brain. Total *Rbfox1* expression levels in different brain regions were analyzed with primers binding to exons 20 and 21 which the majority of transcripts isoforms have in common. Similar levels of *Rbfox1* expression were observed in the different regions analyzed. A significantly higher expression was observed in the cerebellum when compared to midbrain. N=3. Data are shown as the mean ± SEM. *p<0.05; Student's t-test; A paired two-tailed Student t test was used. Expression levels are shown as fold induction compared to midbrain.

Expression levels of the total *Rbfox1* in the juvenile brain were similar across the majority of the analyzed brain regions. Only the cerebellum exhibited a significantly increased (1.3 fold) expression of *Rbfox1* relative to midbrain (Figure 29).

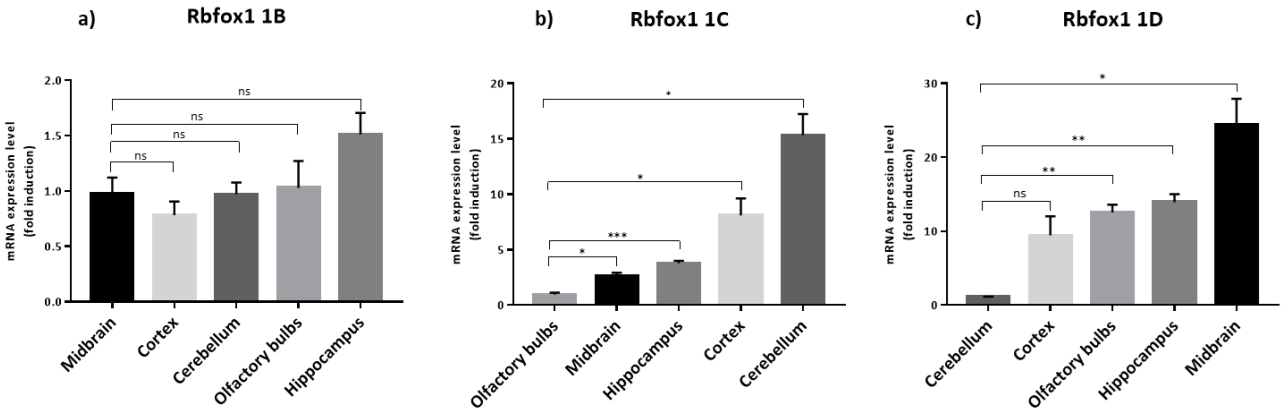

Figure 30. *Rbfox1* transcript-specific expression analysis in different brain regions in the juvenile mouse brain. a) mRNA expression analysis of the Rbfox1 1B transcript in juvenile brain b) mRNA expression analysis of the Rbfox1 1C transcript in juvenile brain. c) mRNA expression analysis of the Rbfox1 1D transcript in juvenile brain. N=3. Data are shown as the mean ± SEM. n.s. not significant, *p < 0.05, **p<0.01, ***p<0.005; A paired two-tailed Student t test was used. Expression levels are shown as fold induction compared to midbrain for Rbfox1 1B, compared to olfactory bulbs for Rbfox1 1C and compared to cerebellum for Rbfox1 1D.

Transcript-specific *Rbfox1* expression analysis showed differential expression between different brain regions for some of the transcript isoforms (Figure 30).

Rbfox1 1B transcript showed similar mRNA levels in the brain regions analyzed (Figure 30a).

Rbfox1 1C transcript was differentially expressed between the brain regions analyzed. Rbfox1 1C relative expression to olfactory bulbs, revealed a significantly 1.7 fold higher expression in midbrain, a 2.9 fold higher expression in the hippocampus, and a 7.1 fold higher expression in the cortex. The highest Rbfox1 1C expression was observed in the cerebellum, where this transcript isoform was 14.5 times more expressed than in olfactory bulbs (Figure 30b).

Expression of Rbfox1 1D revealed different expression levels in the brain regions included in the analysis. Rbfox1 1D relative expression to cerebellum, revealed a 8.3 fold higher expression in cortex, a 11.2 fold higher expression in the olfactory bulbs, and a 12.8 fold higher expression in hippocampus. The highest Rbfox1 1D expression was observed in the midbrain, where this transcript isoform was 23.3 times more expressed than in the cerebellum (Figure 30c).

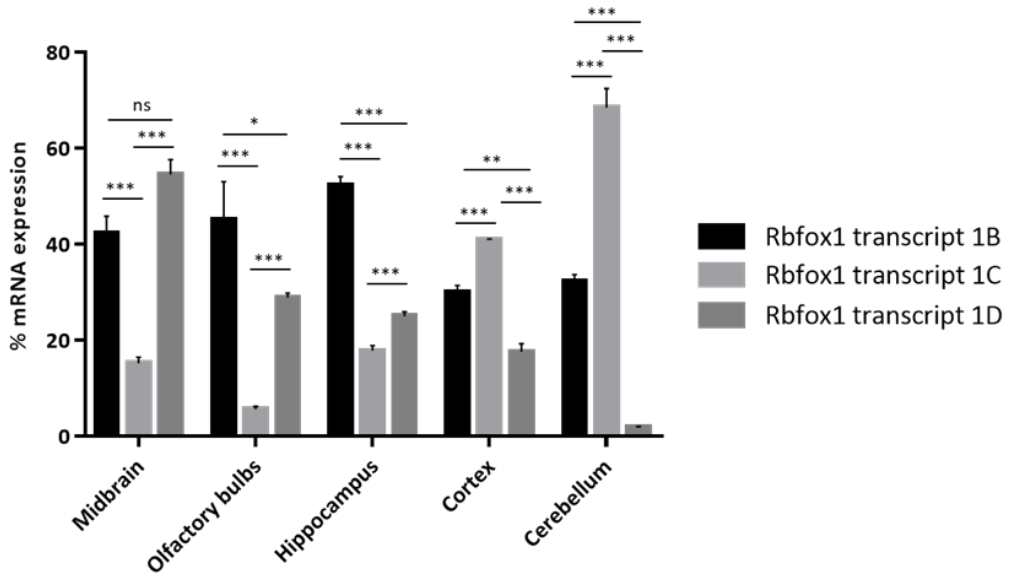

Figure 31. Direct comparison of the expression levels of the different *Rbfox1* transcript isoforms in different brain regions. The sum of expression of Rbfox1 1B, Rbfox1 1C and Rbfox1 D was set to 100%. A probe based RT-qPCR was carried out and primer efficiencies were considered in all calculations for generating reliable results when comparing different primer sets which each other. N=3. Data are shown as the mean ± SEM. n.s. not significant, *p < 0.05, **p<0.01; A paired two-tailed Student t test was used. Expression levels are shown as fold induction compared to midbrain.

Since we used probe-based qPCR assays we were able to compare the transcript levels of the different Rbfox1 isoforms directly after correcting for differences in primer efficiencies (section Materials and Methods). Percentage of expression of each Rbfox1 transcript isoform in the brain

regions analyzed was calculated, revealing different expression patterns of the *Rbfox1* transcripts across the brain regions analyzed (Figure 31).

In midbrain, expression of Rbfox1 1D transcript isoform accounts for 54.5% of total *Rbfox1* expression, being the transcript with the highest mRNA levels in this brain region. In that same brain region, 42.3% of expression was observed with Rbfox1 1B, followed by Rbfox1 1C with a 15.2% of expression.

In olfactory bulbs expression analysis revealed that Rbfox1 1B was the transcript with the highest mRNA levels in this brain region, with 45.2% of expression. On the contrary, Rbfox1 1C was detected to have the lowest mRNA levels, with 5.6% expression rate. 28.9% of expression was detected for Rbfox1 1D in this brain region.

In hippocampus expression analysis revealed that Rbfox1 1B was the transcript with the highest mRNA levels with a 52.2% expression rate, followed by Rbfox1 1D with 25% of expression. Rbfox1 1C was identified as the transcript with the lowest mRNA levels in this brain region, with 17.8% expression rate.

In cortex, Rbfox1 1C was the most expressed transcript isoform with an expression rate of 41%, followed by Rbfox1 1B with approximately 30%. Rbfox1 1D was the less expressed transcript in this brain region with 17.6% expression.

In cerebellum Rbfox1 1C transcript isoform was identified as the most expressed transcript isoform, with an expression rate of 68.4%. On the other hand, Rbfox1 1D was detected to have the lowest expression, accounting only for 1.9% of the total *Rbfox1* expression. Rbfox1 1B showed an expression of 32.2% in the cerebellum (Figure 31).

A transcript-specific *in situ* hybridization experiment was carried out to support and supplement the *Rbfox1* expression analysis data obtained with the RT-qPCR in mature mouse brain. The experiment was performed with 6 weeks-old mouse brain sections.

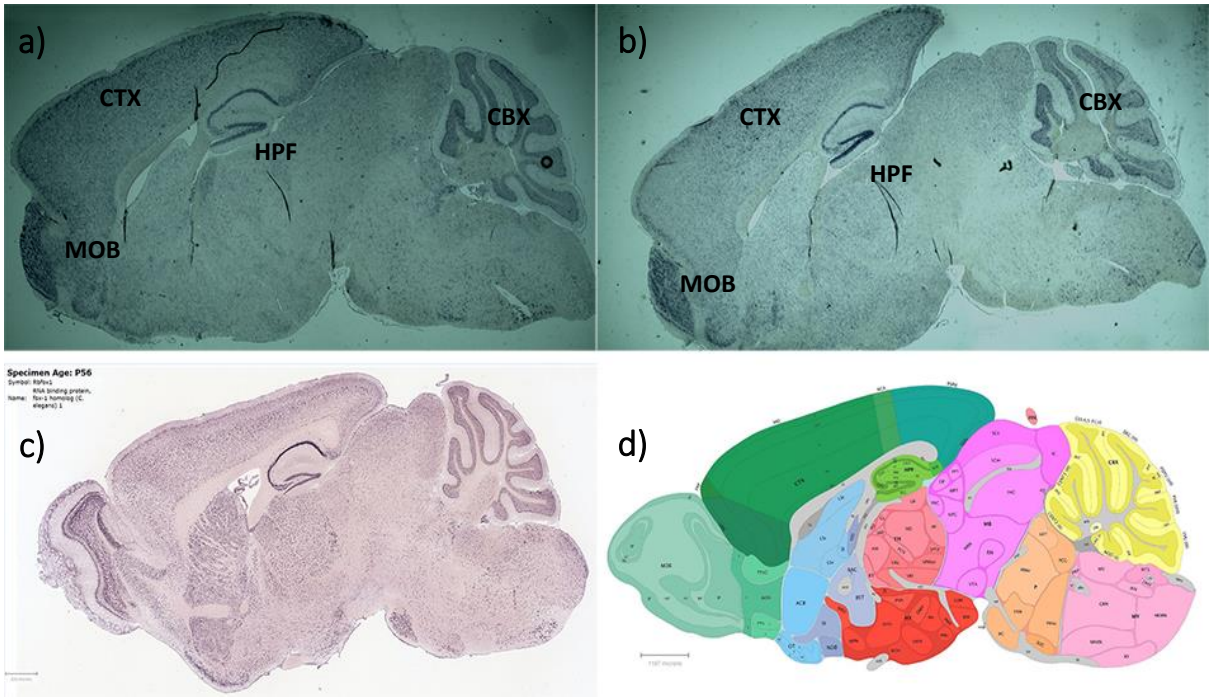

Figure 32. RNA *in situ* hybridization of Rbfox1 *in* juvenile mouse brain. a) *In situ* hybridization experiment using a riboprobe against Rbfox1 transcript 1B. b) *In situ* hybridization experiment using a riboprobe against total Rbfox1 (all transcript isoforms). c) Rbfox1 *In situ* hybridization experiment adopted from the Allen Brain Atlas. d) Schematic representation of the mouse brain (P56) indicating the different brain regions in different colors (Adopted from Atlas Brain map). CTX= cerebral cortex, CBX= cerebellar cortex, MOB= main olfactory bulb, HPF= hippocampal formation.

RNA *in situ* hybridization experiment carried out using a riboprobe against Rbfox1 1B transcript isoform showed expression in the cortex, hippocampus, cerebellum and olfactory bulbs, supporting the expression analysis data obtained with RT-qPCR analysis (Figure 32a). A positive signal in the granular layer of the cerebellar cortex is shown in picture 33a. A close-up of the granular layer showed expression in the folium-tuber vermis (VII), a region of the cerebellar cortex, where expression of Rbfox1 1B was observed in the Purkinje cells in the molecular layer (Figure 33.b). In addition, expression of Rbfox1 1B was also observed in the cerebral cortex and olfactory bulb (Figure 33.c and 33.d). Lastly, expression of Rbfox1 1B was observed in the hippocampal formation, where a strong signal in the molecular layer of the dentate gyrus and in the pyramidal layer was observed (Figures 33f. and 33g.).

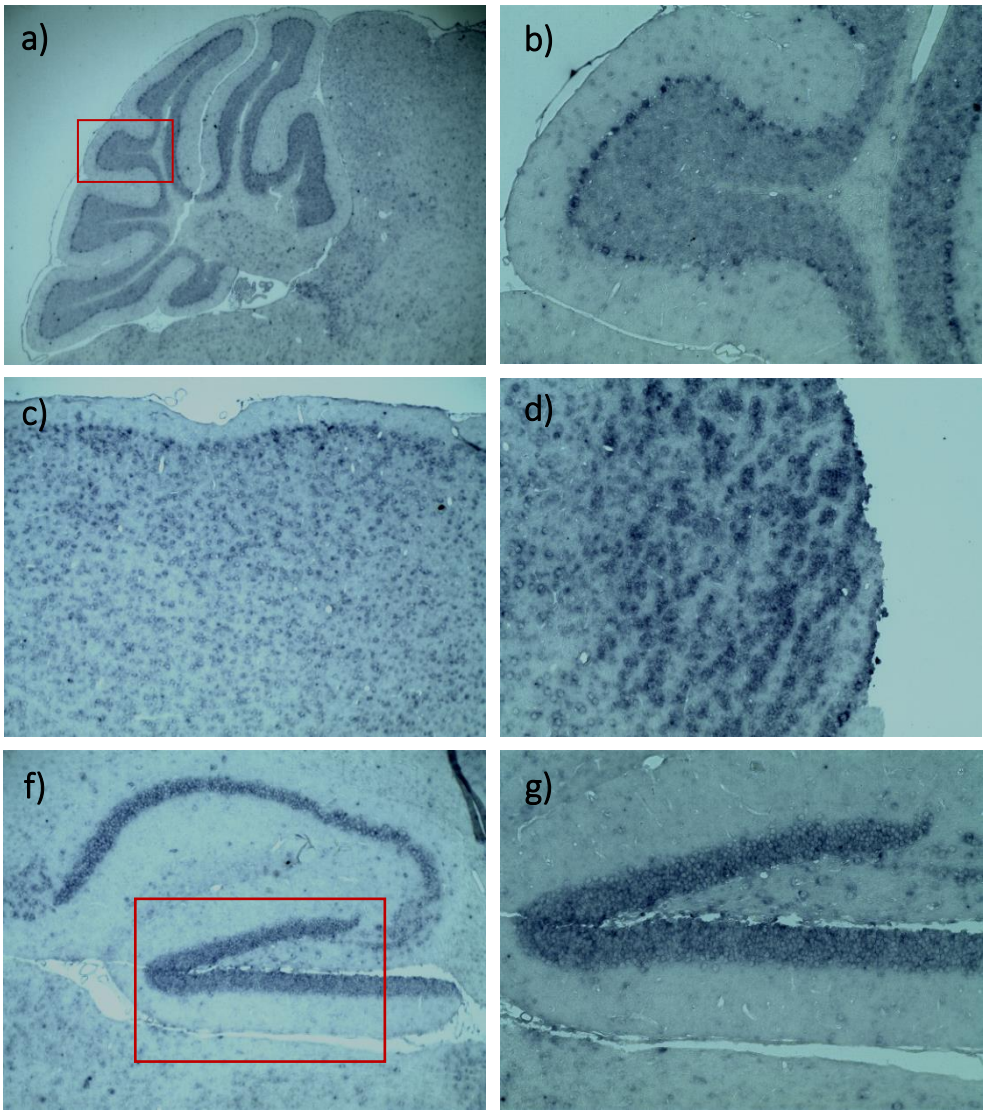

Figure 33. Close up of the *in situ* hybridization positive regions in the juvenile brain using a riboprobe against Rbfox1 1B. a) Positive expression signal for *Rbfox1* transcript 1B observed in the cerebellum (10X). b) Close-up of the cerebellar cortex, where expression of Rbfox1 1B was observed in the granular layer and Purkinje cells (40X) c) Close-up of the cerebral cortex where a positive signal for the Rbfox1 1B expression was observed (20X). d) Close-up of the olfactory bulb (20X). f) Close-up of the hippocampal formation, where a strong positive signal for Rbfox1 1B was observed (20X). g) Close-up of the dentate gyrus where a strong positive signal was observed for Rbfox1 1B. Red boxes indicate amplified regions (40X).

RNA *in situ* hybridization experiment using a riboprobe against total *Rbfox1* (all transcript isoforms) showed a positive signal in the cortex, cerebellum, hippocampus and olfactory bulb (Figure 32b.), supporting the expression analysis data obtained with the RT-qPCR. A positive signal for *Rbfox1* expression was observed in the granular layer of the cerebellar cortex (Figure 34a.). A close-up to the granular layer of the Declive region in the cerebellar cortex showed a positive signal in the Purkinje cells and in the molecular layer (Figure 34b.). In addition, expression of total *Rbfox1* was also observed in the cerebral cortex and olfactory bulbs (Figures 34c. and 34d.). Lastly, a positive signal was also observed in the hippocampal formation giving a strong signal in the molecular layer of the dentate gyrus and in the pyramidal layer, indicating a high expression of *Rbfox1* in this brain region (Figures 34f. and 34g.).

In conclusion, the results obtained from the *in situ* hybridization experiments with riboprobe against total *Rbfox1* mRNA are supported by the results published on the Allan Brain Atlas *Rbfox1 in situ* hybridization experiment, where a positive signal for *Rbfox1* expression was also detected in the cortex, cerebellum, hippocampus and olfactory bulbs (Figure 32c.).

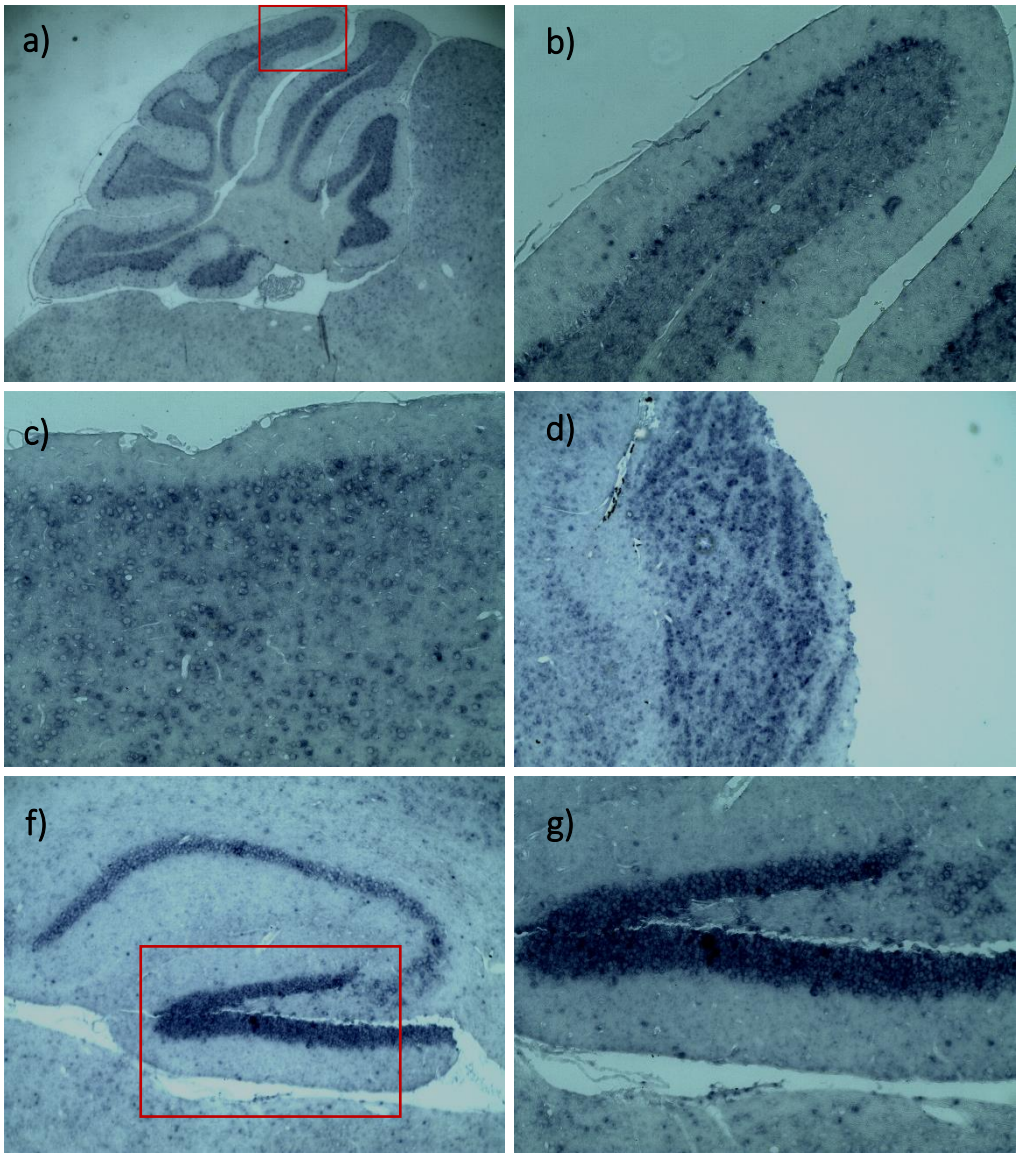

Figure 34. Close up of the *in situ* hybridization positive regions in the juvenile brain using a riboprobe against the total *Rbfox1* (all transcript isoforms). a) A positive signal for *Rbfox1* expression was observed in the cerebellum (10X). b) Close-up of the cerebellar cortex, where the signal in Purkinje cells and in the molecular layer was observed (40X). c) Close-up of the cerebral cortex, where a positive expression for *Rbfox1* was also observed. (40X) d) A positive signal for *Rbfox1* expression was observed in the olfactory bulb (40X). f) Hippocampal formation, where a strong signal for *Rbfox1* expression was also observed (20X). g) Amplification of the dentate gyrus where a strong signal was observed. Red boxes indicate the amplified regions.

Negative control was performed using the sense probe generated for the Rbfox1 1B, showing no binding in any brain region (Figure 35).

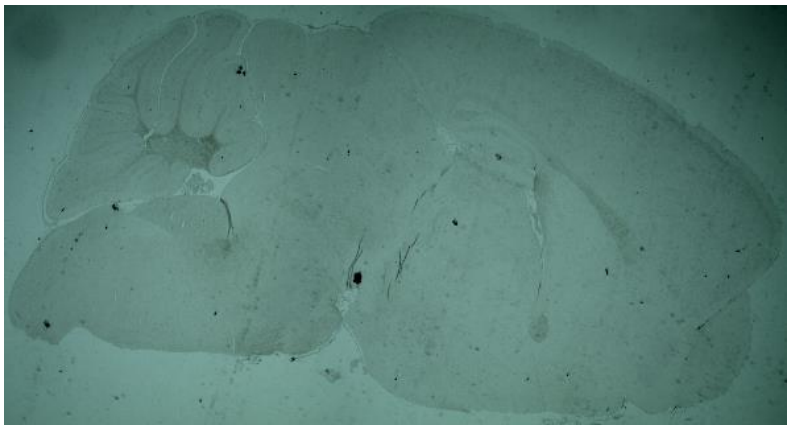

Figure 35. RNA *in situ* hybridization negative control for the juvenile mouse brain. A sense Rbfox1 riboprobe was used as a negative control, showing no binding in the juvenile brain.

3.2 Analysis of *Rbfox1* promoters' activity

To study the activity of the alternative promoter regions that drive expression of *Rbfox1* transcript isoforms 1B, 1C and 1D in the brain, luciferase assays were performed. The alternative promoter regions were named promoter 1B, 1C and 1D according to the transcript isoform they regulated. Since these promoters had not been completely identified and characterized before the onset of this project, fragments of the three different putative promoter regions were amplified from genomic DNA of cerebral cortex of a 6 weeks-old mouse by PCR , and cloned into the Luciferase reporter vector pGL4.10 [luc2] (section Vectors).

Ideally luciferase assays should be performed in a cell line with high endogenous *Rbfox1* expression to ensure high activity of the *Rbfox1* promoter fragments. To identify a suitable

cellular model an *Rbfox1* expression analysis was performed in P19 cells, primary NPCs and primary cortical neurons.

3.2.1 *Rbfox1* expression analysis in different cell types

To study the expression of the different *Rbfox1* transcripts, as well as the total *Rbfox1* expression (all transcripts isoforms) an *Rbfox1 t*ranscript-specific expression analysis by RT-qPCR was carried out in P19 cells, primary NPCs and primary cortical neurons at DIV 4 and DIV 7. The primers used were the same as described in results section 3.1 (see also table 11).

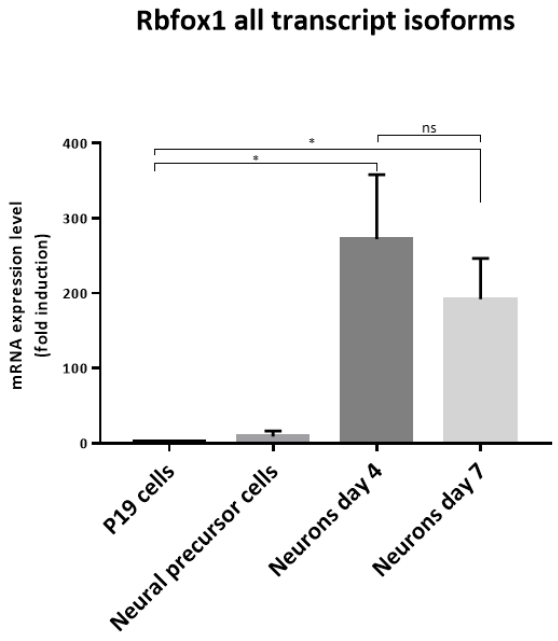

Figure 36. mRNA expression analysis of total *Rbfox1* in different cell lines. A high expression of *Rbfox1* was observed in neurons after 4 days (DIV4) and 7 days (DIV7) in culture. No significant differences were observed between DIV4 and DIV7. N=4. Data are shown as the mean ± SEM. *p<0.05; Student's t-test; An Unpaired two-tailed Student t test was used. Expression levels are shown as fold induction compared to P19 cells.

Expression analysis of the total *Rbfox1* showed a high expression in primary cortical neurons, at DIV4 and DIV7. However, no significant differences were observed in the mRNA levels between DIV4 and DIV7 (Figure 36).

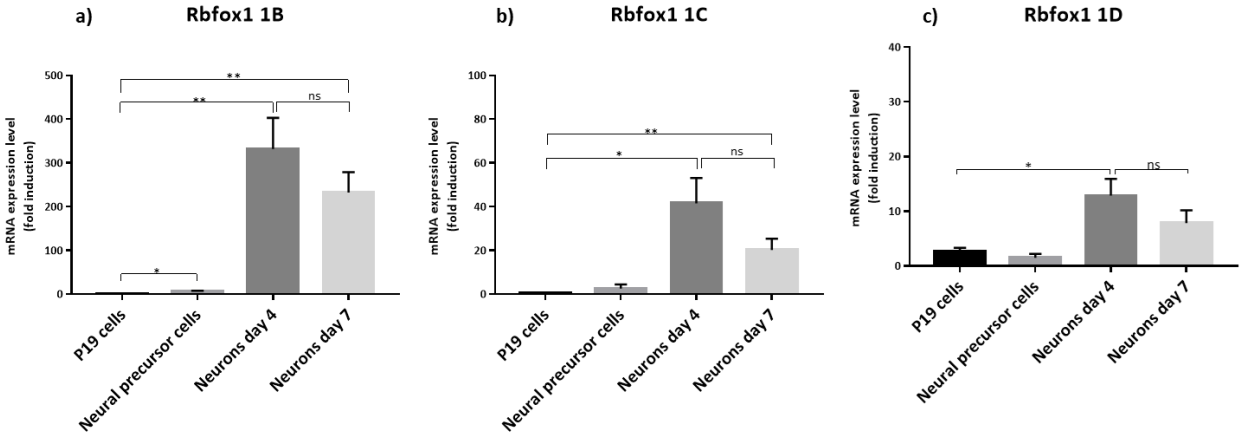

Figure 37. *Rbfox1* transcript-specific expression analysis in different cell lines. a) mRNA expression levels of Rbfox1 1B in P19 cells, NPCs and primary cortical neurons at DIV4 and DIV 7. b) mRNA expression levels of Rbfox1 1C in P19 cells, NPCs and primary cortical neurons at DIV4 and DIV 7. c) mRNA expression levels of Rbfox1 1D in P19 cells, NPCs and primary cortical neurons at DIV4 and DIV 7. N=4. Data are shown as the mean ± SEM. *p < 0.05, **p<0.01; An Unpaired two-tailed Student t test was used. Expression levels are shown as fold induction compared to P19 cells.

Rbfox1 transcript-specific expression analysis revealed a high expression of Rbfox1 1B, Rbfox1 1C and Rbfox1 1D in primary cortical neurons at DIV 4 and 7 (Figure 37). mRNA levels did not show any significant differences between DIV4 and DIV7. Compared to primary cortical neurons, *Rbfox1* expression was low in NPCs.

Altogether, the transcript-specific and the total *Rbfox1* expression analysis data suggested that primary cortical neurons were the most suitable cell host for the luciferase assays. No significant differences were observed between DIV4 and DIV7, therefore experiments were carried out at DIV4.

3.2.2 Identification of putative promoter regions in the *Rbfox1* gene

To identify the putative promoter regions in the *Rbfox1* gene we searched for conserved consensus sequences upstream of the alternative first exons of transcripts 1B, 1C and 1D among different species by *in silico* analysis. For Rbfox1 1B the region from −2147 base pairs to +1039, corresponding to UCSC chr16:5,881,851-5,886,629 on Mouse GRCm38/mm10 Assembly, contained several sequence blocks with a high evolutionary conservation in placental mammals (Figure 38a). For Rbfox1 1C the selected region, which had a high evolutionary conservation in placental mammals, spanned from −989 base pairs to +154, corresponding to UCSC chr16:6,348,047-6,349,505 on Mouse GRCm38/mm10 Assembly (Figure 38b). For Rbfox1 1D, the region having a high evolutionary conservation in placental mammals spanned 2359 nucleotides, corresponding to UCSC chr16:7,037,415-7,039,772 on Mouse GRCm38/mm10 Assembly (Figure 38c).

The selected DNA fragments were amplified by RT-PCR and subsequently cloned into the luciferase reporter vector pGL4.10 (Promega). Luciferase assays were performed in primary cortical neurons and luciferase activity was measured 24h upon transfection.

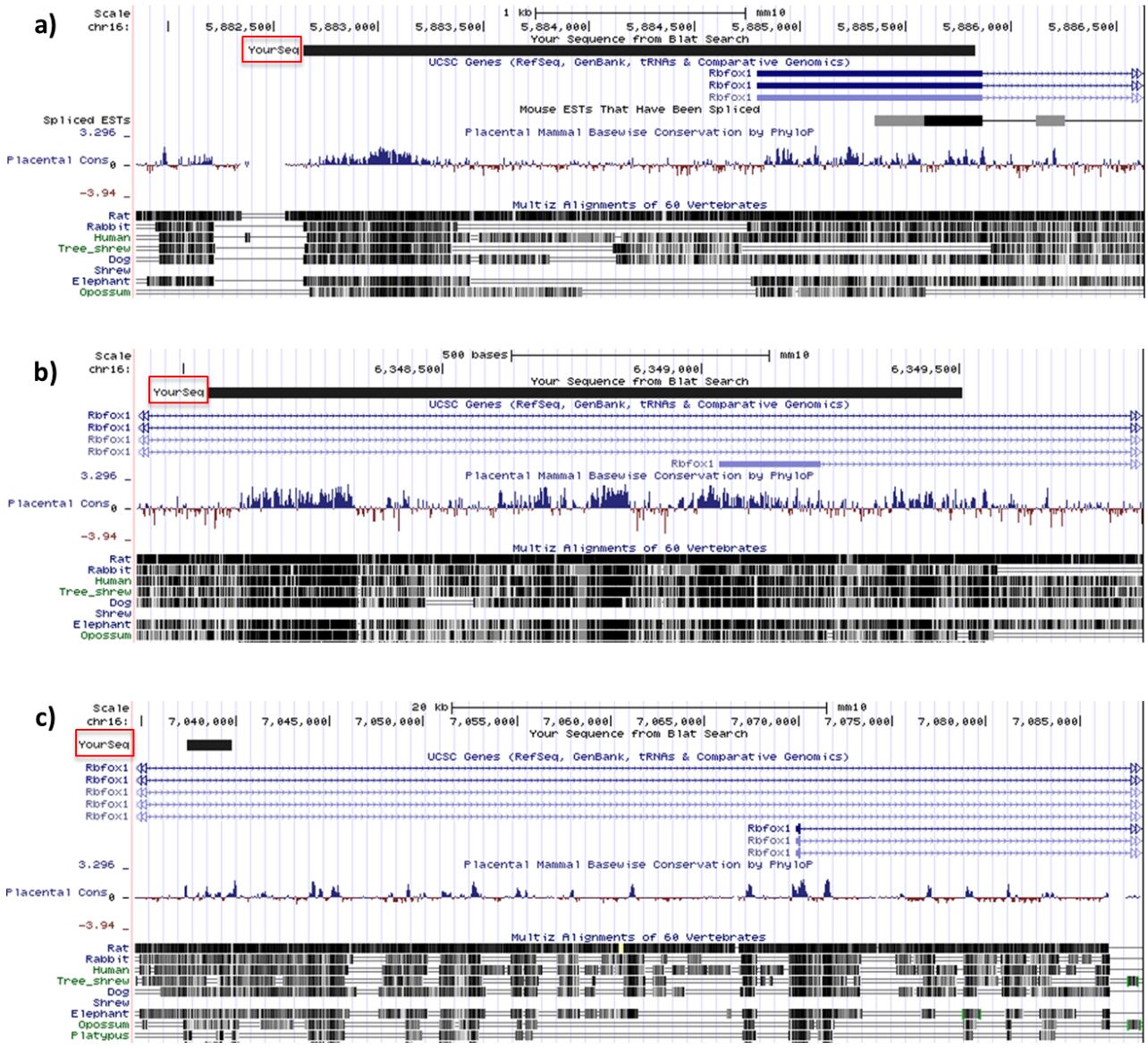

Figure 38. In silico analysis to determine the *Rbfox1* promoter region. A) Rbfox1 1B. b) Rbfox1 1C. c) Rbfox1 1D. Conservation in placental mammals is shown in blue below the gene. The conservation between different species is shown at the bottom of the image. A blast of the cloned promoter 1B, promoter 1C and promoter 1D fragments is shown (red box). Adapted from UCSC Genome Browser.

3.2.3 Analysis of the *Rbfox1* promoters' activity in cortical neurons

A luciferase assay was designed to analyze the activity of the brain-specific promoter fragments. Promoter 1B, promoter 1C and promoter 1D fragments (Figures 38a, 38b and 38c) were cloned into the luciferase reporter vector pGL4.10. Primary cortical neurons were used as a transfection host, and transfected after 3 days in culture. Finally, luciferase activity was measured 24 hours after transfection (see section methods). The renilla plasmid pRL-TK was used for normalization and transfection control. The promoter of miR-302 is silenced in neurons and was therefore used as a negative control.

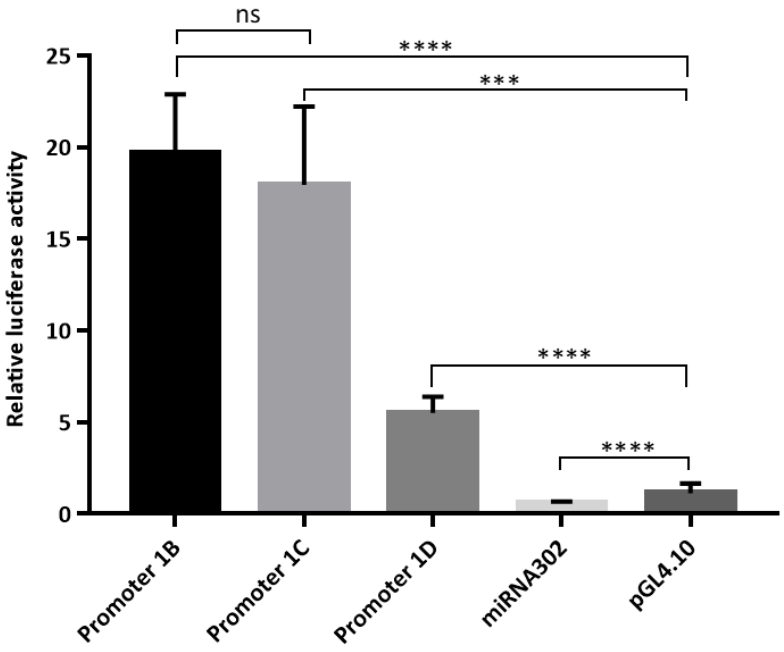

Figure 39. Analysis of the *Rbfox1* promoters' activity. A high activity of promoter 1B and promoter 1C was detected compared to the pGL4.10 vector (mock). Activity of promoter 1D was significantly higher than pGL4.10 vector (mock), but lower than promoter 1B and promoter 1C activity. The negative control (promoter miR-302) showed no activity in primary cortical neurons. The renilla plasmid pRL-TK was used for normalization and transfection control while miR302 was used as a negative control. N=8. Data are shown as the mean ± SEM. ***p < 0,005, ****p <0,001; An Unpaired two-tailed Student t test was used.

Compared to the empty vector an approximately 20-fold increase in luciferase activity was observed for promoter 1B, an 18-fold increase for promoter 1C and a 5.5-fold increase for promoter 1D. No significant difference was detected between promoter 1B and promoter 1C activity. Even though, the relative luciferase activity of the promoter 1D was significantly high compared to the empty luciferase reporter vector, it was much lower than promoter 1B and promoter 1C, suggesting Rbofx1 1B and Rbfox1 1C are the main expressed transcript isoforms in the cortex (Figure 39).

3.2.4 Identification of transcription factor binding sites in promoters 1B and 1C

This part of the project aimed at identifying transcription factor binding sites in the promoter 1B and promoter 1C. First, the cloned sequences were visually screened for evolutionarily conserved short sequence motifs and several E-box / C-box (CANNTG) and G-rich sequences were identified (Figure 40 and Tables 51 and 52) (Refer to Supplemental material for more information about the position of the regulatory elements within the promoters sequence).

Once the binding motifs were identified, a literature search was carried out to identify candidate interacting transcription factors (Tables 51 and 52). Five different E-boxes as well as a G-rich sequence were identified in promoter 1B. Three different transcription factors, c-Myc, NeuroD2 and Hes family members were reported in the literature to bind to these types of C / E-boxes (Laurie Desbarats, 1996; A .J. Walhout, 1998; F. Fisher, 1993; Efil Bayam, 2015). Klf7 was reported in the literature to bind G-rich sequences and was therefore chosen as an additional candidate transcription factor (Lei Lei, 2001).

Six different E-boxes were identified in promoter 1C. The literature search revealed that the transcription factors c-Myc, Mycn and Tcf4 bind to these types of regulatory sequences (Laurie Desbarats, 1996; A.J. Walhout, 1998; F. Fisher, 1993; Derek M. Murphy, 2009; Mari Sepp, 2011; Mari Sepp, 2012).

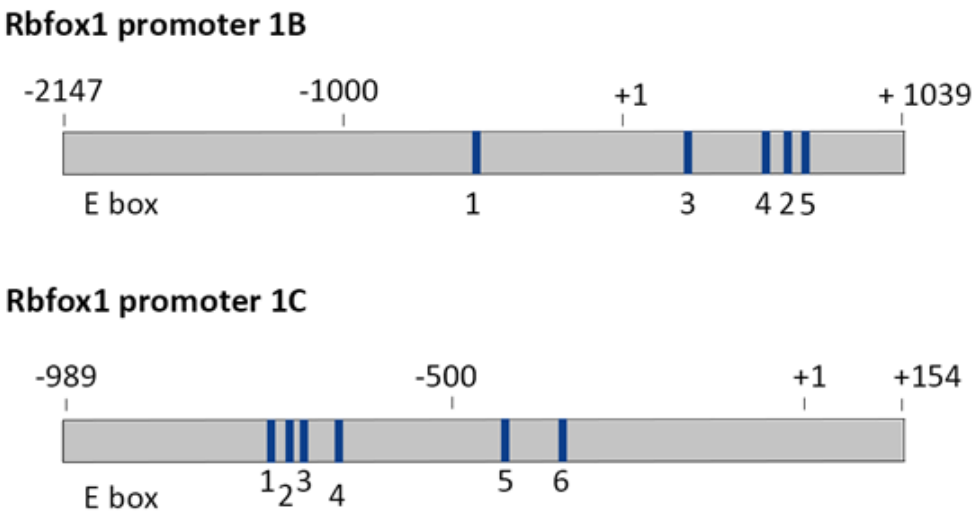

Figure 40. Schematic representation of the *Rbfox1* promoters with the mutated binding sites. A schematic representation of the two *Rbfox1* promoters are indicated as grey bars. Blue vertical bars indicate the position of the mutation in the promoters (not to scale) and the mutation number assigned. Numbers above the grey bar represent the position in the promoter relative to the transcription initiation point. One individual construct was generated per mutation, along with a construct carrying all the mutations.

Table 43. Position of the mutations in the promoter 1B sequence, type of regulatory element, binding motifs, mutations introduced and the transcription factors associated for the *Rbfox1* promoter 1B.

Mutation	***Position***	***Regulatory element***	***Binding motif***	***Mutation introduced***	***Transcription factor associated***
mut: BS1	c1658t_a1659t	E-box	CACATG	**TT**CATG	c-MYC
mut: BS2	c2865t_a2866t	E-box	CATCTG	**TT**CATG	NEUROD2
mut: BS3	c2378t_a2379t	E-box	CACATG	**TT**CGTG	c-MYC
mut: BS4	c2815t_a2816t_c2817t	C-box	CACGCG CGCGTG	**TTT**CTG	HES family
BS5	2889	G-rich sequence	CCCCGCCCC	None	KLF7

Table 44. Position of the mutations in the promoter 1C sequence, type of regulatory element, binding motifs, mutations introduced and the transcription factor associated for the Rbfox1 promoter 1C.

Mutation	*Position*	*Regulatory element*	*Binding motif*	*Mutation introduced*	*Transcription factor associated*
mut: BS1	c332t_a333t	E-box	CAAGTG	**TT**AGTG	TCF4
mut: BS2	c194t_a195t	E-box	CAAGTG	**TT**TGTG	TCF4
mut: BS3	c236t_a237t	E-box	CATGTG	**TT**CGTG	MYCN
mut: BS4	c564t_a565t	E-box	CACCTG	**TT**AGTG	TCF4
mut: BS5	c652t_a653t_c654t	E-box	CACGTG	**TT**CCTG	c-MYC
mut: BS6	c278t_a279t_c280t	E-box	CACGTG	**TT**CGTG	c-MYC

To confirm co-expression of the candidate transcription factors and Rbfox1 *in silico* analyses of *in situ* hybridization data from GenePaint and RT-qPCR experiments were carried out. The online database GenePaint (Online tools) was used to confirm co-expression in the cerebral cortex. GenePaint is a digital atlas of gene expression patterns in mouse, determined by non-radioactive *in situ* hybridization on serial tissue sections. *In situ* hybridization experiments of the transcription factors confirmed their co-expression with Rbfox1 in the cortical plate (Figure 41).

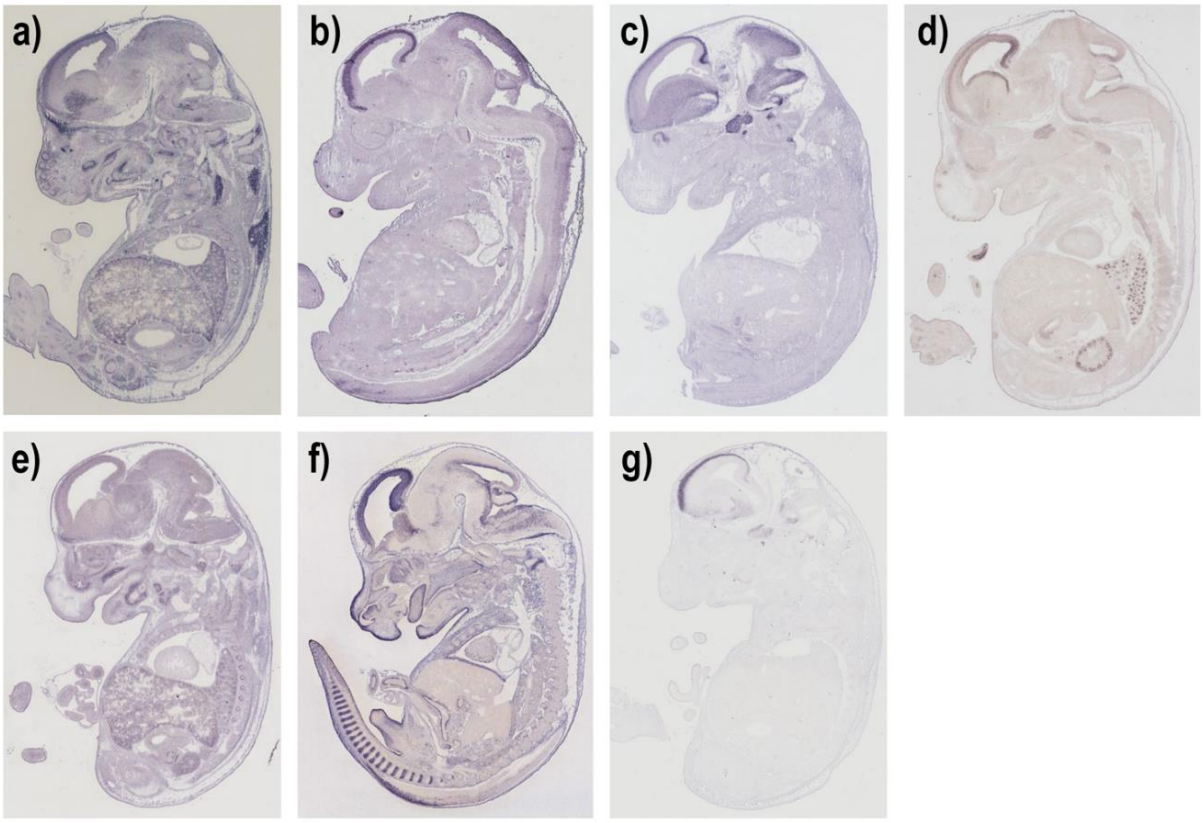

Figure 41. Analyses of RNA *in situ* hybridization experiments of the candidate transcription factors and Rbfox1. a) c-Myc. b) NeuroD2. c) Klf7. d) Mycn. e) Max. f) Tcf4. g) Rbfox1. *In silico* analysis of *In situ* hybridization data of the transcription factors confirmed their expression in the cortical plate, the same cerebral region Rbfox1 is expressed. Experiments were performed in E14.5 mouse embryos. Adopted from GenePaint.

To further validate co-expression of the transcription factors with *Rbfox1* expression analysis of *c-Myc, NeuroD2, Klf7, Mycn, Max* and *Tcf4* by RT-qPCR was performed in P19 cells and primary cortical neurons. Primary cortical neurons were analyzed at two different differentiation days: DIV4 and DIV7. mRNA expression levels were analyzed in order to identify the most suitable time point for cell transfection.

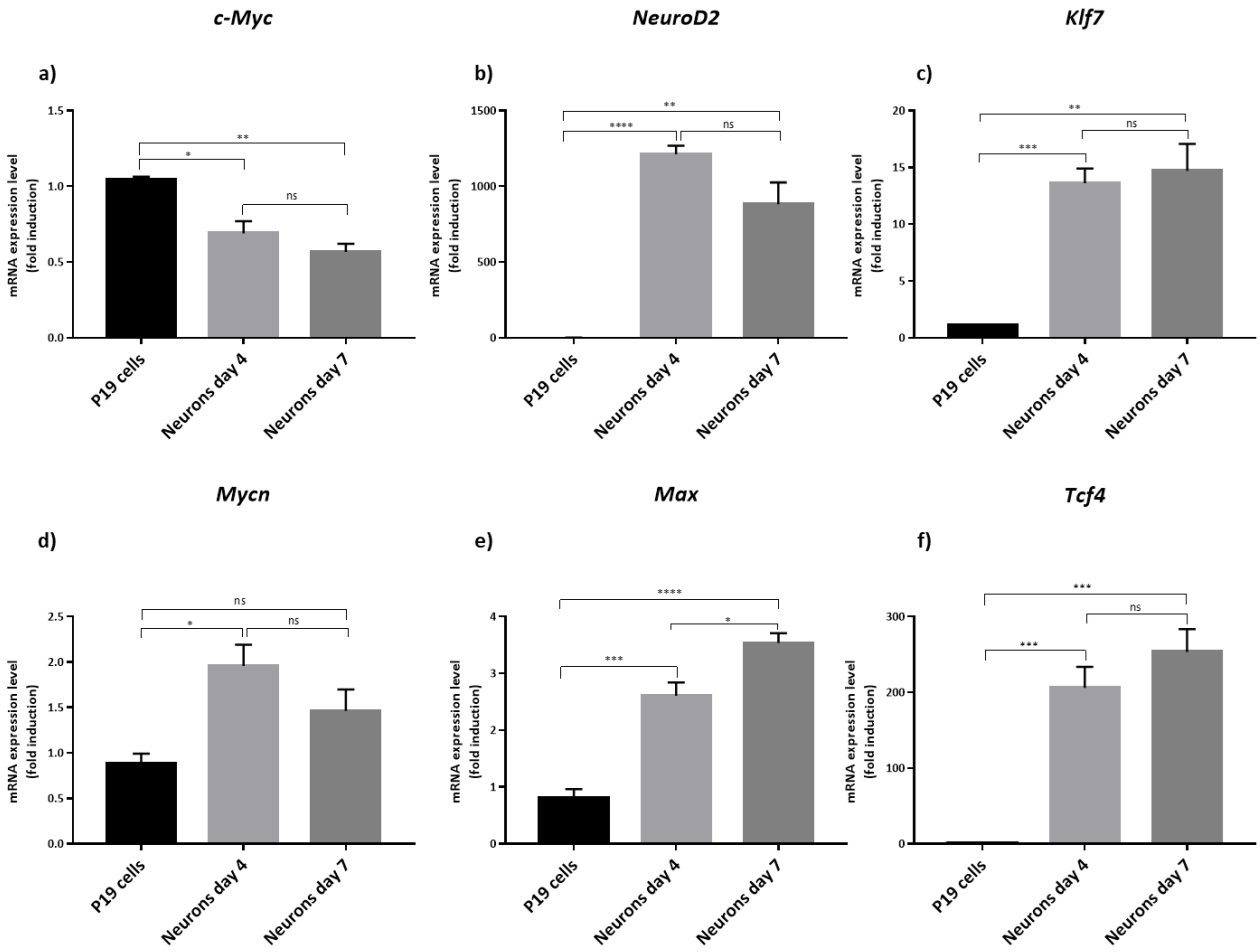

Figure 42. Transcription factors mRNA expression analysis. mRNA expression analysis of *c-Myc, NeuroD2, Klf7, Mycn, Max* and *Tcf4* was performed in P19 cells and primary cortical neurons (DIV4 and DIV7). Except for *c-Myc,* a significant higher expression of the transcription factors was observed in primary cortical neurons. *C-Myc* expression levels decreased during differentiation. Data are shown as the mean ± SEM. N=3 biological replicates. *p < 0.05, **p<0.01, ***p<0.005, ****p<0.001; An Unpaired two-tailed Student t test was used. Expression levels are shown as fold induction compared to P19 cells.

Expression analysis of the candidate transcription factors revealed a high expression of the transcription factors in primary cortical neurons (Figure 42). Relative mRNA levels of *c-Myc* were significantly higher in P19 cells than in primary cortical neurons. A 0.3 and 0.4 fold decrease was observed in DIV4 and DIV7 respectively. No significant differences between DIV4 and DIV7 were

observed (Figure 42a). Expression levels of *NeuroD2, Klf7, Mycn, Max* and *Tcf4* were significantly higher in primary cortical neurons than in P19 cells, with no significant differences between DIV4 and DIV7 for *NeuroD2, Klf7, Mycn* and *Tcf4*.

3.2.5 Analysis of the mutated *Rbfox1* promoters' activity

To elucidate the functional significance of the candidate E/C-boxes, directed mutagenesis was used to introduce mutations into these sequences in the luciferase promoter constructs (Tables 51 and 52). In addition, one construct was generated that carried mutations in all E/C-boxes. Subsequently, changes in the relative luciferase activity were analyzed.

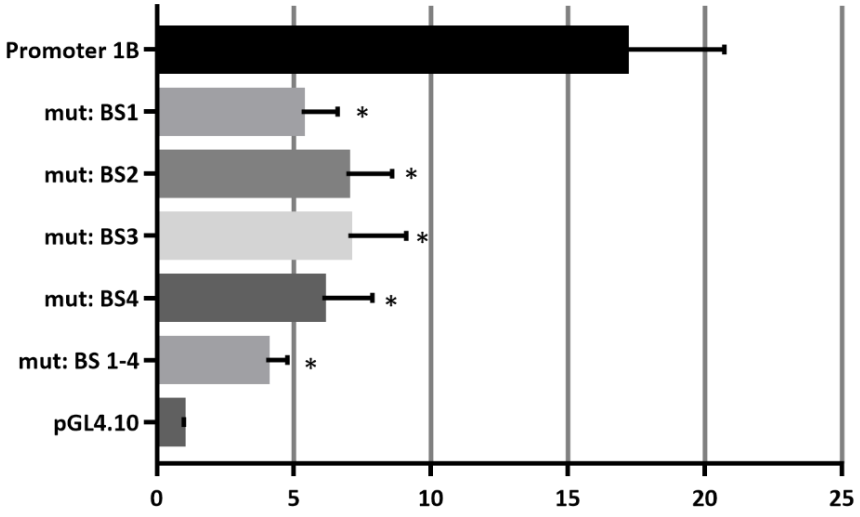

Figure 43. Analysis of the mutated *Rbfox1* promoter 1B activity. Changes in the relative luciferase activity were measured and compared to the wild type promoter 1B. A significant decrease in the relative luciferase activity was observed following transfection of the promoter fragments containing the mutated binding sites. BS 1-4 indicates a construct with all the binding sites mutated. N=6. Data are shown as the mean ± SEM. *p<0,05; An Unpaired two-tailed Student t test was used.

Changes in the relative luciferase activity were measured between the mutated and the wild type promoter 1B constructs. A significant decrease in luciferase activity was observed in all four constructs containing the mutated binding sites compared to the wild type promoter construct. Relative luciferase activity with mut:BS1 was decreased almost 12 fold, with mut:BS2 and mut:BS3 was decreased 10 fold in both cases, and with mut:BS4 was decreased 11 fold. The construct containing mutations in all binding sites showed a 13.1 fold decrease of the luciferase activity relative to the wild type promoter 1B. These results suggested a functional activity of all different E-boxes in regulating Rbfox1 1B expression in cortical neurons. Notably, binding site 4 (mut: BS4) was a putative C-box with predicted repressor activity. However, mutating this C-box resulted in a decrease of luciferase activity suggesting that it acts as an enhancer rather than a repressor. Interestingly, the plasmid containing all four binding sites mutated (mut: BS1-4) gave the lowest luciferase activity, suggesting some additive effects (Figure 43).

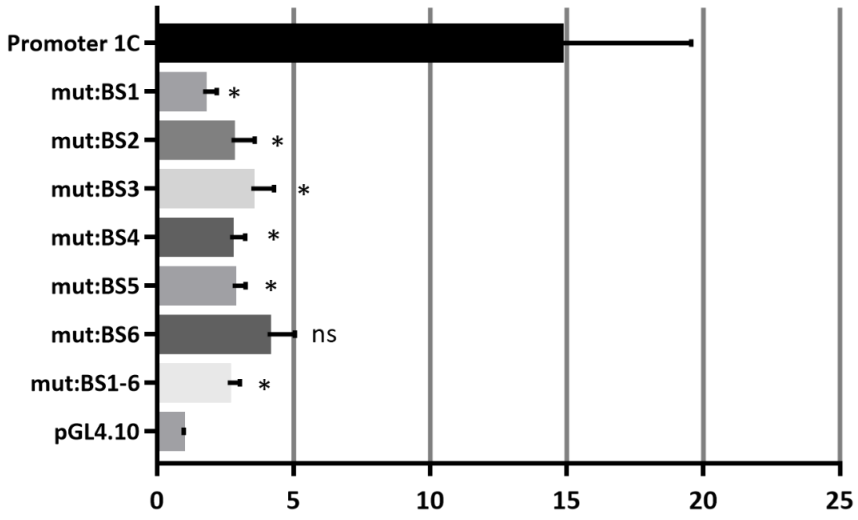

Figure 44. Analysis of the mutated Rbfox1 promoter 1C activity. Changes in the relative luciferase activity were measured and compared to the wild type promoter 1C. A decrease in the promoter 1C activity was observed for all the constructs containing the mutated binding sites. BS 1-6 indicates a construct with all

the binding sites mutated. N=9. Data are shown as the mean ± SEM. n.s., not significant, *p < 0,05; An Unpaired two-tailed Student t test was used.

Changes in the relative luciferase activity were measured comparing the activity of the promoters containing the mutated binding sites to the wild type promoter 1C. A decrease in the luciferase activity was observed with the six different plasmid constructs containing the mutated binding sites. Relative luciferase activity of mut:BS1 was decreased 13.1 fold, with mut:BS2 was decreased 12 fold, with mut:BS3 was decreased 11.3 fold, with mut:BS4 was decreased 12.1 fold, with mut:BS5 was decreased 12 fold and mut:BS6 was decreased 10.7 fold. However, the effect was not significant for BS6. A construct with all the binding sites mutated was generated giving a decrease of the luciferase activity of around 12.1 fold. The decrease in the luciferase activity, with all the mutated binding sites, suggested that the E-boxes are functionally active in regulating Rbfox1 1C expression in cortical neurons (Figure 44).

3.3 Transcription factors knockdown

To test whether the transcription factors that were predicted to bind to the identified motifs regulate *Rbfox1* expression, transcription factor knockdown experiments were carried out. The experiment was performed in primary cortical neurons which were prepared freshly. A pool of siRNA against c-Myc, NeuroD2, Klf7, Mycn, Max and Tcf4 (and a pool of non-targeting siRNA as a control) was used (see Table 18) for the knockdown. 4D-Nucleofector X unit (Lonza) was used to transfect the siRNAs into the nucleus of the cells (transfection in suspension). Cells were cultured for 48 hours before analyzing the changes in *Rbfox1* expression via RT-qPCR.

3.3.1 Electroporation program test

According to the manufacturer's recommendations a set of four pre-selected Nucleofector™ programs were tested with the P3 Primary Cell 4D-Nucleofector™ Kit (see section Kits) in primary cortical neurons. A program test was performed in order to identify the program with the highest transfection efficiency. The test was performed with a pool of siRNAs against NeuroD2 in primary cortical neurons.

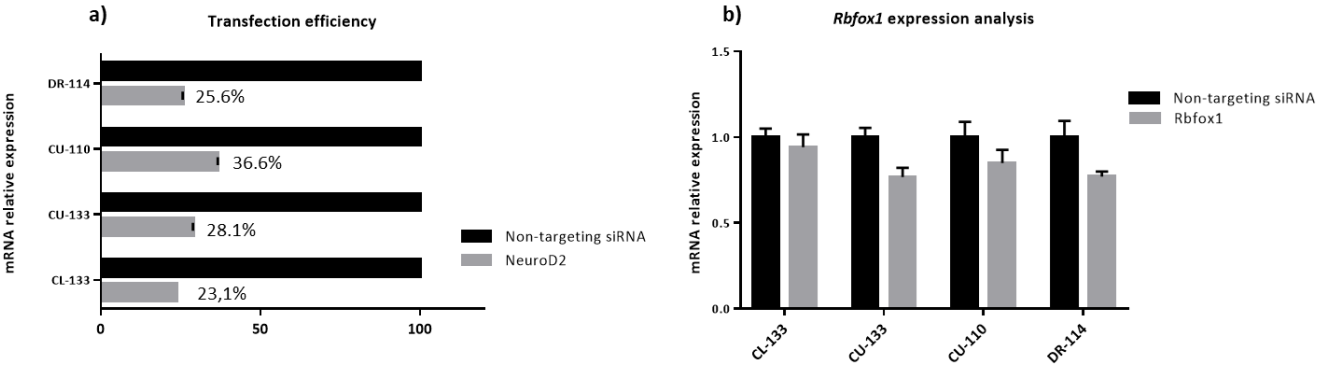

Figure 45. Electroporation program test. Four different 4D-Nucleofector programs were tested to identify the most suitable one. In addition, the effect of *NeuroD2* knockdown on *Rbfox1* expression was assessed. a) Knockdown efficiency of the four different programs tested shown as percentage of mRNA relative to the non-targeting siRNA. b) Changes in the *Rbfox1* expression analyzed upon *NeuroD2* knockdown. *Rbfox1* *e*xpression levels are shown as mRNA levels relative to non-targeting siRNA. This experiment was performed once. Standard errors were calculated from the three technical replicates.

Knockdown efficiency was high with all the four programs tested, reaching more than 50% in all cases (Figure 45a). *Rbfox1 e*xpression analysis, upon *NeuroD2* siRNA transfection revealed a decrease in the expression levels with the four programs tested (Figure 45b). Notably, this

preliminary result suggested a regulation of *Rbfox1* expression by NeuroD2. CU-133 program reached a knockdown efficiency around 72%, it showed a strong decrease of *Rbfox1* mRNA levels, and gave a high cell survival rate. Therefore, the following experiments were performed using the Nucleofector™ program CU-133 for the transfection.

3.3.2 siRNA electroporation

Primary cortical neurons were prepared freshly, from isolated cortices of E14.5 embryos (see section Methods). Cells were electroporated in suspension, with a pool of siRNA against c-Myc, NeuroD2, Klf7, Mycn, Max or Tcf4 with the 4D-Nucleofector (Lonza). Afterwards, transfected neurons were cultured for 48 hours before carrying out the expression analysis. Total *Rbfox1* expression levels, as well as a transcript-specific expression analysis was performed via RT-qPCR. Transfection efficiency was calculated for each siRNA in every assay.

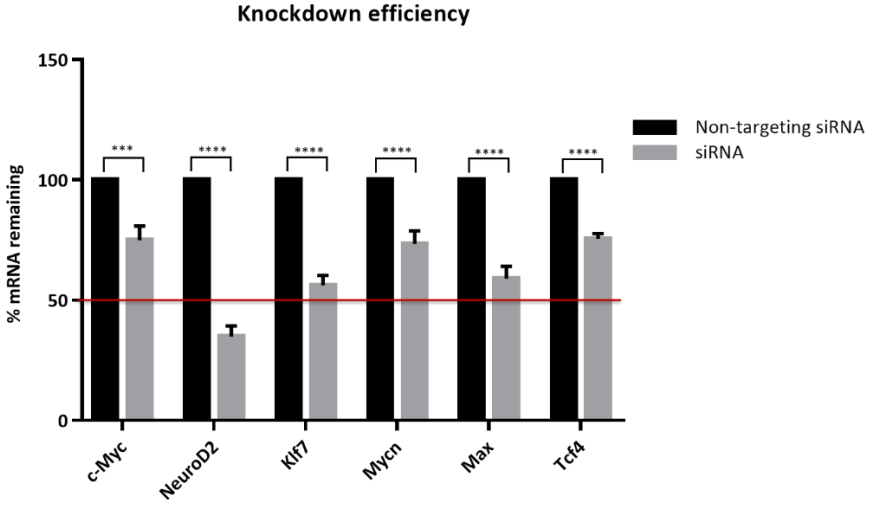

Figure 46. Transcription factors knockdown efficiency. A high knockdown efficiency was reached with the siRNA against NeuroD2, around 65%, whereas the knockdown efficiency reached for c-Myc, Mycn and Tcf4 was rather low. N=8 Data are shown as the mean ± SEM. ***p<0.005, ****p<0.001; An Unpaired two-tailed Student t test was used.

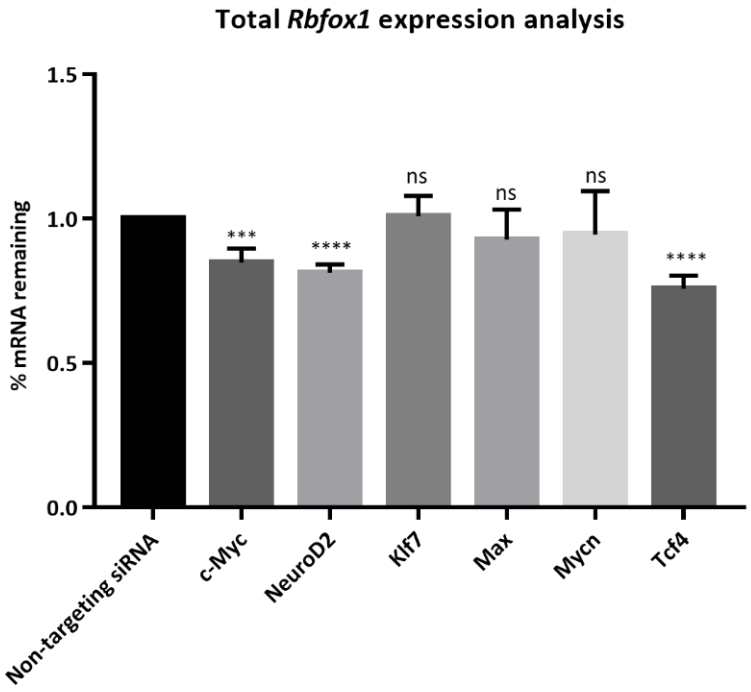

Figure 47. mRNA expression analysis of total *Rbfox1* levels upon transcription factors knockdown. A significant decrease in the Rbfox1 mRNA levels were observed upon knockdown of c-Myc, NeuroD2 and Tcf4. No significant changes in the mRNA levels were observed upon knockdown of Klf7, Max and Mycn. N=8 biological replicates. Data are shown as the mean ± SEM. n.s. not significant, ***p<0.005, ****p<0.001; An Unpaired two-tailed Student t test was used. *Rbfox1 e*xpression levels are shown as % mRNA relative no non-targeting siRNA.

Expression analysis of the total *Rbfox1* levels showed a significant decrease upon c-Myc, NeuroD2 and Tcf4 knockdown (Figure 47). *Rbfox1* mRNA levels decreased by 16% upon c-Myc knockdown, by 19% upon NeuroD2 knockdown, and by 25% upon Tcf4 knockdown. No significant changes in the mRNA levels of *Rbfox1* were observed upon knocking down Klf7, Max and Mycn.

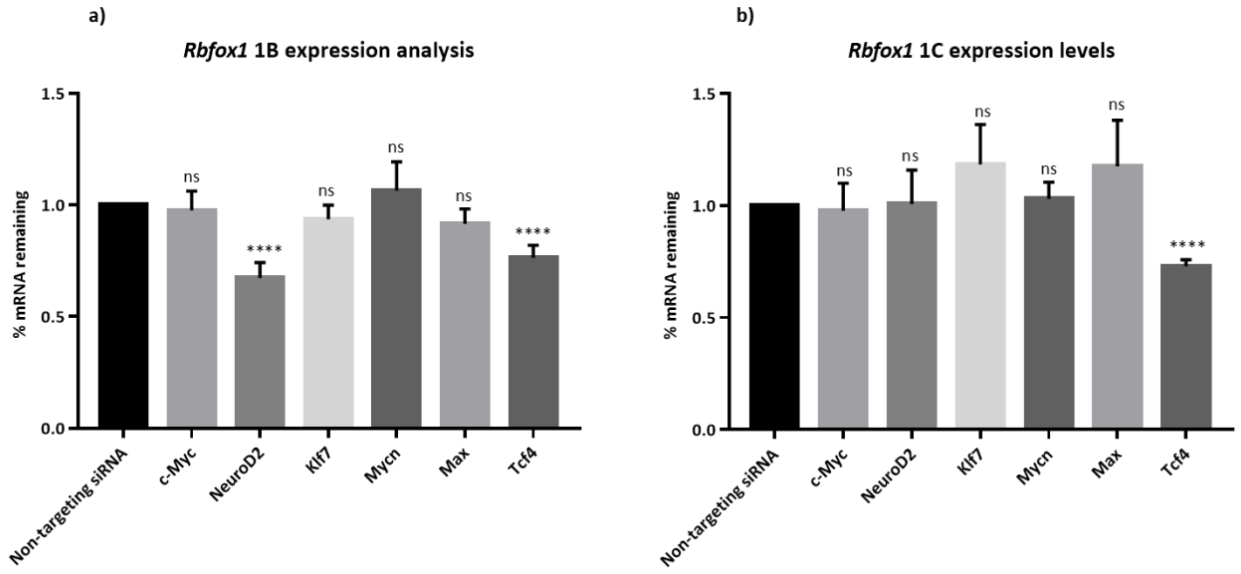

Figure 48. *Rbfox1* transcript-specific expression analysis upon transcription factors knockdown. a) mRNA expression analysis of the *Rbfox1* transcript 1B upon transcription factors knockdown. b) mRNA expression analysis of the *Rbfox1* transcript 1C upon transcription factors knockdown. N=8 biological replicates. Data are shown as the mean ± SEM. n.s. not significant, ****p<0.001; An Unpaired two-tailed Student t test was used. Expression levels are shown as % mRNA relative no non-targeting siRNA.

Expression analysis of the Rbfox1 1B transcript isoform showed a significant decrease in the expression of this transcript upon NeuroD2 and Tcf4 knockdown (Figure 48a). Rbfox1 1B mRNA levels were decreased approximately 33% upon NeuroD2 knockdown, and around 24% upon Tcf4 knockdown. No significant changes in the mRNA levels of Rbfox1 1B were observed upon knocking down any of the other candidate transcription factors.

Expression analysis of the Rbfox1 1C transcript isoform showed a significant 27% decrease of the expression of this transcript upon Tcf4 knockdown (Figure 48b). No significant changes in the

mRNA levels of Rbfox1 1C were observed upon knocking down any of the other candidate transcription factors.

Remarkably, mRNA levels of the total *Rbfox1* decreased 15 % upon c-Myc knockdown (Figure 47). The transcript-specific expression analysis, however, revealed no changes in the mRNA levels of Rbfox1 1B or Rbfox1 1C (Figures 48a and 48b).

Altogether, the results obtained suggest a regulation of *Rbfox1* expression by c-MYC, NEUROD2 and TCF4. At transcript-specific levels, TCF4 seemed to regulate the expression of both transcripts, Rbfox1 1B and Rbfox1 1C, whereas NEUROD2 seemed to regulate only the expression of Rbfox1 1B.

4. Discussion

In this thesis, I have studied the transcriptional regulation of *Rbfox1* in the mouse brain. *Rbfox1* encodes a cell-specific RNA-binding protein which function, among others, is to regulate the splicing of many alternative spliced exons in neurons. To better understand how this gene is transcriptionally regulated in the mouse cortex, I have analyzed the expression pattern of the three different brain-specific *Rbfox1* transcript isoforms. Expression analysis was carried out during cortical development and in the juvenile mouse brain, revealing different expression levels of each *Rbfox1* transcript. Additionally, through *in silico* analysis and luciferase assays, I have identified and characterized the three brain-specific *Rbfox1* promoters. Finally, I have identified several transcription factors which bind to these promoters and regulate the *Rbfox1* expression either globally or in a transcript-specific manner.

4.1 Expression analysis of the splicing regulator *Rbfox1*

4.1.1 *Rbfox1* expression analysis during cortical development

The RT-qPCR experiments with primers detecting all *Rbfox1* transcript isoforms showed a significant upregulation of *Rbfox1* expression during cortical development (Figure 24). In mice, corticogenesis takes place between E11 and E18 (peak of neurogenesis E13), which means, that during this period of time, cell population in the cortex changes from predominantly mitotic multipotent progenitor cells into predominantly neurons (Bradley J. Molyneaux, 2007; Bagirathy Nadarajah, 2002). Therefore, this expression pattern is typical for neuron-specific transcripts. These results are supported by several studies. Nanako Hamada and colleagues already demonstrated that *Rbfox1* is expressed in differentiated neurons but not in mitotically active

progenitor cells in the cerebral cortex (Nanako Hamada, 2013). Furthermore, Brent L. Fogel and colleagues carried out an *in situ* hybridization experiment in 19-weeks human fetal brain, showing that *RBFOX1* was mostly expressed in regions with post-mitotic neurons, giving a reduced signal in the germinal zones (Brent L. Fogel, 2012). Elizabeth A.D. Hammock and colleagues characterized Rbfox1 mRNA localization in the mouse forebrain. The authors performed a series of *in situ* hybridization experiments from E11.5 to P14 allowing them to build an *Rbfox1* expression map during embryonic development. Additionally, they also demonstrated *Rbfox1* expression in post-mitotic projection neurons and interneurons, and implicated *RBFOX1* in the development and maturation of human neurons (Elizabeth A.D. Hammock, 2011).

The observed expression pattern of *Rbfox1* suggested an important role during cerebral cortex development. This hypothesis is supported by several studies. Different RBFOX1 isoforms exist that localize to the cytoplasm or nucleus. Functional studies of these isoforms indicated crucial roles of RBFOX1 during neurogenesis in the cerebral cortex.

A knockdown of the nuclear *Rbfox1* isoform in the developing cerebral cortex revealed defects in radial migration and terminal translocation of the cortical neurons, due to an impaired nucleokinesis (Nanako Hamada, 2016). Additionally, changes in the regulation of axon growth and dendritic arborization were observed. Electrophysiology analysis revealed significant defects in cell membrane and synaptic properties in the Rbfox1-deficient neurons. These results suggested an essential role of the nuclear RBFOX1 in synapse functions, concluding that an impairment of the nuclear RBFOX1 isoform function may induce structural and functional defects in the cerebral cortex (Nanako Hamada, 2016).

The function of the cytoplasmic RBFOX1 has also been studied. A knockdown of the cytoplasmic *Rbfox1* isoform in the developing cerebral cortex revealed defects in radial migration and

terminal translocation of the cortical neurons. Additionally, defects in axon elongation to the contralateral cortex, and in the dendritic arborization formation during corticogenesis were also observed, suggesting a functional impairment of the cytoskeleton system in the RBFOX1-deficient neurons (Nanako Hamada, 2015). More recently, the cytoplasmic RBFOX1 has been implicated in regulating the synaptic transmission in inhibitory neurons (Celine K. Vuong, 2018).

CNVs identified in the *RBFOX1* gene, and associated with neurodevelopmental disorders, are typically located in the 5'-region of the gene, affecting the promoters and intronic regions as well as 5'-UTR exons of some of the *RBFOX1* isoforms (Figure 4). For example, some of these CNVs only affect the 5'-region of Rbfox1 1B but not Rbfox1 1C or 1D, and other CNVs may only affect Rbfox1 1C. In this present study, transcript-specific expression analysis revealed a great importance of Rbfox1 1B, especially during cerebral cortex development, where it was much more strongly expressed than Rbfox1 1C or Rbfox1 1D. Therefore, it may be that CNVs in patients with neurodevelopmental disorders that span the 5'-region of Rbfox1 1B cause defects in cortical development, resulting, for example in an impaired neuronal migration. Rbfox1 1C and Rbfox1 1D were strongly expressed in specific regions of the juvenile mouse brain (Figure 29), i.e. Rbfox1 1C in cortex and cerebellum and Rbfox1 1D in midbrain. CNVs in patients spanning the 5'-region of these transcript isoforms may have a higher impact on the functions of these specific brain regions. However, it is also possible that CNVs that apparently only affect one specific Rbfox1 transcript isoform may nevertheless impair the expression of the other Rbfox1 transcript isoforms, for example by removing important enhancers. In addition species specific differences in the expression of the different Rbfox1 transcript isoforms could exist and it may be difficult to translate the results obtained in mouse to human.

RNA *in situ* hybridization results obtained in this thesis for Rbfox1 1B correlate with the results posted on GenePaint, where expression in the cortical plate and in the spinal cord was observed (Figure 27f and 27g). Likewise, I have also detected expression of the Rbfox1 1B transcript in the same brain regions during embryonic development (Figures 27a and 27b).

4.1.2 *Rbfox1* expression analysis in the juvenile mouse brain

*Rbfox1 e*xpression analysis in the juvenile brain revealed no major differences between the different brain regions analyzed (Figure 28). However, transcript-specific expression analysis revealed different expression of the different transcript isoforms suggesting that, while the overall expression levels of *Rbfox1* are maintained stable, the contribution of each transcript to the total expression levels is different in each brain region (Figure 29).

Besides my study, there is another study that carried out a transcript-specific *Rbfox1* expression analysis (Andrey Damianov, 2010). The authors analyzed the expression of different Rbfox1 transcripts in cerebellum, cortex, striatum, heart and muscle, revealing different mRNA levels of the different transcripts in these regions. Striatum, heart and muscle were not included in my project instead, midbrain, olfactory bulbs and hippocampus were analyzed. Notably, no statistical data was shown in this study.

Damianov and colleagues demonstrated that Rbfox1 1B expression was the highest in cortex. Likewise I also demonstrated expression of Rbfox1 1B in this brain region however, in my analysis Rbfox1 1B expression was the highest in hippocampus (not included in Damianov analysis). Rbfox1 1C (1C.1 in Damianov et al., 2010) expression analysis revealed the highest expression in the cerebellum. Likewise, my Rbfox1 1C expression analysis also revealed the highest expression

of this transcript in cerebellum (Figure 29b). In my analysis, Rbfox1 1D expression was the highest in midbrain (Figure 29c). This brain region was not included in the Damianov study, however they showed expression in striatum, cortex and cerebellum. Likewise, I also demonstrated expression of Rbfox1 1D, in cortex and cerebellum.

In conclusion, this expression pattern may be due to different necessities in the different brain regions, suggesting that each Rbfox1 transcript may play a different role in each brain region.

For example, Rbfox1 1C was strongly expressed in cerebellum. In addition, *in situ* hybridization results gave a strong signal in Purkinje cells (Figures 32b and 33b), which play a fundamental role in controlling motor movement. Therefore, CNVs in autism patients that disrupt Rbfox1 1C may lead to cerebellar dysfunctions. In fact, a study published in 2013 linked ASD with the cerebellum (Tiffany D. Rogers, 2013). This brain region, besides being implicated in motor functions, is also involved in cognitive and emotional functions. Notably, the cerebellum has been found structurally and functionally abnormal in ASD patients. In fact, cerebellar hypoplasia and reduced number of Purkinje cells are consistent findings in ASD patients (S. Hossein Fatemi, 2012). So, that in 2012 Fatemi and colleagues postulated an autism disconnection hypothesis, proposing that a disconnection in the brain of ASD patients, occurs as a result of Purkinje cell loss in the cerebellar cortex (S. Hossein Fatemi, 2012).

Rbfox1 1D was highest expressed in midbrain, which exerts important functions in motor movement, particularly in movements of the eye, and in auditory and visual processing. Several studies have linked midbrain impaired functions to autism, especially to the midbrain auditory system (Gary R. Gaffney, 1988, Nir Oksenberg, 2013).

Expression analysis data, obtained by RT-qPCR, in the juvenile mouse brain agrees with the RNA *in situ* hybridization experiments (Figures 31, 32 and 33). A positive signal for the total Rbfox1 and Rbfox1 1B expression was detected in the cortex, hippocampus, cerebellum and olfactory bulbs (Figure 31a and 31b). Additionally, in situ hybridization experiment of *Rbfox1* posted on the Allen Brain Atlas also correlates with my expression analysis (Figure 31c), showing a strong signal in the cortex, cerebellum, hippocampus and olfactory bulbs.

4.2 Analysis of *Rbfox1* promoters' activity

4.2.1 Analysis of the wild type promoter activity

Based on the *Rbfox1* expression analysis results, which showed a high expression of the different Rbfox1 transcripts in primary cortical neurons at DIV4, these cells were chosen to perform the luciferase assays (Figure 35 and 36). An *in silico* analysis was carried out to identify the putative regulatory regions of the three different brain-specific Rbfox1 transcripts (Figure 37).

Luciferase assays carried out for promoter 1B, promoter 1C and promoter 1D revealed different activity levels in primary cortical neurons (Figure 38). Despite the fact that luciferase assays are in general an artificial system the results obtained with the *Rbfox1* promoter fragments are in agreement with the expression analysis. Therefore, luciferase assays were a suitable system to study regulation of *Rbfox1* promoter activity.

Higher activity of promoters 1B and 1C than promoter 1D was observed, correlating with the high expression levels of Rbfox1 1B and Rbfox1 1C (Figure 36a and 36b).

Altogether these results suggest that all sequence elements necessary for the induction of *Rbfox1* expression were included in the promoter fragments.

4.2.2 Identification of candidate transcription factors

Candidate transcription factors to bind *Rbfox1* promoters and regulate their activity were predicted as described in section 3.2.4. Additionally, co-expression of these transcription factors with *Rbfox1* in the cortical plate was confirmed by *in situ* hybridization experiments performed in E14.5 mouse embryos (Figure 40).

Expression analysis of the candidate transcription factors was carried out in P19 cells and primary cortical neurons at DIV4 and DIV 7 (Figure 41). Analysis revealed strong expression of *NeuroD2, Klf7, Mycn, Max* and *Tcf4* in primary cortical neurons (Figures 41b, 41c, 41d, 41e and 41f). This expression profile was expected, since all candidate transcription factors are neurogenic, meaning they are implicated in cell differentiation in the cortex during development (section 1.3). Therefore, expression analysis reassured them as good candidates to regulate *Rbfox1* expression.

Expression analysis of *c-Myc*, revealed lower levels in primary cortical neurons (DIV4 and DIV7) relative to P19 cells, suggesting that this transcription factor is more expressed pluripotent cells rather than differentiating neurons (Figure 41a). Notably, high expression levels of *c-Myc* often correlate with cellular processes such as proliferation, suppression of differentiation, transformation and apoptosis (A.J. Walhout, 1998). Therefore, low expression levels in differentiating neurons are expected. However four binding motifs for this transcription factor were identified in both promoter sequences, two in promoter 1B and two in promoter 1C (Figure 39 and Tables 43 and 44). In fact, c- MYC regulates mammalian cell proliferation and apoptosis (Bruno Amati, 1994) but to date, no specific function has been reported in cortical development for this transcription factor. Actually, this is the first work implicating c-MYC in the transcriptional regulation of a neuron-specific gene. Additionally, in the literature, there are many studies showing that c-MYC, besides binding to E-box sequences by itself, often heterodimerizes with

MAX to function as a transcription factor (Laurie Desbarats, 1996; A.J. Walhout, 1998; F. Fisher, 1993). Therefore expression analysis of the transcription factor MAX was also carried out, revealing a strong expression in differentiating neurons (Figure 41e).

NEUROD2 expression analysis revealed a high expression in primary cortical neurons, and also one NEUROD2 binding site was identified in promoter 1B (Figure 39 and Table 43). Some evidences reveal that this transcription factor binds to the *Rbfox1* promoter region. Indeed, a genome-wide ChIP-seq study of NEUROD2 targets during embryogenesis (E14.5) identified *Rbfox1* as a target (Efil Bayam, 2015). The authors identified several putative NEUROD2 binding sites in the *Rbfox1* gene, many of them in the 5' UTR of the first exon, correlating with our findings.

Expression analysis of *Klf7* was also carried out, since a G-rich sequence, identified as a binding site for KLF7 (Lei Lei, 2001), was detected in the promoter 1B sequence (Figure 39 and Table 43). No mutations were introduced to this binding site but it was included in the knockdown experiment.

Tcf4 expression analysis revealed strong expression in differentiating neurons, and two different TCF4 binding motifs were identified in promoter 1C (Figure 39 and Table 44). TCF4 transcription factor is associated with Pitt–Hopkins syndrome, intellectual disability, schizophrenia and other rare cognitive disorders, and several studies implicated TCF4 in correct neuronal development and migration. For example a study showed that homozygous *Tcf4* knockout ($Tcf4^{-/-}$) mice die within 24 h after birth demonstrating that TCF4 is a crucial transcription factor required for normal development. Subsequent analysis of the transgenic brains revealed a reduction in the number of neurons forming the pontine nucleus and an accumulation of ectopic neurons outside this region which failed to migrate to their correct location (Adriano Flora, 2007). Another recent

study demonstrated that neuronal activity and protein kinase A signaling induce a TCF4-controlled transcription in primary cortical neurons (Mari Sepp, 2017).

MYCN expression analysis revealed strong expression in differentiating neurons, and one binding motif was identified in promoter 1C (Figure 39 and Table 44).

In promoter 1B, a binding site for HES family repressors was identified (Figure 39 and Table 43). Even though expression analysis was not performed for specific transcription factors belonging to this family, the binding motif was indeed included in the luciferase assay.

4.2.3 Analysis of the mutated *Rbfox1* promoters' activity

Directed mutagenesis was used to introduce mutations in the putative binding motifs identified, and subsequently changes in the luciferase activity were measured for both, promoter 1B and promoter 1C (Figure 42 and Figure 43).

In promoter 1B, we identified five different binding sites predicted to be bound by four different transcription factors, c-MYC, NEUROD2, HES family and KLF7. Four out of the five sites were mutated: two for c-MYC, one for NEUROD2 and one for HES family. in Mutations were not introduced in the KLF7 binding site (BS5) therefore, changes in the luciferase activity were not measured. Binding sites 1, 2 and 3 were designated E-boxes, and binding site 4 was identified as C-Box (Table 43).

We show that luciferase activity was significantly decreased with each of the 4 different mutated motifs, demonstrating that these binding sites actively regulate promoter 1B activity (Figure 42). These results confirm c-MYC (mut:BS1 and mut:BS3) and NEUROD2 (mut:BS2) as good candidate transcription factors to bind to the *Rbfox1* promoter 1B and regulate its expression.

Interestingly, binding site 4 (mut:BS4) in the promoter 1B sequence is a putative binding site for HES family repressors. Therefore an increase in luciferase activity was expected after mutating this site. However, a decrease in the luciferase activity was observed, suggesting that this binding site acts as an enhancer. A major question arises from this result. It is widely known that *in vivo* many transcription factors competitively interact with the same binding motif, affecting the interpretation of results for reporter gene assays (Kazuo Niwano, 2006). In another words, multiple transcription factors exist that bind to the same DNA element yet have very different biological functions. If we have a closer look to the HES family functions, we do not expect their expression in differentiating neurons. They are transcriptional repressors of the proneural genes (Makoto Ishibashi, 1995; Jun Hatakeyama, 2004), and have also been shown to repress cell differentiation and to regulate cell fate decisions (Ryoichiro Kageyama, 2007). Moreover, it has been published that HES1 and HES5 directly repress proneural gene expression and thereby inhibit neuronal differentiation (Ryoichiro Kageyama, 2015). Therefore, in differentiating neurons, a transcriptional activator may bound to this DNA element acting as E-box instead of C-box.

We also demonstrated that luciferase activity was the lowest when the construct harboring all four mutated binding sites (mut:BS1-4) was transfected indicating an additive effect and supporting the hypothesis that all the binding sites identified are transcriptionally active (Figure 42).

In summary, all mutated binding sites in the promoter 1B sequence actively decreased luciferase activity, demonstrating that they are active regulatory elements in the *Rbfox1 1B* expression regulation. We also demonstrated that c-MYC and NEUROD2 are good transcription factor candidates.

We identified six different binding sites in *Rbfox1* promoter 1C: three TCF4 binding sites, one MYCN binding site and two c-MYC binding sites. All the identified binding sites were designated as E-boxes (Table 44). We showed a decrease in the relative luciferase activity with all six mutated constructs: mut:BS1, mut:BS2, mut:BS3, mut:BS4, mut:BS5, mut:BS6 and mut:BS1-6 (construct harboring all the mutated binding sites). We also showed a significant decrease in the luciferase activity with the construct harboring all the six mutated binding sites (mut:BS1-6) indicating an additive effect and supporting the hypothesis that all the binding sites identified are transcriptionally active (Figure 43).

In summary, all mutated binding sites in promoter 1C sequence actively decreased the luciferase activity, demonstrating that they are active regulatory elements in the *Rbfox1 1C* expression regulation. We also demonstrated that c-MYC and TCF4 and MYCN are good transcription factor candidates.

In conclusion, even if further studies must be done to identify the complete transcription machinery responsible for *Rbfox1* expression, we identified the promoter region of the three brain-specific *Rbfox1* transcript isoforms. Additionally, we located specific regulatory sequences within the promoters and recognized several transcription factors predicted to bind to the regulatory sequences and regulate *Rbfox1* expression. Furthermore, up to date, no studies demonstrating the transcriptional regulation of *Rbfox1* by c-MYC, NEUROD2, MYCN and TCF4 have been published. This thesis is the first study predicting a regulation of *Rbfox1* expression by these transcription factors.

4.3 Transcription factors knockdown

To finally confirm whether the identified candidate transcription factors are implicated in the regulation of *Rbfox1* expression, a knockdown of c-*Myc, Neurod2, Mycn* and *Tcf4* (predicted in the luciferase assay as good candidates), and *Klf7* and *Max* was carried out. Subsequent changes in *Rbfox1* expression were analyzed by RT-qPCR. As mentioned previously, c-MYC must heterodimerize with MAX to exert its functions as a transcription factor (Laurie Desbarats, 1996; A.J. Walhout, 1998; F. Fisher, 1993). Therefore, a knockdown of *Max* was also carried out, to determine if it is also involved in regulating *Rbfox1* expression through this complex formation. Additionally, even though mutations were not introduced to the KLF7 binding site in the luciferase assay, a knockdown of this transcription factors was indeed carried out.

We measured the knockdown efficiency for all the siRNA, and we found that the highest was with *NeuroD2*, around 69%. Unfortunately, the knockdown efficiency reached with the other siRNAs was not higher than 40% (Figure 45).

We found that c-MYC, NEUROD2 and TCF4 transcription factors regulate the expression of the total *Rbfox1* (Figure 46). Moreover, expression analysis at transcript-specific level demonstrated that NEUROD2 regulates the expression of Rbfox1 1B and TCF4 regulates expression of both transcript isoforms, Rbfox1 1B and Rbfox1 1C (Figures 47a and 47b).

As mentioned before, a genome-wide study analyzing NEUROD2 targets throughout the genome identified *Rbfox1* as a target gene (Elif Bayam, 2015). In this published study NEUROD2 target genes were investigated at E14.5, which is the peak of neurogenesis and also when *Rbfox1* and *NeuroD2* are both highly expressed. They found that within a gene, NEUROD2 peak sequences were enriched in E-box motifs, and calculations revealed that NEUROD2 binding was most likely

to be located in the first 5'UTR exon instead of having a random distribution. Actually, they identified a total of forty seven NEUROD2 peaks mapping within the *Rbfox1* gene (chr16:5,884,793-7,412,480), most of them located in the 5'UTR region, confirming that *in vivo* NEUROD2 preferentially binds to transcription start sites located within or upstream of 5'UTR exons (Elif Bayam, 2015). Notably, one out of the forty seven NEUROD2 peaks, mapping to the genomic position chr16:5,884,574-5,885,866 on Mouse GRCm38/mm10 Assembly, overlaps the promoter 1B sequence (chr16:5,882,646-5,885,831) cloned in this thesis. Moreover, within the promoter 1B sequence, the NEUROD2 motif is located in the position chr16: 5,885,511-5,885,516 on Mouse GRCm38/mm10 Assembly which overlaps the region identified in the published study. In conclusion, the finding in this study correlates and supports our result, confirming the hypothesis that NEUROD2 transcription factor binds to the promoter region of *Rbfox1* 1B and regulates its expression.

We found that Rbfox1 1B expression was significantly decreased upon *Tcf4* knockdown, however no binding site for this transcription factor was identified in the promoter 1B sequence cloned. Three major possibilities arise from this result. The first is that TCF4 binds to the E-boxes in promoter 1B, even though they are not bona fide TCF4 binding sites, and regulate Rbfox1 1B expression directly. The second is that TCF4 regulates Rbfox1 1B expression indirectly, either through another transcription factor or forming a complex with another protein, which will be the one physically bound to DNA. Such binding will explain why no TCF4 binding site was identified in the promoter 1B sequence. For example, the yeast transcription factors Mbp1 and Swi6 form the MBF complex and Mbp1 is the one interacting DNA directly at ACGCGT sequences (Ian A. Taylor, 2000). It is known that TCF4 can form complexes with other proteins to regulate gene expression. For example, the complex β-catenin-TCF4 that regulate expression of target

genes, such as *Axin2*, *c-Myc* and *Cyclin D1* (Hyun-Woo Shin, 2014). The third possibility may be that the TCF4 binding site was not included in the promoter 1B sequence cloned and analyzed in the luciferase assays, correlating with the fact that we did not observe any change in the luciferase activity. To further investigate this and to elucidate whether TCF4 regulates *Rbfox1* expression directly or indirectly a chromatin immunoprecipitation (ChIP) assay should be performed.

Regarding c-MYC transcription factor, on one hand, we found that the total *Rbfox1* expression was decreased upon *c-Myc* knockdown (Figure 46), indicating a regulation of the expression by this transcription factor. However, the transcript-specific expression analysis showed no changes of either Rbfox1 1B or Rbfox1 1C after *c-Myc* knockdown. This may be an indicator of the existence of another Rbfox1 transcript, whose expression is regulated by c-MYC, and contributes to the total Rbfox1 levels. No specific function of c-MYC has been reported in cortical development to date, hence this thesis is the first work implicating this transcription factor in the transcriptional regulation of a gene expressed exclusively in neurons.

On another hand, as mentioned before c-MYC must heterodimerize with MAX to exert its functions as a transcription factor. However we observed no changes in the *Rbfox1* expression, neither at total Rbfox1 levels nor at transcript-specific level upon *Max* knockdown. This may be due to the low knockdown efficiency reached for the siRNA against *Max* (40%), which may be too low to exert an effect on *Rbfox1* expression. Nevertheless, it is also plausible that c-MYC regulates *Rbfox1* expression partnering with another transcription factor. There are several candidates for DNA-binding proteins, other than Max, that interact with c-MYC and are implicated in gene expression/repression. For example, a study showed physical and functional interaction between c-MYC and TFII-I, a transcription initiation factor. In this study, the authors demonstrated that

the c-MYC-TFII-II complex inhibits the transcription initiation (Ananda L. Roy, 1993). Another study demonstrated inhibition of the transcriptional regulator Yin-Yang-1 (YY1), a transcription factor that regulates the transcription of many genes, including the oncogenes *c-FOS* and *c-MYC*. Depending on the context, YY1 acts as a transcriptional repressor, a transcriptional activator, or a transcriptional initiator. In this study the authors showed that *in vitro*, c-MYC inhibits both the repressor and the activator functions of YY1, which suggests that c-MYC functions by modulating the activity of YY1 (A. Shrivastava, 1993). There are also several studies implicating c-MYC in gene expression by itself, without the necessity to interact with another transcription factor. For example, a study showed that c-MYC activates the expression of telomerase by inducing expression of its catalytic subunit, telomerase reverse transcriptase (TERT). Telomerase is a ribonucleoprotein complex expressed in proliferating and transformed cells, in which it preserves chromosome integrity by maintaining telomere length. In this study, the authors identified numerous transcriptionally active c-MYC-binding sites located in the TERT promoter and, through luciferase assays they were able to show regulation of the telomerase activity by transcriptional activation of TERT induced by c-MYC. In addition, they were able to demonstrate that TERT expression was directly induced by transcription factor c-MYC (Kou-Juey Wu, 1999). Given all these evidences, c-Myc may regulate *Rbfox1* expression either interacting with proteins other than MAX or acting as a gene expression regulator by itself.

We also identified a KLF7 binding motif in the sequence of promoter 1B, however, expression analysis after KLF7 knockdown demonstrated that this transcription factor does not regulate *Rbfox1* expression. Knockdown efficiency of the siRNA against KLF7 was around 43%, allowing for the possibility of either being too low to see an effect on *Rbfox1* expression or the binding site is not transcriptionally functional. A study showed that KLF7 is required for neuronal

morphogenesis and axon guidance in the cortex, but its activity may be required in another cellular context and timeline (Massimiliano Caiazzo, 2010; Massimiliano Caiazzo, 2011).

Finally, even though a change in the luciferase activity was detected with the transcription factor MYCN in the luciferase assay experiment here, we demonstrated, through a knockdown, that this transcription factor does not regulate *Rbfox1* expression. These contradictory results can be explained by the fact that luciferase experiments are very artificial and do not reflect the *in vivo* environment of the promoter (Fabio Gasparri, 2010).

In summary, we here demonstrated that the transcription factors c-MYC, NEUROD2 and TCF4 regulate the total *Rbfox1* expression. Transcript-specific expression analysis demonstrated that the transcription factor NEUROD2 regulates expression of the Rbfox1 1B transcript isoform, whereas the transcription factor TCF4 regulates both Rbfox1 1B and Rbfox1 1C. In any case, further functional studies, such as chromatin immunoprecipitation (ChIP), should be conducted to confirm the physical interaction between the identified transcription factors and the *Rbfox1* promoter sequence. More importantly, it is necessary to identify more transcription factors that regulate the *Rbfox1* expression in a transcript-specific manner, to better comprehend the function of each *Rbfox1* transcript isoform.

5. Conclusion

RBFOX1 is an RNA-binding protein which regulates alternative splicing and RNA stability in neurons. RBFOX1 plays an important role in neurodevelopment, but little is known about how its transcriptional activity is regulated.

Expression analysis of the *Rbfox1* gene revealed a strong upregulation during cortical development, whereas expression levels were relatively constant between different subregions of the juvenile brain. Furthermore, transcript-specific analysis revealed different contribution of the alternative Rbfox1 transcript isoforms to the total Rbfox1 levels, suggesting that a complex organization of the *Rbfox1* gene, with its alternative promoters, is necessary to ensure constant Rbfox1 levels in different developmental stages and brain subregions. Although further studies should be performed with transcript-specific knockouts in mice or human cell models, these findings may pave the way to understand the causative role of reduced *RBFOX1* expression in neurodevelopmental disorders.

In addition, characterization of the *Rbfox1* promoters revealed that its expression in primary cortical neurons is driven by promoters 1B and 1C. Promoter 1B seems to be important to drive *Rbfox1* expression in the developing cerebral cortex and in most juvenile brain subregions, whereas expression of Rbfox1 isoforms transcribed from promoter 1C was highest in the cerebellum of the juvenile mouse brain.

Finally, through knockdown experiments, I was able to show that transcription factors C-MYC, NEUROD2 and TCF4 regulate total *Rbfox1* expression, whereas expression of Rbfox1 1B, and Rbfox1 1C was demonstrated to be regulated by NEUROD2 and TCF4, and TCF4 respectively.

Results obtained in this thesis predict that reduced expression of only one of the two brain specific Rbfox1 transcript isoforms suffices to decrease *Rbfox1* expression in different brain regions and may contribute to the pathogenesis of autism in *RBFOX1* deletion carriers. I have also identified for the first time transcription factors that bind to either promoter 1B or 1C and regulate their expression in the brain, either at transcript-specific level or at total Rbfox1 levels.

Although further functional studies such as ChIP experiments to confirm the physical interaction between c-MYC, NEUROD2 and TCF4 with the *Rbfox1* promoter region need to be conducted, this thesis offers the potential of unveiling the transcriptional network and pathways regulating the cortical differentiation.

References

- Amati B., Land H. (1994). Myc-Max-Mad: a transcription factor network controlling cell cycle progression, differentiation and death. *Current Opinion in Genetics and Development*, 4(1):102-8. https://doi.org/10.1016/0959-437X(94)90098-1.
- Amir R.E., Van den Veyver I.B., Wan M., Tran C.Q., Francke U., Zoghbi H.Y. (1999). Rett syndrome is caused by mutations in X-linked MECP2, encoding methyl-CpGbinding protein 2. *Nature Genetics*, 23(2):185-8. http://doi:10.1038/13810.
- Auweter S.D., Fasan R., Reymond L., Underwood J.G., Black D.L., Pitsch S., Allain F.H. (2006) Molecular basis of RNA recognition by the human alternative splicing factor Fox-1. *The EMBO Journal,* 25, 163–173. http://doi:10.1038/sj.emboj.7600918.
- Barash Y., Calarco J.A., Gao W., Pan Q., Wang X., Shai O., Blencowe B.J., Frey B.J. (2010). Deciphering the splicing code. *Nature* 465(7294), 53-9. Htpp://doi:10.1038/nature09000.
- Bayam E., Sahin G.S., Guzelsoy G., Guner G., Kabakcioglu A., Ince-Dunn G.(2015) Genome-wide target analysis of NEUROD2 provides new insights into regulation of cortical projection neuron migration and differentiation. *BMC Genomics*, 16,681. htpp://doi:10.1186/s12864-015-1882-9.
- Beaulieu M.E., McDuff F.O., Frappier V., Montagne M., Naud J.F., Lavigne P. (2012). New structural determinants for c-Myc specific heterodimerization with Max and development of a novel homodimeric c-Myc b-HLH-LZ. *Journal of Moplecular Recognition,* 25(7), 414-426. http://doi:10.1002/jmr.2203.

- Bertrand, N., Castro S. D., Guillemot F. (2002) Proneural genes and the specification of neural cell types. *Nature Reviews Neuroscience*, 3(7), 517–530. htpp:// doi:10.1038/nrn874.
- Bhalla K., Phillips H.A., Crawford J., McKenzie O.L., Mulley J.C, et al. (2004). The de novo chromosome 16 translocations of two patients with abnormal phenotypes (mental retardation and epilepsy) disrupt the A2BP1 gene. *Journal of human Genetics*, 49, 308-311. http://doi:10.1007/s10038-004-0145-4.
- Blumenthal G.M., Dennis P.A. (2008). PTEN hamartoma tumor syndromes. *European Journal of Human Genetics*, 16(11), 1289-300. Htpp://doi:10.1038/ejhg.2008.162.
- Brodeur G.M., Seeger R.C., Schwab M., Varmus H.E., Bishop J.M. (1984). Amplification of N-myc in untreated human neuroblastomas correlates with advanced disease stage. *Science,* 224(4653), 1121-1124. htpp://doi:10.1126/science.6719137.
- Caiazzo M., Colucci-D'Amato L., Volpicelli F., Speranza L., Petrone C., Pastore L., Stifani S., Ramirez F. (2011). Krüppel-like factor 7 is required for olfactory bulb dopaminergic neuron development. *Experimental Cell Research,* 317(4), 464–473. https://doi.org/10.1016/j.yexcr.2010.11.006.
- Caiazzo M., Colucci-D'Amato L., Esposito M.T., Parisi S., Stifani S., Ramirez F., di Porzio U. (2010). Transcription factor KLF7 regulates differentiation of neuroectodermal and mesodermal cell lineages. *Experimental Cell Research,* 316 (14), 2365–2376. https://doi.org/10.1016/j.yexcr.2010.05.021.
- Carreira-Rosario A., Bhargava V., Hillebrand J., Kollipara R.K., Ramaswami M., Buszczak M. (2016), Repression of pumilio protein expression by Rbfox1 promotes germ cell

differentiation. *Developmental Cell,* 36(5), 562–571. http://doi:10.1016/j.devcel.2016.02.010.

- Courchesne E., Pierce K., Schumann C.M., Redcay E., Buckwalter J.A., Kennedy D.P.,et al.(2007). Mapping early brain development in autism. *Neuron*, 56(2), 399-413. htpp://doi:10.1016/j.neuron.2007.10.016.
- Chahrour M., Zoghbi H.Y.(2007).The story of Rett syndrome: from clinic to neurobiology. *Neuron*, 56(3):422-37. htpp://doi:10.1016/j.neuron.2007.10.001.
- Chen Y., Zubovic .L, Yang F., Godin K., Pavelitz T., Castellanos J., Macchi P., Varani G. (2016). Rbfox proteins regulate microRNA biogenesis by sequence-specific binding to their precursors and target downstream Dicer. *Nucleic Acids Research*, 44(9), 4381-95. http://doi:10.1093/nar/gkw177.
- Chisaka O., Musci T.S., Capecchi M.R. (1992). Developmental defects of the ear, cranial nerves, and hindbrain resulting from targeted disruption of the mouse homeobox gene Hox-1.6. *Nature*, 355(6360), 516-520. htpp://doi:10.1038/355516a0.
- Conciatori M., Stodgell C.J., Hyman S.L., O'Bara M., Militerni R., Bravaccio C., et al. (2004). Association between the HOXA1 A218G polymorphism and increased head circumference in patients with autism. *Biological Psychiatry* 15;55(4), 413-9. htpp://doi:10.1016/j.biopsych.2003.10.005.
- Convoy J.G., (2016) Developmental regulation of RNA procesing by Rbfox proteins. *RNA*, 8(2). http://doi:10.1002/wrna.1398.
- Damianov A., Black D.L. (2010). Autoregulation of Fox protein expression to produce dominant negative splicing factors. *RNA,* 16(2), 405-416. http://doi:10.1261/rna.1838210.

- Damianov A., Ying Y., Lin C.H., Lee J.A., Tran D., Vashisht A.A., Bahrami-Samani E., Xing Y., Martin K.C., Wohlschlegel J.A., et al. (2016). Rbfox proteins regulate splicing as part of a large multiprotein complex LASR. *Cell* , 165(3), 606–619.. http://doi:10.1016/j.cell.2016.03.040.
- Davis L.K., Maltman N, Mosconi M.W., Macmillan C., Schmitt L., Moore K., Francis S.M., Jacob S., Sweeney J.A., Cook E.H. (2012). Rare inherited A2BP1 deletion in a proband with autism and developmental hemiparesis. *American Journal of Medicine Genetics*, 158A(7), 1654-61. htpp://doi:10.1002/ajmg.a.35396.
- Desbarats L., Gaubatz S., Eilers M. (1996). Discrimination between different E-box-binding proteins at an endogenous target gene of c-myc. *Genes and Develppment,* 10(4):447-60. http://doi:10.1101/gad.10.4.447.
- Elia J., Gai X., Xie H.M., Perin J.C., Geiger E., Glessner J.T., D'Arcy M., de Berardinis R., Frackelton E., Kim C., et al. (2010). Rare structural variants found in attention-deficit hyperactivity disorder are preferentially associated with neurodevelopmental genes. *Molecular Psychiatry,* 5(6):637-46. http://doi:10.1038/mp.2009.57.
- Fanciulli M., Pasini E., Malacrida S., Striano P., Striano S., Michelucci R, Ottman R., Nobile C. (2014). Copy number variations and susceptibility to lateral temporal epilepsy: a study of 21 pedigrees. *Epilepsia* 55(10), 1651-8. htpp://doi: 10.1111/epi.12767.
- Fatemi S.H., Aldinger K.A., Ashwood P., Bauman M.L., Blaha C.D., Blatt G.J., et al. (2012). Consensus paper: pathological role of the cerebellum in autism. *Cerebellum,* (3):777-807. http://doi: 10.1007/s12311-012-0355-9.

- Fisher F., Crouch D.H., Jayaraman P.S., Clark W., Gillespie D.A., Goding C.R. (1993). Transcription activation by Myc and Max: flanking sequences target activation to a subset of CACGTG motifs in vivo. *The EMBO Journal*, 2(13):5075-82.
- Flora, A. et al. (2007) The E-protein Tcf4 interacts with Math1 to regulate differentiation of a specific subset of neuronal progenitors. *Proceedings of the National Academy of Sciences of the United States of America*, 104(39), 15382-15387. htpp://doi:10.1073/pnas.0707456104.
- Florio M., Huttner W. B. (2014) Neural progenitors, neurogenesis and the evolution of neocortex. *Development,* 141(11), 2182-2194. htpp://doi:10.1242/dev.090571.
- Fong A.P., Yao Z., Zhong J.W., Cao Y., Ruzzo W.L., Gentleman R.C., Tapscott S.J. (2012). Genetic and epigenetic determinants of neurogenesis and myogenesis. *Developmental Cell*, 22(4), 721-735. Htpp://doi:10.1016/j.devcel.2012.01.015.
- Forrest M.P., Hill M.J., Quantock A.J., Martin-Rendon E., Blake D.J.4. (2014). The emerging roles of TCF4 in disease and development. *Trends in Molecular Medicine,* 20(6), 322-331. http://doi: 10.1016/j.molmed.2014.01.010.
- Gaffney G.R, Kuperman S., Tsai L.Y., Minchin S. (1988). Morphological evidence for brainstem involvement in infantile autism. *Biological psychiatry,* 24(5), 578-586.
- Gallant N.M., Baldwin E., Salamon N., Dipple K.M., Quintero-Rivera F. (2011). Pontocerebellar hypoplasia in association with de novo 19p13.11p13.12 microdeletion. *American Journal of Medical Genetics*, 155A (11), 2871-8. http://doi: 10.1002/ajmg.a.34286.

- Gasparri F., Galvani A. (2010). Image-based high-content reporter assays: limitations and advantages*. Drug Discovery Today Technologies*, Spring, 7(1):e1-e94. http://doi: 10.1016/j.ddtec.2010.04.003.
- Gauthier J., Siddiqui T.J., Huashan P., Gauthier J., Siddiqui T.J., Huashan P., et al. (2011). Truncating mutations in NRXN2 and NRXN1 in autism spectrum disorders and schizophrenia. *Human Genetics*, 130(4), 563–573. htpp://doi:10.1007/s00439-011-0975-z.
- Gehman, L.T., Stoilov, P., Maguire, J., Damianov, A., Lin, C.H., Shiue, L., Ares, M. Jr., Mody, I. and Black, D.L. (2011). The splicing regulator Rbfox1 (A2BP1) controls neuronal excitation in the mammalian brain. *Nature Genetics*, 43(7), 706-711. http://doi:10.1038/ng.841.
- Geschwind, D.H. (2011). Genetics of autism spectrum disorders. *Trends in Cognitive Science,* 15(9), 409–416. https://doi:10.1016/j.tics.2011.07.003.
- Gkogkas C.G., Khoutorsky A., Ran I., Rampakakis E., Nevarko T., Weatherill D.B., et al. (2013). Autism-related deficits via dysregulated eIF4E-dependent translational control. *Nature*, 493(7432), 371-377. htpp://doi:10.1038/nature11628.
- Götz M., Huttner W. B. (2005). The cell Biology of neurogenesis. *Nature Reviews Molecular Cell Biology, 6(10), 777-788.* htpp://doi: 10.1038/nrm1739.
- Griswold AJ.., Dueker N.D., Van Booven D., Rantus J.A., Jaworski J.M., et al. (2015). Targeted massively parallel sequencing of autism spectrum disorder-associated genes in a case control cohort reveals rare loss-of-function risk variants. *Molecular Autism,* 6:43. http://doi:10.1186/s13229-015-0034-z.

- Guven-Ozkan T., Busto Germain U., Schutte Soleil S., Cervantes-Sandoval I., O'Dowd D. K., Davis R .L. (2016). MiR-980 is a memory suppressor microRNA that regulates the autism-susceptibility gene A2bp1. *Cell Reports*, 14(7), 1698-1709. http://doi:10.1016/j.celrep.2016.01.040.
- Hadjixenofontos A., Schmidt M.A., Whitehead P.L., Konidari I., Hedges D.J., Wright H.H., et al. (2013). Evaluating mitochondrial DNA variation in autism spectrum disorders. *Annals of Human Genetics*, 77(1), 9-21. http://doi:10.1111/j.1469-1809.2012.00736.x.
- Håndstad T., Rye M., Močnik R., Drabløs F., Sætrom P. (2012). Cell-type specificity of ChIP-predicted transcription factor binding sites. *BMC Genomics,* 13:372. http://doi:10.1186/1471-2164-13-372.
- Hamada N., Ito H., Iwamoto I., Mizuno M., Morishita R., Inaguma Y., Kawamoto S, Tabata H., Nagata K. (2013). Biochemical and morphological characterization of A2BP1 in neuronal tissue. *Journal of Neuroscience Research,* 91(10), 1303-1311. http://doi:10.1002/jnr.23266.
- Hamada N., Ito H., Iwamoto I., Morishita R., Tabata H., Nagata K. (2015). Role of the cytoplasmic isoform of RBFOX1/A2BP1 in establishing the architecture of the developing cerebral cortex*. Molecular Autism*, 6, 56. http://doi:10.1186/s13229-015-0049-5.
- Hamada N., Ito H., Nishijo T., Iwamoto I., Morishita R., Tabata H., Momiyama T., Nagata K. (2016). Essential role of the nuclear isoform of *RBFOX1*, a candidate gene for autism spectrum disorders, in the brain development. *Scientific Reports*, 6, 30805. http://doi:10.1038/srep30805.

- Hammock E.A., Levitt P. (2011). Developmental expression mapping of a gene implicated in multiple neurodevelopmental disorders, A2bp1 (Fox1). Developmental Neuroscience, 33(1): 64–74. htpp://doi:10.1159/000323732.
- Hatakeyama J., Bessho Y., Katoh K., Ookawara S., Fujioka M., Guillemot F., Kageyama R. (2004). Hes genes regulate size, shape and histogenesis of the nervous system by control of the timing of neural stem cell differentiation. *Development*, 131(22):5539-50. http://doi: 10.1242/dev.01436.
- Hemara-Wahanui A., Berjukow S., Hope C.I., Dearden P.K., Wu S.B., Wilson-Wheeler J., et al. (2005). A *CACNA1F* mutation identified in an X-linked retinal disorder shifts the voltage dependence of the Cav1.4 channel activation. *Proceedings of the National Academy of Sciences of the United States of America,* 102(21), 7553-8. htpp://doi:10.1073/pnas.0501907102.
- Hodgkin J., Zellan J.D., Albertson D.G. (1994). Identification of a candidate primary sex determination locus, fox-1, on the X chromosome of Caenorhabditis elegans. *Development*. 120(12), 3681-3689.
- Hu X.L., Wang Y., Shen Q. (2012). Epigenetic control on cell fate choice in neural stem cells. *Protein Cell,* 3(4), 278-90. http://doi:10.1007/s13238-012-2916-6.
- Ince-Dunn G., Hall B.J., Hu S.C., Ripley B., Huganir R.L., Olson J.M., Tapscott S.J., Ghosh A. (2006). Regulation of thalamocortical patterning and synaptic maturation by NeuroD2. *Neuron,* 2; 49 (5), 683-95. http://doi:10.1016/j.neuron.2006.01.031.
- Ince-Dunn G1, Hall BJ, Hu SC, Ripley B, Huganir RL, Olson JM, Tapscott SJ, Ghosh A.

- Iossifov I., Ronemus M., Levy D., Wang Z., Hakker I., et al. (2012). De Novo Gene Disruptions in Children on the Autistic Spectrum. *Neuron*, 74(2), 285-299. http://dx.doi.org/10.1016/j.neuron.2012.04.009.
- Ishibashi M., Ang S. L., Shiota K., Nakanishi S., Kageyama R.,Guillemot, F. (1995). Targeted disruption of mammalian hairy and Enhancer of split homolog-1 (HES-1) leads to up-regulation of neural helix-loop-helix factors, premature neurogenesis, and severe neural tube defects. *Genes and Devdelopment,* 15;9(24):3136-48.
- Jin Y., Suzuki H., Maegawa S., Endo H., Sugano S., Hashimoto K., Yasuda K., Inoue K. (2003). A vertebrate RNAbinding protein Fox-1 regulates tissue-specific splicing via the pentanucleotide GCAUG. *The EMBO Journal*, 22(4):905-912. http://doi:10.1093/emboj/cdg089.
- Kandel E.R.; Schwartz J.H.; Jessell, T.M. (2000). Principles of Neural Science (Fourth edition). *United State of America: McGraw-Hill,* 324. ISBN 0-8385-7701-6.
- Kato G.J., Lee W.M., Chen L.L., Dang C.V. (1992). Max: functional domains and interaction with c-Myc. *Genes & Development,* 6(1),81-92. htpp://doi:10.1101/gad.6.1.81.
- Kageyama R., Shimojo H., Imayoshi I. (2015). Dynamic expression and roles of Hes factors in neural development. *Cell and Tissue Research,* 359(1), 125-33. http://doi: 10.1007/s00441-014-1888-7.
- Kageyama R., Ohtsuka T., Kobayashi T. (2007). The Hes gene family: repressors and oscillators that orchestrate embryogenesis. *Development,* 134(7):1243-51. http:// doi:10.1242/dev.000786.

- Kaushik, G., Zarbalis K. S. (2016). Prenatal Neurogenesis in Autism Spectrum Disorders. *Frontiers in Chemistry* 4, 12. htpp:// doi:10.3389/fchem.2016.00012
- Kiehl T.R., Shibata H., Vo T., Huynh D.P., Pulst S.M. (2001). Identification and expression of a mouse orthologue of A2BP1. *Mammalian Genome,* 12(8):595-601.
- Kim K.K., Yang Y., Zhu J., Adelstein R.S., Kawamoto S.(2014). Rbfox3 controls the biogenesis of a subset of micro- RNAs. *Nature Structural&Molecular Biology*, 21(10), 901-10. http://doi:10.1038/nsmb.2892.
- Kim K.K., Adelstein R.S., Kawamoto S. (2009) Identification of neuronal nuclei (NeuN) as Fox-3, a new member of the Fox-1 gene family of splicing factors. *Journal of Biological Chemistry,* 284(45):31052-31061. http://doi:10.1074/jbc.M109.052969.
- Klinck R., Fourrier A., Thibault P., Toutant J., Durand M., Lapointe E., Caillet-Boudin M.L., Sergeant N., Gourdon G., Meola G., et al. (2014). RBFOX1 cooperates with MBNL1 to control splicing in muscle, including events altered in myotonic dystrophy type 1. *PLoS One*, 9(9): e107324. http://doi:10.1371/journal.pone.0107324.
- Krey J., Dolmetsch R. (2007). Molecular mechanisms of autism: a possible role for Ca2+ signaling. *Current Opinion in Neurobiology,* 17(1), 112-9. htpp://doi:10.1016/j.conb.2007.01.010.
- Kuroyanagi H. (2009). Fox-1 family of RNA-binding proteins. *Cellular and Molecular Life Sciences,* 66(24): 3895–3907. http://doi:10.1007/s00018-009-0120-5.
- Kuroyanagi H., Ohno G., Mitani S., Hagiwara M. (2007). The Fox-1 family and SUP-12 coordinately regulate tissue-specific alternative splicing in vivo. *Molecular Cell Biology*, 27(24), 8612–8621. http://doi:10.1128/MCB.01508-07.

- Lai M.C., Lombardo M.V., Baron-Cohen S. (2013). Autism. *Lancet,* 383(9920), 896-910. http:// doi:10.1016/S0140-6736(13)61539-1.
- Lal D., Pernhorst K., Klein K.M., Reif P., Tozzi R., Toliat M.R., Winterer G., Neubauer B., Nürnberg P., Rosenow F., et al. (2015). Extending the phenotypic spectrum of RBFOX1 deletions: Sporadic focal epilepsy. *Epilepsia*, 56(9), e129-33. htpp://doi: 10.1111/epi.13076.
- Lal D., Reinthaler E.M., Altmuller J., Toliat M.R., Thiele H., Nurnberg P., Lerche H., Hahn A., Moller R.S., Muhle H., et al. (2013). RBFOX1 and RBFOX3 mutations in rolandic epilepsy. *PLoS ONE* 8(9), e73323. htpp://doi:10.1371/journal.pone.0073323.
- Lam C.W., Yeung W.L., Ko C.H., Poon P.M., Tong S.F., Chan K.Y., et al. (2000). Spectrum of mutations in the MECP2 gene in patients with infantile autism and Rett syndrome. *Journal of Medical Genetics*, 37(12), E41. htpp://doi:10.1136/jmg.37.12.e41.
- Laub F. Lei L., Sumiyoshi H., Kajimura D., Dragomir C., Smaldone S., Puche A.C., Petros T.J., Mason C., Parada L.F., Ramirez F. (2005). Transcription factor KLF7 is important for neuronal morphogenesis in selected regions of the nervous system. *Molecular Cell Biology* 25(13), 5699-5711. htpp://doi: 10.1128/MCB.25.13.5699-5711.2005.
- Laumonnier F, Roger S, Guerin P, Molinari F, M'rad R, Cahard D, et al. (2006). Association of a functional deficit of the BKCa channel, a synaptic regulator of neuronal excitability, with autism and mental retardation. *American Journal of Psychiatry,* 163(9):1622-9. htpp://doi:10.1176/ajp.2006.163.9.1622.
- Lei L., Ma L., Nef S., Thai T., Parada L.F. (2001). mKlf7, a potential transcriptional regulator of TrkA nerve growth factor receptor expression in sensory and sympathetic neurons. *Development,* 128(7), 1147-1158.

- Levy D., Ronemus M., Yamrom B., Lee Y.H., Leotta A., Kendall J. (2011). Rare de novo and transmitted copy-number variation in autistic spectrum disorders. *Neuron,* 70(5), 886-897. http://doi: 10.1016/j.neuron.2011.05.015.
- Le-Niculescu H., Patel S.D., Bhat M., Kuczenski R., Faraone S.V., Tsuang M.T., McMahon F.J., Schork N.J., Nurnberger J.I., Jr., Niculescu A.B., III. (2009). Convergent functional genomics of genome-wide association data for bipolar disorder: comprehensive identification of candidate genes, pathways and mechanisms. *American journal of Medical Genetics Part B (Neuropsychiatric Genetics),* 150B (2), 155-181. htpp://doi:10.1002/ajmg.b.30887.
- Lee, J.A., Damianov A., Lin C.H., Fontes M., Pariksshak N. N.., Anderson E. S., Geschwind D. H., Black D. L. Martin K. C. (2016) Cytoplasmic Rbfox1 Regulates the Expression of synaptic and Autism-related Genes. *Neuron*, 89(1), 113-128. http://doi: 10.1016/j.neuron.2015.11.025.
- Lee J.A., Tang Z.Z., Black D.L. (2009). An inducible change in Fox-1/A2BP1 splicing modulates the alternative splicing of downstream neuronal target exons. *Genes and Development*, 23(19), 2284-2293. http://doi:10.1101/gad.1837009.
- Lichtenstein P., Carlström E., Råstam M., Gillberg C., Anckarsäter H.(2010) The genetics of autism spectrum disorders and related neuropsychiatric disorders in childhood. *The American Journal of Psychiatry,* 167(11), 1357-63. https://doi.org/10.1176/appi.ajp.2010.10020223.
- Lintas C., Persico A.M. (2009). Autistic phenotypes and genetic testing: state-of-the-art for the clinical geneticist. *Journal of Medical Genetics,* 46(1), 1-8. Htpp://doi:10.1136/jmg.2008.060871.

- Makki N., Capecchi M.R. (2011). Identification of novel Hoxa1 downstream targets regulating hindbrain, neural crest and inner ear development. *Developmental Biol*ogy, 357(2), 295-304. htpp://doi:10.1016/j.ydbio.2011.06.042.
- Maris C., Dominguez C., Allain F.H. (2005) The RNA recognition motif, a plastic RNA-binding platform to regulate post-transcriptional gene expression. *The FEBS journal,* 272(9), 2118–2131. http://doi:10.1111/j.1742-4658.2005.04653.x.
- Martin C.L., Duvall J.A., Ilkin Y., Simon J.S., Arreaza M.G., et al. (2007). Cytogenetic and molecular characterization of A2BP1/FOX1 as a candidate gene for autism. *American journal of Medical Genetics Part B (Neuropsychiatric Genetics),* 144B(7), 869-76. http://doi:10.1002/ajmg.b.30530.
- Massari M.E., Murre C. (2000) Helix–loop–helix proteins: regulators of transcription in eucaryotic organisms. *Molecular and Cellular Biology,* 20, 429-440. http://doi:10.1128/MCB.20.2.429-440.2000.
- Mikhail F.M., Lose E.J., Robin N.H., Descartes M.D., Rutledge K.D., et al. (2011). Clinically relevant single gene or intragenic deletions encompassing critical neurodevelopmental genes in patients with developmental delay, mental retardation, and/or autism spectrum disorders. *American Journal of Medical Genetics,* 155A(10), 2386-96. htpp.//doi:10.1002/ajmg.a.34177.
- Molyneaux B.J., Arlotta P., Menezes J.R., Macklis J.D. (2007). Neuronal subtype specification in the cerebral cortex. *Nature Reviews. Neuroscience,* 8(6), 427-37. http:// doi:10.1038/nrn2151.
- Mosca S.J., Langevin L.M., Dewey D., Innes A.M., Lionel A.C., Marshall C.C., Scherer S.W., Parboosingh J.S., Bernier F.P. (2016). Copy-number variations are enriched for

neurodevelopmental genes in children with developmental coordination disorder. *Journal of Medical Genetics*, 53(12), 812-819. htpp://doi:10.1136/jmedgenet-2016-103818.

- Murphy D.M., Buckley P.G., Bryan K., Das S., Alcock L., Foley N.H., Prenter S., Bray I., Watters K.M., Higgins D., Stallings R.L. (2009). Global MYCN transcription factor binding analysis in neuroblastoma reveals association with distinct E-box motifs and regions of DNA hypermethylation. *PLoS One*, 4(12), e8154. htpp://doi: 10.1371/journal.pone.0008154.
- Nadarajah B., Parnavelas J.G. (2002). Modes of neuronal migration in the developing cerebral cortex. *Nature Reviews. Neuroscience,* 3(6), 423-32. htpp://doi: 10.1038/nrn845.
- Nakahata S., Kawamoto S. (2005). Tissue-dependent isoforms of mammalian Fox-1 homologs are associated with tissue-specific splicing activities. *Nucleic Acids Res*search, 33, 2078–2089. http://doi:10.1093/nar/gki338.
- Neale, B.M.; Kou Y.; Liu L.; Ma'ayan A.; Samocha K.E.; Sabo A.et al. (2012) Patterns and rates of exonic de novo mutations in autism spectrum disorders. *Nature* 485 (7397), 242–245. htpp://doi:10.1038/nature11011.
- Need A.C., Attix D.K., McEvoy J.M., Cirulli E.T., Linney K.L., Hunt P., et al. (2009). A genomewide study of common SNPs and CNVs in cognitive performance in the CANTAB. *Human Molecular Genetics*; 18(23), 4650-4661. htpp://doi:10.1093/hmg/ddp413.
- Need A.C., Ge D., Weale M.E., Maia J., Feng S., Heinzen E.L., et al. (2009). A genomewide investigation of SNPs and CNVs in schizophrenia. *PLoS Genetics,* 5(2):e1000373. htpp://doi:10.1371/journal.pgen.1000373.

- Neves-Pereira M., Müller B., Massie D., Williams J.H., O'Brien P.C., Hughes A., et al. (2009). Deregulation of EIF4E: a novel mechanism for autism. Journal of *Medical Genetics*, 46(11), 759-765. Htpp://doi:10.1136/jmg.2009.066852.
- Niwano K., Arai M., Koitabashi N., Hara S., Watanabe A., Sekiguchi K., Tanaka T., Iso T., Kurabayashi M. (2006). Competitive binding of CREB and ATF2 to cAMP/ATF responsive element regulates eNOS gene expression in endothelial cells. *Arteriosclerosis, Thrombosis and Vascular Biology*, 26(5), 1036-1042. http://doi:10.1161/01.ATV.0000215179.76144.39.
- Oksenberg N., Stevison L., Wall J.D., Ahituv N. (2013). Function and regulation of AUTS2, a gene implicated in autism and human evolution. *PLoS,* 9(1):e1003221. http://doi: 10.1371/journal.pgen.1003221.
- Persico, A.M., Napolioni, V. (2013). Autism genetics. *Behavioural Brain Research,* 251, 95-112. https://doi.org/10.1016/j.bbr.2013.06.012.
- Pfaffl, M.W. (2001). A new mathematical model for relative quantification in real-time RT-PCR. *Nucleic Acids Research*, 29(9): p. e45.
- Prochownik E.V., VanAntwerp M.E. (1993). Differential patterns of DNA binding by myc and max proteins. *Proceeding of the National Academy of Sciences of the United States of America,* 90(3), 960-964.
- Rabbani B., Mahdieh N., Hosomichi K., Nakaoka H., Inoue I. (2012). Next-generation sequencing: impact of exome sequencing in characterizing Mendelian disorders. *Journal of Human Genetics* 57(10), 621-32. htpp://doi:10.1038/jhg.2012.91.
- Rakic, P. (2009). Evolution of the neocortex: a perspective from developmental biology. *Nature Reviews Neuroscience,* 10 (10), 724–735. Htpp://doi:10.1038/nrn2719.

- Rakic P. (1988) Specification of cerebral cortical areas. *Science*, 241(4862), 170-176. http.//doi:10.1126/science.3291116.
- Rogers, T.D., McKimm, E., Dickson, P.E., Goldowitz, D., Blaha C.D., Mittleman G. (2013). Is autism a disease of the cerebellum? An integration of clinical and pre-clinical research. *Frontiers in Systems Neuroscience,* 7(15), 1-16. https://doi.org/10.3389/fnsys.2013.00015.
- Ronald A., Happé F., Bolton P., Butcher L.M., Price T.S., Wheelwright S., Baron-Cohen S., Plomin R. (2006). Genetic heterogeneity between the three components of the autism spectrum: a twin study. *Journal of the American Academy of Child and Adolescent Psychiatry*, 45(6), 691-9. http://dx.doi.org/10.1097/01.chi.0000215325.13058.9d.
- Roy A.L., Carruthers C., Gutjahr T., Roeder R.G. (1993). Direct role for Myc in transcription initiation mediated by interactions with TFII-I. *Nature,* 365(6444), 359-361. http://doi:10.1038/365359a0.
- Roybon L., Mastracci T.L., Ribeiro D., Sussel L., Brundin P., Li J.Y. (2010). GABAergic differentiation induced by Mash1 is compromised by the bHLH proteins Neurogenin2, NeuroD1, and NeuroD2. *Cerebral Cortex*, 20(5), 1234-1244. http://doi:10.1093/cercor/bhp187.
- Rubeis Silvia de., He X.; Goldberg A., Poultney P., Christopher S., Samocha K., Cicek A. et al. (2014). Synaptic, transcriptional and chromatin genes disrupted in autism. *Nature* 515 (7526), 209–215. http://doiI:10.1038/nature13772.
- Sanders S.J.; Murtha M.T.; Gupta A.R.; Murdoch J.D.; Raubeson M.J.; Willsey, A. J. et al. (2012). De novo mutations revealed by whole-exome sequencing are strongly associated with autism. *Nature* 485 (7397), 237–241. http://doi:10.1038/nature10945.

- Sanders S.J., Ercan-Sencicek A.G., Hus V., Luo R., Murtha M.T., Moreno-De-Luca D. et al. (2011) Multiple recurrent de novo CNVs, including duplications of the 7q11.23 Williams syndrome region, are strongly associated with autism. *Neuron,* 70(5), 863-885. http://doi: 10.1016/j.neuron.2011.05.002.
- Sandin S., Lichtenstein P., Kuja-Halkola R., Larsson H., Hultman C.M., Reichenberg A. (2014). The Familial risk of Autism. *Jama Journals,* 311(17), 1770-1777. http://doi:10.1001/jama.2014.4144.
- Sebat J.; Lakshmi B.; Malhotra D.; Troge J.; Lese-Martin C.; Walsh T.et al. (2007). Strong association of de novo copy number mutations with autism. *Science*, 316 (5823, 445–449. http://doi:10.1126/science.1138659.
- Sebat J., Lakshmi B., Malhotra D., Troge J., Lese-Martin C., Walsh T., Yamrom B., Yoon S., Krasnitz A., Kendall J., et al. (2007). Strong association of de novo copy number mutations with autism. *Science*, 316(5823), 445-9. http://doi:10.1126/science.1138659.
- Sepp M., Vihma H., Nurm K., Urb M., Page S.C., Roots K., Hark A., Maher B.J., Pruunsild P., Timmusk T. (2017). The Intellectual Disability and Schizophrenia Associated Transcription Factor TCF4 Is Regulated by Neuronal Activity and Protein Kinase A. *The journal of Neuroscience,* 7(43), 10516-10527. htpp://doi:10.1523/JNEUROSCI.1151-17.2017.
- Sepp M., Pruunsild P., Timmusk T. (2012). Pitt-Hopkins syndrome-associated mutations in TCF4 lead to variable impairment of the transcription factor function ranging from hypomorphic to dominant-negative effects. *Human Molecular Genetics,* 21(13), 2873-2888. htpp://doi: 10.1093/hmg/dds112.

- Sepp, M. et al. (2011) Functional diversity of human basic helix–loop–helix transcription factor TCF4 isoforms generated by alternative 5' exon usage and splicing. *PLoS ONE* 6(7):e22138. https://doi.org/10.1371/journal.pone.0022138.
- Shibata H., Huynh D.P., Pulst S.M. (2000). A novel protein with RNA-binding motifs interacts with ataxin-2. *Human Molecular Genetics*, 9(12), 1903.
- Shin H.W., Choi H., So D., Kim Y.I., Cho K., Chung H.J., et al. (2014). ITF2 prevents activation of the β-catenin-TCF4 complex in colon cancer cells and levels decrease with tumor progression. *Gastroenterology*, 147(2), 430-442.e8. http://doi:10.1053/j.gastro.2014.04.047.
- Shrivastava A., Saleque S., Kalpana G.V., Artandi S., Goff S.P, Calame K. (1993). Inhibition of transcriptional regulator Yin-Yang-1 by association with c-Myc. *Science,* 262(5141), 1889-1892.
- Spitz F., Furlong E.E. (2012). Transcription factors: from enhancer binding to developmental control. *Nature Reviews. Genetics,* 13(9), 613-626. http://doi:10.1038/nrg3207.
- Splawski I., Timothy K.W., Sharpe L.M., Decher N., Kumar P., Bloise R., et al.(2004). Ca(V)1.2 calcium channel dysfunction causes a multisystem disorder including arrhythmia and autism. *Cell*, 119(1):19-31. htpp://doi:10.1016/j.cell.2004.09.011.
- Stefansson H., et al. (2009). Common variants conferring risk of schizophrenia. *Nature* 460(7256), 744–747. http://doi:10.1038/nature08186.
- Song R.R., Zou L., Zhong R., Zheng X.W., Zhu B.B., Chen W., et al. (2011). An integrated meta-analysis of two variants in HOXA1/HOXB1 and their effect on the risk of autism spectrum disorders. *PLoS ONE,* 6(9), e25603. Htpp://doi:10.1371/journal.pone.0025603.

- Tang Z.Z., Zheng S., Nikolic J., Black D.L. (2009). Developmental control of CaV1.2 L-type calcium channel splicing by Fox proteins. *Molecular Cell Biology,* (17), 4757-65. http://doi:10.1128/MCB.00608-09.
- Taverna, E. Götz M., Huttner W.B. (2014). The Cell Biology of Neurogenesis: Toward an Understanding of the Development and Evolution of the Neocortex. *Annual Review of Cell and Developmental Biology*, 30, 465-502. http://doi:10.1146/annurev-cellbio-101011-155801.
- Taylor I.A., McIntosh P.B., Pala P., Treiber M.K., Howell S., Lane A.N., Smerdon S.J. (2000). Characterization of the DNA-binding domains from the yeast cell-cycle transcription factors Mbp1 and Swi4. *Biochemistry*, 39(14), 3943-3954. http://doi:10.1021/bi992212i.
- Underwood J.G., Boutz P.L., Dougherty J.D., Stoilov P., Black D.L. (2005) Homologues of the Caenorhabditis elegans Fox-1 protein are neuronal splicing regulators in mammals. *Molecular Cell Biology,* 25(22), 10005-10016. http://doi:10.1128/MCB.25.22.10005-10016.2005.
- Vaags A.K., Lionel A.C., Sato D., Goodenberger M., Stein Q.P., Curran S., et al. (2012). Rare deletions at the neurexin 3 locus in autism spectrum disorder. *American Journal of Human Genetics*, 90(1), 133–141. htpp://doi:10.1016/j.ajhg.2011.11.025.
- Voineagu I., Wang X., Johnston P., Lowe J.K., Tian Y., et al. (2011). Transcriptomic analysis of autistic brain reveals convergent molecular pathology. *Nature* 474, 380-384. http://doi:10.1038/nature10110.
- Walhout A.J., van der Vliet P.C., Timmers H.T. (1998). Sequences flanking the E-box contribute to cooperative binding by c-Myc/Max heterodimers to adjacent binding sites.

Biochimica et Biophysica Acta, 1397(2):189-201. https://doi.org/10.1016/S0167-4781(97)00227-3.

- Wechsler D.S., Papoulas O., Dang C.V., Kingston R.E. (1994). Differential binding of c-Myc and Max to nucleosomal DNA. *Molecullar and Cellular Biology,* 14(6), 4097-4107.
- Weiss L.A. (2009). Autism genetics: emerging data from genome-wide copy-number and single nucleotide polymorphism scans. *Expert Review of Molecular Diagnostics,* 9(8), 795-803. htpp://doi: 10.1586/erm.09.59.
- Weiss L.A., Escayg A., Kearney J.A., Trudeau M., MacDonald B.T., Mori M., et al. (2003). Sodium channels SCN1A, SCN2A and SCN3A in familial autism. *Molecular Psychiatry*, 8(2):186-94. htpp://doi: 10.1038/sj.mp.4001241.
- Wenzel M., Schüle M., Casanovas S., Strand D., Strand S., Winter J. (2016). Identification of a classic nuclear localization signal at the N terminus that regulates the subcellular localization of Rbfox2 isoforms during differentiation of NMuMG and P19 cells. *FEBS,* 590(24), 4453-4460. http://doi:0.1002/1873-3468.12492.
- Weyn-Vanhentenryck S.M., Mele A., Yan Q., Sun S., Farny N., Zhang Z., Xue C., Herre M., Silver Pamela A., Zhang Michael Q., et al. (2014). HITS-CLIP and integrative modeling define the Rbfox splicing-regulatory network linked to brain development and autism. *Cell Reports*, 6(6), 1139-1152. http://doi:10.1016/j.celrep.2014.02.005.
- Wintle R.F., Lionel A.C., Hu P., Ginsberg S.D., Pinto D., Thiruvahindrapduram B., Wei J., Marshall C.R., Pickett J., Cook E.H., et al. (2011). A genotype resource for postmortem brain samples from the Autism Tissue Program. *Autism Research,* 4(2), 89-97. htpp://doi: 10.1002/aur.173.

- Wu K.J., Grandori C., Amacker M., Simon-Vermot N., Polack A., Lingner J., Dalla-Favera R. (1999). Direct activation of TERT transcription by c-MYC. *Nature Genetics,* 21(2), 220-224. http://doi:10.1038/6010.
- Zahir F.R., Baross A., Delaney A.D., Eydoux P., Fernandes N.D., Pugh T., et al. (2008). A patient with vertebral, cognitive and behavioural abnormalities and a de novo deletion of NRXN1 alpha. *Journal of Medical Genetics,* 45(4):239-43. htpp://doi:10.1136/jmg.2007.054437.
- Zhang C., Frias M.A., Mele A., Ruggiu M., Eom T., Marney C.B., Wang H., Licatalosi D.D., Fak J.J., Darnell R.B. (2010). Integrative modeling defines the Nova splicing-regulatory network and its combinatorial controls. *Science*, 329(5990), 439-43. http://doi:10.1126/science.1191150.
- Zhao, W.W. (2013). Intragenic deletion of *RBFOX1* associated with neurodevelopmental/neuropsychiatric disorders and possibly other clinical presentations. *Molecular cytogenetics*, 6(1), 26. htpp://doi:10.1186/1755-8166-6-26.

6. Supplements

6.1 Vectors information

6.1.1 pGEM-T easy vector

Lenght: 3015 bp

T7 RNA polymerase transcription initiation site: 1

SP6 RNA polymerase transcription initiation site: 141

M13 Reverse Sequencing Primer binding site 176–197

M13 Forward Sequencing Primer binding site 2949–2972

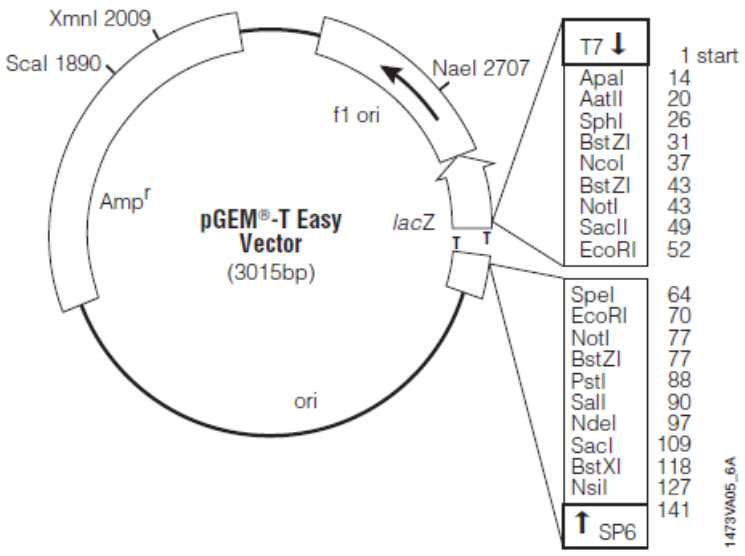

Figure 49. pGEM®-T Easy Vector features list map.

6.1.2 pGL4.10 [luc2] vector

Length: 4242 bp

Key sites

KpnI: 18

Hind III: 66

XhoI: 34

Bgl ll: 47

Vector features:

Multiple cloning region 1–70

luc2 reporter gene 100–1752

SV40 late poly(A) region 1787–2008

Reporter Vector primer 4 (RVprimer4) binding region 2076–2095

Synthetic "-lactamase (Ampr) coding region 3124–3984

Synthetic poly(A) signal/transcriptional pause site 4089–4242

Reporter Vector primer 3 (RVprimer3) binding region 4191–4210

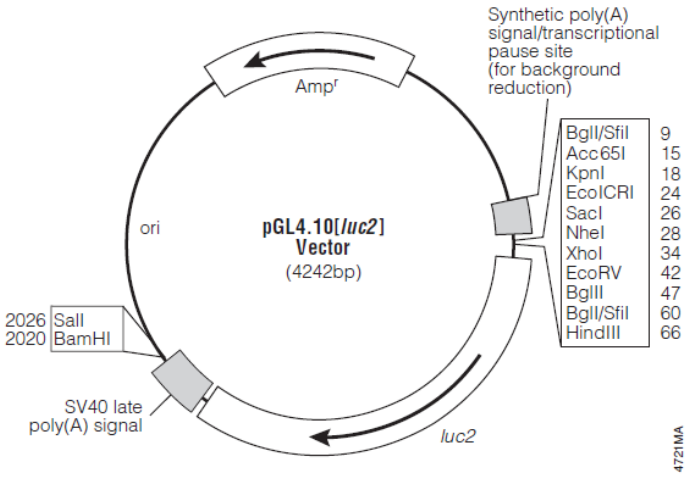

Figure 50. pGL4.10 [luc2] vector features list and map

6.1.3 pRL-TK vector

Base pairs 4045

HSV TK promoter 7-759

Chimeric intron 826-962

T7 RNA polymerase Promoter (-17 to +2) 1006-1024

T7 RNA polymerase transcription initiation site 1023

Rluc reporter 1034-1969

SV40 late polyadenylation signal 2011-2212

Beta-lactamase (AmpR) 2359-3219

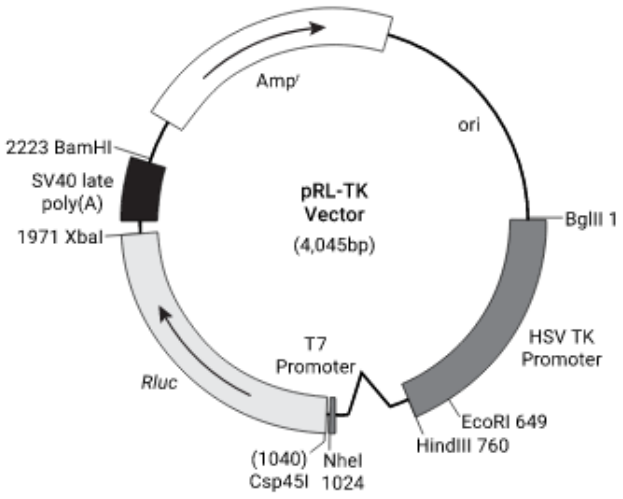

Figure 51. pRL-TK vector features list and map.

6.2 In situ hybridization probes and sequences

6.2.1 Rbfox1 transcript 1B probe

Rbfox1 DNA showing Exon 1 in red. Primers binding site are highlighted in yellow. PCR Product: 197 bp.

AAGTGGACCAGGGCAAGGGGTCTCCATACCCTTAGGCCTTTTGAGATTCCTTTTCCTACC
TTGCCTATGAGGACAAGGGGGAGGCGTTCAGGATGGAGAGCTCATTTAGGGGCTGGCTGA
GCAAACCCACTTTGGGAAGAGGAAGGCCTCAATCTAAGGACGTGTGTTCTCTGCTCCACC
CACTCTGGAAGGCAACTTTCACCCCTTGTGCACTTTAGGAAGAAGAGACTAGGGGCACCT
AGTCCCTTGCCCACAGCGGCTGCTGGAATTCAAGGCTGCAAGCGTGACCGTGACCGCGGC
GGCAGCACTGGAGAGGGAAGGGGGAGGGGGCGCTCCCTGGTGCTCGGGATTATTTTTGGC
TCGCCAGCCCGGCTGCTCGCTGCCTGTCGCGCGCGCGCGCGGGCACACACAGACACAC
ACACTCACACACACACACAGAGAGACACACACACACACATGCACACATTTTTCTCGCGCT
CTCCCTAGCTCTCCGCTCTCCTTTGTTTATTTTCTAATCTGGATTTTGTTGGTTGCGCTC
TTCTTTGCTTCTCCTCCGGTCCAGCTTGCCAGCACTCCCGTGGGCCACCCAGTGCTCGCC
TGCTGCTCCCAAATCAGCGTCACCCGGTCCCCTCCTCCCGGCCTCCTGGAGCGCGGGGTT
TGAAGGTCACCTCCTTTCTAGTTCCCCCTGCGAGCCGAGCCGCCTCCACCCTCCTCCGTC
TGGATCCCAGAAGTGTCAGTCGCAGCGGCTGATACCTCGGATAGGGGTCCGCGCGTGGTA
GCAGGGAGGGGAGCCCGAACTCAGAGTCGAGGGGGAATTACTCCCTCTTCTTATCGCGCC
AGACCCGGCTGCACCACGGAAGAGTGGGGGCGCTCTGCCAGCCACAGGACCCACGCGTGC
GCCTCGCGGACCCGAGAAACCACCAGTGAGTCGCTCAGCTCGCATCTGGAGGGGACAGCC
GTGCGCCCCGCCCCAGCGTCCGGAGCCGACAACTCCGAGCGTCCTCCCAGCTCAGGACAG
ATCTGAGAGGACCTAGCGCATCTCCAGATCCCGGAAACCCCTGCGCTTCAGACCAGGTGG
CCTTGGACACCAGGGCCCCTTAGGAGTGATCCGGACCTTCGCCGCGCCCAGTAGTAGGGC
GCGGCTGACCTGCCGCGAAGTTGTGGCCAGCTGGAGTGAGAGAAGCCAACATCCTAATTC
GTTGCCTCTGGTGGATGCTGAACGCGGCTGGGGTCACACAGAGAACTGAGGAATCCAGGA
GCAGGCAACAACTGCCAAGCTCGCCAGGAGTTCTAGGTAAGTCCAGGCAGAGTCGCCCAC
TTTTGCGCTACCTAATCCGGACCCAACCCAAAGGGTCCCAGGAAAGAAAAACCGAGGTTC
CAGCAAAGGTGGCCTCCTCCCAGAGCCACTCTGGGTGTGATGCACCTGGAAGTTTTACAG
GGCATGAAGAGCAATCTCTTGGCACGTTCCTGGAGAGGGACTTAACCATGAGCCCCCTAC
TCCACCTCCACACATTGTCTCTTCTCCCTTCTTATCTTTCCTTGCCCCCAGGGTATCCCT
CCTAAGCTCCCAGGATGCCTCCTCTGGCCTCCCATTGCATCCCAGGGGCAGCAGCTGCAG

6.2.2 Rbfox1 all transcripts probe

Rbfox1 DNA showing Exons 6 and 7 in red. Primers binding sites are highlighted in yellow. PCR Product: 242bp.

TGTACAGACCTCAGAAAGTAGTATTGGAGGTCTAGGGAGTGTGATGTCATCGTGTTCCTT
GATCTTTTGTTTCCATCTGTAAATTGAGAATGATGATGATCACCATTTGCTCATAGTGTG
TGGTGAGGCTTGGCTGAGAAGCCAATCCTTAGGGCCCTGCAAAGAGTGCTGGGGCTCAGT
TCCTGTAATGTGGGGGGACAGTTCTGTTTGTGGAGCTCTAATGGTGTTCTCTTCCCTTCT
CTTTTTCTTTTCTTCCCACAGGGTAATCAGGAAGCAGCCGCCGCCCCTGACACAATGGCT
CAGCCTTATGCCTCAGCGCAGTTCGCACCACCCCAGAATGGCATCCCTGCAGAATACACG
GCCCCTCATCCTCATCCCGCGCCAGAGTACACCGGCCAGACCACTGTCCCTGACCACACA
TTAAACCTGTATCCTCCTACACAGACGCACTCGGAGCAGAGTGCTGACACCAGTGCGCAG
ACCGTCTCCGGCACCGCCACAGTAAGTGGATGCTATGTCCAGGACCTGGAGGGTGCTGTC
CCTGAACAGGTGCCCTGGCCCTTAAGCCTGGAACTTAGTGGACAGAGTACCCTGTGTGCT
GGGGATTTTGGCAAGCAAAGAAGCTTTAAACCTCCCCATACACTATCAGCTTCCCAGAGA
TGGGACCAAGTCCTCATAGAACACACCCTGCCGTTTCTGGGAAGAGACGATATTGGGACC
TAGTGCTTACTTTCCTTTTGTTTTGTTTCTTGTTCCTTTAGCAGACAGATGATGCAGCCC
CGACCGACGGCCAGCCCCAGACACAACCTTCTGAAAACACAGAAAGCAAGTCCCAGCCCA
AGCGGCTGCATGTGTCCAACATCCCTTTCCGGTTCCGGGATCCAGACCTCCGACAAATGT
TTGGTGTAAGTACTGCCTTCATCCTCAGTTTGCTCCTTGTGGGAGTTCTGAGACTGTCTC
ACTCTAAGGTAGAATGTTGTTATAGAATGAAGGCATTTTAGCATCTAATACCTGGGTCTA
TGGGGGTAGGTCCCCTTAGGGGTGATAGGAGACATTGATTTGTTTTAGTTGTACTCATGG

6.3 *Rbfox1* promoters sequences

6.3.1 Promoter 1B

PCR Primers: Rbfox1_Prom1_kpnI_F, Rbfox1_Prom1_hindIII_R **PCR product: 3186 bp**

GACGCCTGGCTCTTGATAAATATTTTTAAGCCTAGTAGCAAGGC
AGGCATCAGTAGTTACCTCTGACCTTTGATACTGATATATAAAAACCTATTTCTACTCCC
AAATAATTAAATCAGAACCGATTCAAACTGATCTTGGTTTTTGGATTGGTAGCTTTTACC
TTATTGATTATTGTAAAATTATGTATTTACAATAATAAATTAGTTCATCCATCGTCCATT
TAGTGAAGCAACAGCCAGTGTCTCTGCCTCGAGTGCTTAGGTCTGTATCTTCCCCCTCAG
AACCCAGGAGCAGAGCACAGAGAAGCAGTTCAGCAGAACTCACCATTAGCTGACACTTAT
TTCTTCTCCTGTTATTGATAACTTGACTTTAAGTTGAGAATACTTCTTTTTTAAGCCATG
GCATCTCCCTGTATGGCTAGACAATTACATTTAAACTTAGCAACTCTCCTGATGCAAACA
GTTTCTGGGGGAGATGATTATGATGTTACTAACCTGGATTTATGGCTTCTTTGTGCTTTC
TGGGGAGGATAAGAGACTGTGAGAAAGGAAAACACAGTTGTGTGCATACAAATACATTAT
TATTGGAGAGTGTTTTGAGAAAGGTCATGGTCAAACAAAACCCAAAGTGCAAATAGCTGG
TGCCAGAGATAGGGACCACATTGTAGGGTTTTCAAGGTTACTTTCTCAAATAAGTATGAC
TTCAAATTGGGTGGTTTTAATAAATTGATGGTTGTGGATAGCAGAACATTGTGTTTCCTA
GATGTGGGAGGAAACTGTAGAAACAATAATAATAATAAATAATAATAATGTGATGTAGAG
ATGTCGAGACTAGTGAGTCTGTCATTGATGAGGCCCTGGGGTCATTCAATCTGGGAACAT
CCAAAGGAACACAGGGGACATGGGCTTTGCTGTCAACCCAGAAACCAGGCTGTGAGCAAG
AGTCTCAGGTCAGGGGCCCATGATGAAGTCTGGTCTTTCCTAAGCTACCTGCCCATAAGT
GGCAGGGTGGTACAGTGCCTTCCTTGGGAAATGAGGTAGACCTGCCAAGGGGAATCCTGG
ATCCTGGCAGAGGACTTGGTGATCTCCAGCAAATGTTAGAGCGGGCTTCAGGGAAGATTT

TCTTGTGTAACATAATCATTTGAAATGTAAATGAGAGAGGGAGGGAGGGGGGAGGAAGAG
GGGGGGAGGGCAGATGGAGGAGAAGGGAGGGAAGGAGAGAATGAAGGAGGGAGGAAGGGG
AGGGGAAAGAAGATCTGGAAGAAAGAAAAGAGGAAAGAAAGAGAAGGAAGACAGGAGGGA
GAAAAAGAAGGGAGAAAGAAATTAGGGAAGAGAGGCAGAAGAGAGGAGAGAAGGGAGGAA
AAAAGGAGAGAAAGAATATAGAATCAATAGGGAGAAGGAAGGAGAGAGGAAGAAGAGGGA
AAGAGGAAGAAAGAAAAGAGAGGGAAGGGGGGAAGAGCAGGCAAAAGGGAAAGATGGAGA
ACAGAAGGAAAAGGAAAAAAAGTGAAATAGCATTTCTGGCTGGGGAGCCCAGGCAGGGCA
CAAGGAAAAGCCCTGCTTTAGCTTCTGATACCTCAACTTTCTAACATGGGAAATGGGCAG
ATTCAGGGTATCCTCTCTGTCTTGTTGAGATGACAGTGCAAACTATGTAAGCAACACATG
GTAGTGTGACCTGAGTACTAGAGAGGCCTAAGAAGAATCATGGATGGGCCTGTCAGCTAG
CTGCTCAGAGAACAAACCCCAGCCTCCAACCCAGAAGCACTTCTGCCCACCAAGAAGAGG
TGGCTGCTCAGATGAGGTCAGGCCAGACCTGCAGCTCAGAGGTAGAGATTATCCAGGTGG
GTGTAACTTTTTGTTTCAGGACTGGGGCTCCATCTCTGCCAGGCAGAGAGCTTTAAGAGT
TCCCCAGAAACTTCTTTGAAAGTGGACCAGGGCAAGGGGTCTCCATACCCTTAGGCCTTT
TGAGATTCCTTTTCCTACCTTGCCTATGAGGACAAGGGGGAGGCGTTCAGGATGGAGAGC
TCATTTAGGGGCTGGCTGAGCAAACCCACTTTGGGAAGAGGAAGGCCTCAATCTAAGGAC
GTGTGTTCTCTGCTCCACCCACTCTGGAAGGCAACTTTCACCCCTTGTGCACTTTAGGAA
GAAGAGACTAGGGGCACCTAGTCCCTTGCCCACAGCGGCTGCTGGAATTCAAGGCTGCAA
GCGTGACCGTGACCGCGGCGGCAGCACTGGAGAGGGAAGGGGGAGGGGGCGCTCCCTGGT
GCTCGGGATTATTTTTGGCTCGCCAGCCCGGCTGCTCGCTGCCTGTCGCGCGCGCGCGCG
CGGGCACACACAGACACACACACTCACACACACACACAGAGAGACACACACACACACATG
CACACATTTTTCTCGCGCTCTCCCTAGCTCTCCGCTCTCCTTTGTTTATTTTCTAATCTG
GATTTTGTTGGTTGCGCTCTTCTTTGCTTCTCCTCCGGTCCAGCTTGCCAGCACTCCCGT
GGGCCACCCAGTGCTCGCCTGCTGCTCCCAAATCAGCGTCACCCGGTCCCCTCCTCCCGG
CCTCCTGGAGCGCGGGGTTTGAAGGTCACCTCCTTTCTAGTTCCCCCTGCGAGCCGAGCC
GCCTCCACCCTCCTCCGTCTGGATCCCAGAAGTGTCAGTCGCAGCGGCTGATACCTCGGA
TAGGGGTCCGCGCGTGGTAGCAGGGAGGGGAGCCCGAACTCAGAGTCGAGGGGGAATTAC
TCCCTCTTCTTATCGCGCCAGACCCGGCTGCACCACGGAAGAGTGGGGGCGCTCTGCCAG
CCACAGGACCCACGCGTGCGCCTCGCGGACCCGAGAAACCACCAGTGAGTCGCTCAGCTC
GCATCTGGAGGGGACAGCCGTGCGCCCCGCCCCAGCGTCCGGAGCCGACAACTCCGAGCG
TCCTCCCAGCTCAGGACAGATCTGAGAGGACCTAGCGCATCTCCAGATCCCGGAAACCCC
TGCGCTTCAGACCAGGTGGCCTTGGACACCAGGGCCCCTTAGGAGTGATCCGGACCTTCG
CCGCGCCCAGTAGTAGGGCGCGGCTGACCTGCCGCGAAGTTGTGGCCAGCTGGAGTGAGA
GAAGCCAACATCCTAATTCGTTGCCTCTGGTGGATGCTGAACGCGGCTGGGGTCACACAG
AGAACTGAGGAATCCAGGAGCAGGCAACAACTGCCAAGCTCGCCAGGAGTTCTAGGTAAG

CACATG → mut:BS1 and mut:BS3. C-Myc binding sites

CATCTG → mut:BS2. NeuroD2 binding site

CCCCGCCCC → G-rich sequence. Klf7 binding site

CACGCGTG → mut:BS4. Hes family binding site

6.3.2 Promoter 1C

PCR Primers: Rbfox1_Prom2_XhoI_F, Rbfox1_Prom2_ext_Bgl II_R **PCR product 1459bp**

AGTACAGCTACCTCGTGGGGGATATGAAGAGGTAGGGAGGGGGGTCTCCCAGCCTCCCGG
AATTCCTCCATGAAGTCGCAGATTGGAAATCATAAATACTGGCTATGGACATTTTGAATA
ATGCAGGGAGTAGCGTAAGTAATTGCCAGCGCTGATATCCTGCCTTGGACATCTCATTGC
TCCTGAGTTAAAATTGGTTGTCAAGTGAGGACTCTGGGGACTGTGCAAGGTGCCCTATTC
TGTCATGTGGTACATATTTAATGCTTGAAAGAACAAGGGAAGAGACACGTGCTGGGGGGG
GGGTGGTGGTGAGATTATGCCATCAGTTTGCTCACTTTCCAAGTGCTTGGCAAAGGGGGT
GGCTTGCAGTTCTTCCCTCAGTTGCTAGACTTGGTAAAAATTAAAATAAAAACCAGGCGT
CCAGTTCATCTGTCCGTCATGTCGCTGTCAGCGCCGCATGGCAGTAGGCTTGTCTTTGTG
TGTTCCTGGAGCTTTGATTACCTCCCTGCACCGCGCGCTCGCTCTTGTGCCTGCTGGATC
TCTGGCCCTCTCGCTTGTTCAAGGCCTTGAACACCTGCTGGTGGCTGGAGCAAAACAGCC
CAGGCAGGCGAAGGCGCGGCCAGCCCAGCAGAGAGAGCTAGAATCATTGGCATTGCTAGC
ACGTGGGTACCATTCTCTGCTGCTGCTGCTGCCCCGGCACTTCTCCCGCCTTGCGTTTCT
CCCAATGCGATGTAGCAAGAGAGGGAGCAGGAGGCGCTTTTGCAGCGGGCGATGAAATCC
TGGCAGCTAATTGCAGTCGTGGGAGATGCCCTTCAGGTAAGGCGAGCGAGGGAGGCACGG
AGACACTGTGGGAGGGGGAGCAAGAGACTGGATGGGAGGGAGGGGAGGCAACTCTGGCAC
CAGCATCCGAGCATCCCGAAGCCCGCTGGACGGATGCTTGGGAGGAGGGCGCGCAGGGAC
GGGGGCGGGCGGCAGGGGGAGGAGTGTGCGAATTGACATTCGGGGCTGCCTGTGGCAGGC
GAGCCGCCGCCAGCCGCTGTCCAACGTTAGCTCAGAGAAGGTGGCGGGCGGGCGTGTGCA
CCTCTGGGGCCGCGGATCAGAATCCGGACCTGGCGGTGGATGGAGCTCAGGGAGTCTTGA
GAGGCAATGGCAGGACGCAAATGTGTTTGCAGCGAGTGAATTACACAGGGTAGGTAAGTT
CAGCTCCGGAGTCCTGTGGGATACAATCTGGGATTCGCCCTGGGCTCCCCGAGGGTCCCC
GAGGGTCCCTCAATACCCAGGGAGCTTAGACGGGCTGGGGGACCAGAGGGTGGATGGATT
CACTTTTACCAAGTGGAAGTTCGCGGGGAACTTCCCTGGAAATAGCCATTGGCTCTGTTG
AACTTTATTCCCAGAGATGAATAAGCGTTTATTAAGGACTGGTGTTACAAGACCCGCAGG
CTAGGGCTGGATTTTGCAAAGAAGATG

CAAGTG→ mut:BS1 and mut:BS2. Tcf4 binding sites

CATGTG → mut:BS3. Mycn binding site

CACCTG → mut:BS4. Tcf4 binding site

CACGTG → mut:BS5 and mut:BS6. C-Myc binding sites

6.3.3 Promoter 1D

PCR Primers: Rbfox1_Prom4_XhoI_F, Rbfox1_Prom4_Bgl II_R **PCR product: 2359 bp**

AGACTGTAGTTTTTTCCAGTGTCTGATTGAAAAAGAAAAAAATCTCTGCAGTTAAAAAAA
ATATCTGAAGTAAAGAAAAAAAAAAAAGAAGAAGGAGCAAGACAGACTGAAAAGCCAAGC
TCTCTGTGGTCTTTCATTCTTTTTCATTGGCTCACGGAATTATGAAATAAAACTAAGTAC
AAAGATGGAAAGTAAGGAAAGAGGTACTGGATGTTTGCGTGAGTCAGAGCTTGTGTGACA
AATGCCACCGATTTCTGAGACAACGTGTAGCAAGCCGGTTTTTCTTTTCTGAATACTGTC
TGCCAGCCCTCTTACCCCCAACCAGCCCCAGAAACACTTTGCCCTTGCTCTCCCAGCCCT
GCAAAGGACTCACAAAGCGTTAAAAAGGCTGCTGAGTGGCCATTGAGTTGACAGGATACA
AGAACCCCCACAAAATAATTTGAGGAGTGGGTTTGCAAAGTGGAAGGTGGAAATGAACAG
TTAGGCTGGTTGGGGCCCAGTGGAGACATTATCGGTTTTGATACCGTTTCAGAAAACAGC
ACCTAACCTAGCCATGGGACCATCCTCTCCTTTCCATCAGAAAGCATTTGATTAGTCTGC
CAAGTGAATTGTGTCTTGCACGCTGCGGGATCAGTCTAGAAGATTCTAGAAGTCTAGAGG
GAGTGTGGGGAGCACCTATGGGGATGGCCTTTGAGTGGCTTCTTGCCTCAAAGTCCCTTC
CTGAAAGAAACCGTCCCTCCACACCCCCAGCGGTGGCTCTGCCCTGCATGGTTGGCACCA
ACCCTCACCTGGGATTCTTTGAGAGAACCAAACAACCCAGGTTCTAGTGAAACCTTTCTC
AGAGAATAAAATAAAAAAAGAAAGAAAAGAAAAGAAACTCAATCACTAGCTCAAAATAAA
TCTGTATAAAGTATGGCAACTATTCCTGATCATAATTTTACTATTGCCAGGATTTTACCC
CTTGTGGGAATCAAGGACGAGTTAGAGTCTTCATATTTTCTCTTAATTCACAGATCACAT
CCCTTTTTATTGCATAAAGACTAACGAAATCCACTAATGAATAATTATTACTTCATAAGA
TAAAGGGGAGGGGAAAGATCCGCCTGCAAGAGTGGAATGTTAATTTGACCAACGAGGCCA
GACAAGAGGAGAAAATATAAAATAAAACCATTTCAATTTGTTCTTTGCCTCACGCACAAT
AATCTCTTACCAGACAGGGACTTTTGCCCACTCCTTGCATTTATAATTGAGAAGACCAGC
AGGTTCTAGCCTGGAAGGAGGCCCCTCGAATTCACCTAACAGCTGCGGTGGATTCTCCGG
TTTAGCCTCCAGGCTTGGGGCTGCCCCGGAGGGGCTGATTCCAGGGGGAAAGCAGCGTCC
GGAACACCGCGGGGGGCCCAGGAACCTCTTTATTGCTCCCTCCCCCCTCAGCACCCCAAA
CCTTGGAGTGTCCATCACCCCCAAGCTTCTTACAAAAGGGGAATTCCTTTTCATGTGTTT
ATTTGCCAACGAGTCAGGCAAACAAACCGCCGACTGAAAATCTCCCGGACTCCTCAGGGT
CCCAGCTGAGCAGTCTTGTTAATGGTCCAGCTCCTTTGATTGCTGGAGATGTGGGGCGCT
CACATGCTCGATCTCCCTCCCCTCGAAGGATTTTAGCAGACAAAATTTAAATTTTAGCGA
GTCCCTTTTTTAAAAAGAAAGAAACGCACAACCCTGCCCCTGGACCTCCTTGGCAAATGA
GAAGACTCCCAGCATCAGCACCAAGCAAGTGAGCGACAGAGAAGCTGTAAGTCAAAATCA
ATTTCTCTCTCTCTCTCTCTCTCTCTCTCTCTCTCTCTCTCTCTCTCTCTCTCTCTCTCT
CTCTCTCTCTCTCTCTCTCTCTCTCTCTCTCTCTCCTCCTACCCCTCTCCCTCCCCCT
CCCCATTTCCCCTCTCCTCTTCCTTTCTCTCCTTCCCCCCTTCTTTCTCCTCCTCCCCCT
CCCTACTCCATCTCTCCCTGTTTCCTCTCTAGCATCTCTATCAGAGCATCTTAACCCCCT
GTCTTTCATAGAAGGCGACTTTGACCATTCTTGTCACCTTTAGGGGGTAGTGGGGTGGGG
TGAGGGGCACCTTCCACTTTAAGAGCGCTCCAATAACAGGCCCAATAAGCCGAGGGAACC
AACACACTACTTCCCTGCCTCTCCAAGAGTCTTTAGTTGAAGGCTGATGAAAGCTGGGTA
CTAGCAAACCCGAGGGCGAGGAGAGCCAGGGAGGAGGGACTCTCTTGGGGTGCCGTGGAG
GGGAGGGAGAAAGAGAGAGACGAAAGAGGAAGAGAGAGAGCAAGAGGGACATCCACTGCT
GTGTGAGTTAGATAATCGGCAAAAATTAAAAAAGGGGGGGGGGGGGAAAGCTG